Erklärung über frühere Promotionsversuche

Hiermit erkläre ich, dass vorher keine weiteren Promotionsversuche unternommen worden sind, oder an einer anderen Stelle vorgelegt wurden.

Hamburg, den 24.04.08

(Unterschrift)

Eidesstattliche Versicherung

Hiermit erkläre ich an Eides statt, dass die vorliegende Dissertationsschrift selbständig und allein von mir unter den angegebenen Hilfsmitteln angefertigt wurde.

Hamburg, den 24.04.08

(Unterschrift)

A mis padres.

Muchas gracias.

“Study of the inhibitors in the acidic attack on steel surfaces during the elimination of oxide scales”

Beim Department Chemie
der Universität Hamburg
eingerichte Dissertation zur Erlangung des Doktorsgrades

vorgelegt von “master in sciences”
Laura María Fernández Díaz

Gutachtern :

1. Prof. Dr. J.A.C. Broekaert
2. Prof. Dr. N.H. Bings

Datum der letzten mündlichen Prüfung:

7. November 2008

The present work was carried out from August 2003 to August 2007 in the Department Oberflächen Analytik of ThyssenKrupp Steel. Part of this work was realized under the Marie Curie fellowship with contract number G5TR-CT-2000-00017.

Acknowledgements

I would like to thank Prof. Dr. J. A. C. Broekaert for his supervision and help.

To my supervisor in ThyssenKrupp Steel, Dr. Appel, I would like to thank for assisting me in my development as a scientist.

The whole electrochemical part of this work would not have been done without the very helpful advice and guidance of Dr. Ostwald and Mr. Bendick, who has been always very patient and has taken all the necessary time to explain concepts and proceedings. Also I would like to thank him for the very interesting conversations kept to make time shorter while the experiments were taking place.

All explanations and advice of Dr. Müller has been of great help to introduce me in the "fantastic ToF-SIMS world" and he has been always keen to answer my questions and give explanations. I should thank also Mr. Netthöfel for his time and patient supervising the infrared results.

I would like to thank my workmates for the help and support provided through all these years, preventing me of stepping into "the dark side", and for all the good times, conversations and jokes shared during this period.

I would like to thank especially all those who had taken the time of reading and correcting my work.

There are many people who are partially responsible that this work has come out to a good end. It would be impossible to name them all, nevertheless I can not omit the following people:

- My parents and brother. This work belongs more to them than to me. I would like to thank them for all they have given me along my life. I would not have reached this status without all the effort that my parents have made for me and without the sometimes wise and some other times very funny words which with my brother has always supported and encouraged me to go on.

- Ildefonso, for all those hours of endless talking whenever I had needed it, his support in the most difficult times and his efforts to make me believe in myself. Thanks also for bringing things into perspective and overall for all that we have shared, I have grown up a lot by your side.
- Praveen, not only for the good times shared and his unconditional emotional support but for the time and effort he has taken from his (very busy) life to help me with my “very poor English”.
- Johnson, first of all for bringing me into my senses when I was out of them and then to use his time and effort to read and correct part of this work.
- Paco and Mari, thanks for all their support through the difficult times and all you have given me.
- Astrid, thanks for all her love and emotional growing up help. Her very sensitive perceptions have helped me a lot to realize about many important things.
- Irma, thanks for all the conversations and work together to find the emotional stability and for all the advice and listening.
- Julio, for all his advice regarding anything but mostly computer problems and his encouragement when things were difficult. Also for all the laughing brought to my life with his crazy wisecracks.
- Maria, I do not think I would have ever obtained my degree without her help, support, care and sometimes the governess roll that she has taken to make me study. Without that step I would have never reached this point.
- Efrain, Virginia, Tonja, Angela, Martin and so many others, thanks for the help in different matters, the support given, the incredible times and conversations shared together, the experiences, the jokes, the laughing… thanks for the very good times and all your care, encouragement and support in the bad ones.

To all these people and all those who are not mentioned here, whose advice and good talks with had been of great help not only to keep me in the way to finally finish this work but to grow as person and human being, I would like to heartily express my profound gratitude; please consider this work partly yours.

Introduction

Pickling process is commonly used in machine-construction industry during punching, pressing, welding, etc. and also in power plants for acid washing of steam boilers and other installations. This is effective for cleaning surface layers, corrosion products and encrustations that are formed during the operation of the installations. Pickling, however, mostly takes place in metallurgy to eliminate the formation of surface layers during steel heat treatment processes. These layers must be necessarily removed to achieve desired properties and to guarantee the quality of semi-finished products such as pipes, sheets and bands.

Though technically important, the costs associated with the pickling process can increase exorbitantly, as the hot acids used for this process not only dissolve the scale but also the steel bulk material, when no cautions are taken. In fact pickling with HCl is proven to be more effective and also faster than H_2SO_4. While the use HCl for pickling presents some advantages, large corrosion-resistance containers required for its storage and transport at concentrations of about 20 to 25 % makes it problematic. This makes H_2SO_4 more attractive and is commonly used in many processes.

Indeed, when H_2SO_4 concentrations even as low as 10 % H_2SO_4 are used at 40°C, iron dissolves six times faster than ferrous oxide[1]. Only 5 % of the quantity of H_2SO_4 used is consumed for the dissolution of the scale[1]. The costs of the acid during steel surface treatment can be divided as follows:

- 55 % for the dissolution of steel
- 25 % in lost during washing
- 15 % overflow with solutions used
- 5 % for the dissolution of the scale.

It is important therefore to ensure that the dissolution and loss of metal is as low as possible, as here most of the acid is consumed and the economical loss is at largest. This fact asks for the use of acid corrosion inhibitors.

Different corrosion inhibitor compounds have been largely used along the years to prevent corrosion. The effectiveness of these compounds enormously depends on various factors like the nature and the concentration of the used acid, the alloy to be protected or the temperature of the medium. Even though these inhibitors have been long known to be effective depending on the experimental conditions used, their underlying mechanisms have not been well known[2]. Up to now not all inhibitors have been studied in detail.

The ultimate purpose of their study should be the development of predictive criteria for the inhibition effectiveness more than the mere delivering on explanation of experimental results and a possible mechanism. Both latter attempts have been far from successful in providing a satisfactory understanding of practical inhibitor phenomena. This demands extremely detailed studies about the compounds formed are necessary to discover patterns that can be applied to predict the general behaviour of inhibitors[2].

The study of corrosion and its effects is a vast field. The effects of corrosion and protection from corrosion at the surface of a metal can be studied by means of different superficial methods such as scanning electron microscopy, x-ray photoelectron spectroscopy, secondary neutral mass spectroscopy, time of flight secondary ion mass spectrometry[3], white light interferometry, glow discharge optical emission spectroscopy, atomic force microscopy, etc. However, corrosion process itself, as a result of its electrochemical nature[4], mainly can be studied by means of electrochemical methods[5] which provide not only for thermodynamic but also for kinetic information about the process and therefore allow a comparison of the different inhibitors effects and help in improving their effectiveness[6]. The most common electrochemical methods which provide thermodynamic and kinetic information about the corrosion reactions are open circuit potential measurements, recording of polarization curves and impedance spectroscopy[7, 8].

The objective of this work is to perform a methodological study of the inhibition mixture and each of its components currently in use at the pickling plants of the steel company ThyssenKrupp Steel AG (Dortmund, Duisburg). This will contribute to the development of a scientific methodology for predicting the inhibitor effectiveness as well as to contribute to an optimization of pickling parameters at pickling plants in general. For this study H_2SO_4 is used. H_2SO_4 is a by-product in the conversion of coal to cokes and therefore it is used in the pickling plants in order to recycle it.

2. Theoretical Part

2.1 Overview on steel production processes and theoretical concepts

In this section a brief description of the chemistry of iron and adsorption processes are presented. Detail description of steel as a working material and about industrial steel making process and especially about the pickling step, which is the main topic of this investigation, are given.

2.1.1 Brief description of the iron chemistry and some of its compounds

Iron is the second most abundant metal after aluminium and the fourth most abundant element in earth's crust. It is a metallic greyish tinge lustrous and fairly soft metal which is quite reactive. There are rich deposits of iron ores in many parts of the world and the free energy required to isolate iron from its oxide ores is less than the half of that required for the production of aluminium metal[2, 5].

At 298 K it is in the solid state. In moist air it quickly oxidizes to hydrous Fe^{III} oxide, which is known most commonly as rust. Rust has no protective properties, it flakes off and the fresh metal surface again is exposed to environmental conditions. In a finely divided (grated) form, iron is pyrophoric.

Iron metal rapidly dissolves in dilute mineral acids. When no air and no oxidizing agents are present, compounds are formed. However when there is air in the reaction place or warm diluted nitric acid is used, part of the iron is oxidized to Fe^{III}[9].

Some important iron oxides include:

FeO: (iron (II) oxide). At low temperatures, FeO is less stable than Fe and Fe_3O_4. It has rock salt (NaCl) type crystallographic structure and typical composition $Fe_{0.95}O$. FeO is found as the mineral wustite[4,5,10,11].

Fe_2O_3: This oxide can be obtained by heating the hydrous oxide [FeO(OH)] at 200°C. It is found as hematite and has a corundum structure with the oxide ions forming a hexagonally close-packed array with Fe^{III} ions at the octahedral interstices. There is also a rare form of this oxide called β-Fe_2O_3[12-14].

Fe_3O_4: this oxide is present in nature as the mineral magnetite. It is a Fe^{II}-Fe^{III} mixed oxide with an inverse spinel structure. Fe^{II} ions occupy the octahedral interstices. Half of the Fe^{III} ions are in the tetrahedral and half in the octahedral interstices of a cubic densely packed array of oxide ions. It has a very high electrical conductivity (~10^6 that of Fe_2O_3), which probably is due to rapid valence oscillations between the Fe sites[11,15-17]. Magnetite can be used as a black pigment.

Solid iron has a body centred cubic (bcc) polycrystalline structure. It consists of a cubic array of cubic cells groups where a metallic iron atom occupies each of the corners of the cube and another iron atom is in the centre of the cube.

The metal bulk consists of an assembly of several crystals with such a structure connected together. The interface between the crystals is called grain boundary. The lattice has defects and imperfections and contains segregated or soluble impurities. All these imperfections show up at the surface and determine greatly how the iron will react. Structure imperfections accordingly have a great influence on the dissolution rate.

The alloys of iron and carbon have specific importance because they are used in steel production. The iron phase diagram explains the different structures possible, which depends on temperature and composition[18-20].

2.1.2 Adsorption

Adsorption may lead to an increase in the concentration of a dissolved substance at the interface of a condensed and a liquid phase as a result of the operation of surface forces. Adsorption can also occur at the interface of a condensed and a gaseous phase[21]. The potential energy of a surface adsorbing a molecule decreases as the molecule approaches the surface. The degree of adsorption greatly depends on the specific nature of the solid and of the molecules being adsorbed and it is a function of pressure (or concentration) and temperature[22]. An adsorbate is a molecular species of a gas or a substance dissolved in liquid which adheres to or is adsorbed in an extremely thin surface layer on a solid substance. An adsorbent (or substrate) is a condensed phase at the surface of which adsorption may occur.[5]

- **Physisorption and chemisorption:**

There are two kinds of adsorption: physical adsorption (or physisorption) and chemical adsorption (or chemisorption)[21-24]. The difference between them lies in the nature of molecular interactions involved. In the case of physisorption (non specific) they are weak intermolecular and long range van der Waals forces. Such small energies can be absorbed as an increase of the thermal vibrations of the lattice. A molecule bouncing across the surface will gradually lose its energy and finally adsorb on it in a process called accommodation. The small enthalpy change involved is insufficient to lead to a cleavage of bonds. Accordingly, a physisorbed molecule retains its identity, although it might be distorted by the presence of the surface. Once a monolayer has been formed, intermolecular interactions between the molecules of the adsorbate and the non-adsorbed molecules of the same substance can lead to the formation of a second layer of adsorbed species. Physical adsorption is readily reversed by lowering the pressure of the gas or the concentration of the solute and degree of interactions is smaller at higher temperatures. The equilibrium generally is achieved rapidly and is readily reversible.

In the case of chemisorption (highly specific) a stronger interaction takes place, such as a chemical bond (usually covalent). It may not occur at an appreciable rate at low temperatures because it has higher activation energy. The atoms or molecules tend to find sites that maximize their coordination number with the substrate. Once a monolayer of the adsorbate covers the solid surface no further chemical reaction between the adsorbate and the adsorbent can occur. The enthalpy of chemisorption is much greater than the one involved in physisorption. The distance between the surface and the closest adsorbate atom typically is also shorter in chemisorption than in physisorption. A chemisorbed molecule can be torn apart at the demand of the unsaturated valences of the surface atoms and the existence of molecular fragments at the surface as a result of chemisorption is one of the reasons why solid surfaces catalyse reactions. This process is called dissociative adsorption. When the species have unshared electron pairs or multiple bonds they can be chemisorbed without dissociating (nondissociative or molecular adsorption) [21-24].

The enthalpy of adsorption depends on the extension of the surface coverage, mainly because the adsorbate particles interact. When the particles repel each other the adsorption becomes less exothermic as the coverage increases.

The characteristics of the physisorption and the chemisorption is summarized in **table 1**.

PHYSICAL ADSORPTION	CHEMICAL ADSORPTION
Enthalpy of adsorption less than about - 40 kJ/mol	Enthalpy of adsorption greater than about -80 KJ/mol
Adsorption appreciable only at temperatures below the boiling point of the adsorbate	Adsorption can occur at high temperatures
Each infinitesimal increase in pressure or concentration of adsorbate generates an infinitesimal increase in amount adsorbed	Each infinitesimal increase in amount adsorbed decreases with each infinitesimal increase in pressure of adsorbate
Amount of adsorption on surface a function more of adsorbate than adsorbent	Amount of adsorption characteristic of both adsorbate and adsorbent
No appreciable activation energy involved in adsorption process	Activation energy may be involved in adsorption process
Multilayer adsorption occurs	Adsorption leads to a monolayer, at most

Table 1. Characteristics of physical and chemical adsorption.

- **Adsorption isotherms**:

The adsorptive is the material that is present on the bulk phases and capable of being adsorbed.[18]The adsorption isotherm for a single gaseous adsorptive on a solid is a function which applies at constant temperature and relates the amount of substance adsorbed at equilibrium to the pressure (or concentration) of the adsorptive in the gas phase. The surface excess amount rather than the amount adsorbed is the quantity accessible to experimental measurements. However at low pressures the difference between the two quantities becomes negligible.[10]

There are different kinds of isotherms that can be used depending on the working condition that apply.

2.1.3 Arrhenius equation

The rate equation and the value of the rate coefficient (rate constant) for a reaction can be deduced from rate of reaction measurements at a fixed temperature. The rate of the reaction can be expressed as[19-21]:

Rate = k(T) x (x, the concentration is the dependent term)

It is known that the rate constant rises as the temperature is increased and several experiments have shown that this dependence to be strong[25-27]. In 1889 Arrhenius observed exponential dependence of the rate constant with the temperature and presented his findings in an empirical relationship in the form:

$$k = Ae^{(-Ea/RT)} \quad \textbf{(1)}$$

A is the pre-exponential factor (also called frequency factor), which has the same units as the rate constant and E_a is the activation energy. A and E_a are called the Arrhenius parameters. T is the temperature in degrees Kelvin and R the ideal gaseous constant.

When the logarithm of the rate constant is plotted against the inverse of the absolute temperature a straight line should be obtained. Both the pre-exponential factor A and E_a can be deduced from such graphs[25-27].

2.1.4 Corrosion

2.4.1.1 The corrosion process

Corrosion can be defined as the destructive result of chemical reaction between a metal or metal alloy and its environment[25].

The same energy that is necessary to extract the chemical elements from their minerals is released during the corrosion processes. Corrosion reactions transform the elemental form of a metal into compounds which are very similar or even identical to the minerals from which the metals were extracted. That is why corrosion can be considered as extractive metallurgy in reverse[25].

According to IUPAC recommendations[26], corrosion is “an irreversible interfacial reaction of a material (metal, ceramic, polymer) with its environment which results in consumption of the material or in dissolution of the material by a component of the environment”. Often, but not necessarily, corrosion results in effects which are detrimental to the usage of the material considered. Only physical or mechanical processes such as melting or evaporation, abrasion or mechanical fracture are not included in the term corrosion. In the same paper a short reference to electrochemical corrosion is given and it is mentioned that this kind of corrosion always involves electrode reactions (for example the corrosion of a metal by dissolution of metal ions or by formation of an oxide film). There are always two types of electrode reactions: the anodic and the cathodic one. They simultaneously proceed on the same surface or on spatially separated areas, which means that there is a flow of an electric current between the anode and the cathode.

Corrosion can take place in different ways:

-Uniform corrosion: When the time average of the corrosion current through a unit area of any microscopic dimension is independent on the position on the surface.

-Non-uniform corrosion: when the time average of the corrosion current through a unit area depends on its position on the surface. This form of corrosion can occur as a result of inhomogeneities of the environment. Pitting or intergranular corrosion are examples of non-uniform corrosion and some times are called localized corrosion.

-Selective corrosion: is the corrosion of a single phase having more than one component. Here the ratio of the corrosion rates of the components differs from the ratio of the bulk mole fraction. This kind of corrosion changes the composition of the material in the interfacial region.

There are more known types of corrosion such as galvanic corrosion, crevice corrosion, pitting corrosion, environmentally induced cracking, hydrogen damage, intergranular corrosion, dealloying and erosion corrosion.

2.4.1.2 Corrosion mechanisms in aqueous environment

Corrosion in aqueous environment has an electrochemical nature because nearly all processes imply transfer of electric charge. A general equation describing the overall process taking place can be written as:

$$M + n\,H^{+} \longrightarrow M^{+n} + n\,H_2\,(g) \qquad \textbf{(2)}$$

The metal reacts with the solution by which it is dissolved in it and hydrogen gas is liberated to the atmosphere. This equation can be seen as the sum of two different reactions, namely:

$$M \longrightarrow M^{n+} + n\,e^{-} \qquad \text{(anodic reaction)} \qquad \textbf{(3)}$$

$$n\,H^{+} + n\,e^{-} \longrightarrow n/2\,H_2 \quad \text{(cathodic reaction)} \qquad \textbf{(4)}$$

The cathodic reaction is not unique, as besides the one of hydrogen several reductions can take place:

$$O_2 + 4\,H^+ + 4\,e^- \xrightarrow{\hspace{4em}} 2\,H_2O \qquad \textbf{(5)}$$

$$Fe^{3+} + e^- \xrightarrow{\hspace{4em}} Fe^{2+} \qquad \textbf{(6)}$$

The first reaction explains the reduction of dissolved oxygen in acid solutions exposed to ambient air and the second one the reduction of ions from salts present in the solution. In the case of steel the presence and reduction of Fe^{3+} ions is very common.

The anodic reaction is an oxidation, in which the metal increases its valence number by delivering electrons, while the cathodic reaction is a reduction reaction where the oxidation state of hydrogen decreases from +1 to 0 consuming electrons and forming molecular hydrogen.

The processes taking place during aqueous corrosion can be described as represented in **figure 1**.

When an excess of electrons is supplied the rate of corrosion, expressed by the anodic reaction, slows down while the rate of the cathodic reaction increases.

The interpretation of corrosion phenomena is based on the knowledge of the kinetics of the electrochemical reactions. The study of the corrosion in the case of metals of the iron group is especially difficult because a large number of parameters influence the anodic metal dissolution: for example, the structure of the surface greatly influences the rates of anodic dissolution. Further on, parameters such as the selective dissolution of one of the alloy components or absorption of hydrogen into the metallic lattice also can influence the structure which can greatly change the speed of metal dissolution. Further chemisorption of substances from the electrolyte may change the interface metal/electrolyte, act as catalysts or inhibitors of the metal dissolution or change the reaction path.

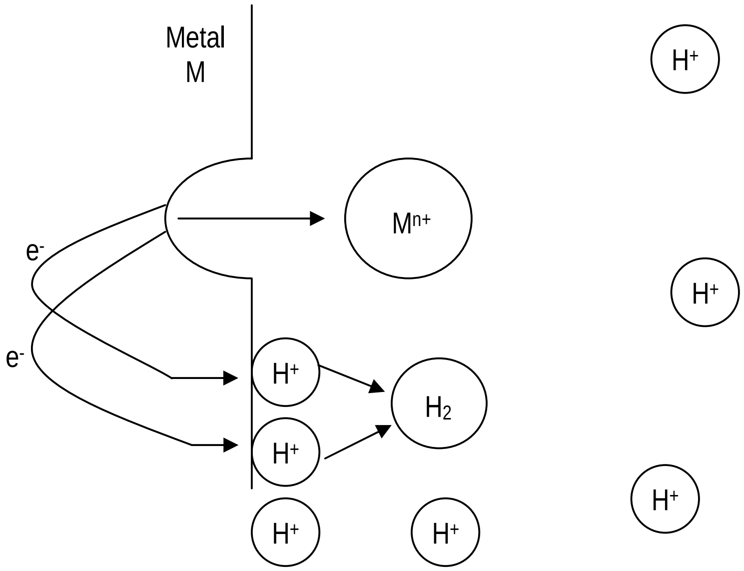

Figure 1. Representation of the corrosion process where the metal is dissolved in the solution as M^{n+} delivering electrons to reduce the hydrogen ions to hydrogen gas.

To understand the corrosion mechanism it is necessary to understand what is going on when a piece of metal is introduced into an aqueous solution. The metal is rich in mobile electrons, which interact with the aqueous solution forming a complex interface. The water molecules, possessing H atoms with a partially positive charge and O atoms with a partially negative charge, interact with the surface and form an oriented solvent layer. The structural situation is represented in **figure 2**.

The solvent layer formed on top of the metal prevents a further approach of charged molecules (ions) from the bulk solution. Ions in aqueous solution are also solvated and the molecules that surround them interact with the water molecules on the surface. These water molecules hamper the direct contact between the electrode and the ions. The plane compressed between the metal and the closest positively charged ions is known as the Helmhotz plane (**figure 2**). The diffuse layer is a three dimensional region in which non-specifically adsorbed ions are distributed. It extends from the outer Helmhotz plane into the bulk of the solution. Its thickness depends on the total ion concentration in the solution. The resulting structure consists of an interface with separate charges (double layer), of which the behaviour very much resembles a capacitor (**figure 2**). This charge distribution complicating the approach of the ions to the surface avoids an easy interchange of charge and therefore electrochemical reactions. Accordingly the structure of the double layer very much affects the electrode processes[27-29].

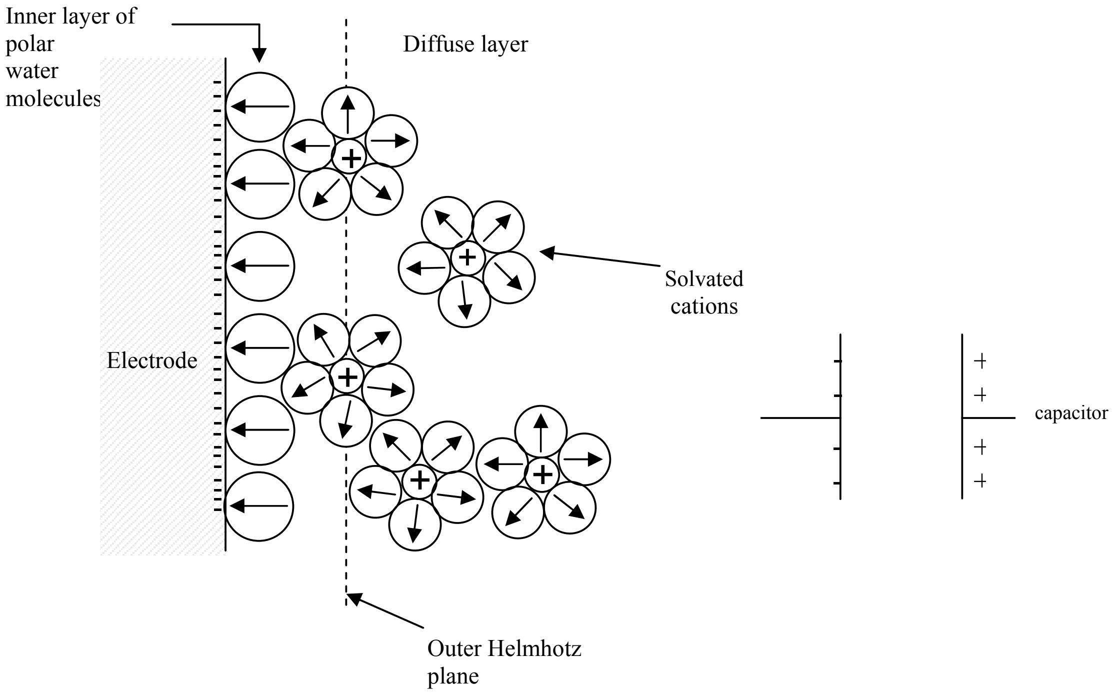

Figure 2. Layer system formed when a metal is introduced to an aqueous solution and electric equivalence to a capacitor.

2.1.5 Steel

2.1.5.1 Steel as material

According to the UNE 36-004 standard e.g. (Spanish standard for steel specifications, promoted by AENOR) steel is a material in which iron is predominant, where the content of carbon generally is inferior to 2% and which contains also other elements. Although a limited number of steels has contents of carbon higher that 2%, this is the normal limit which distinguishes steel from cast iron.

Nowadays, steel not only includes all forgeable iron based materials but also highly alloyed metallic materials in which the element iron is an important component but which are not necessarily forgeable[6, 9].

The wide diversity of steels relates to the polymorphism of the iron crystals and the capacity of iron to form alloys with other elements by the existence of solid solutions or compounds. It is possible to modulate the microstructure of a steel finished product by controlling the composition, the heat treatment and the forming conditions. It is a way to come also to the desired final characteristics of the material obtained [6, 9].

2.1.5.2 Corrosion of steel

To study the corrosion of steel it is crucial to understand the phase diagram for iron and steel, which shows the different microstructures obtained from the mixture in different proportions of carbon and iron, ranging from pure iron to cast irons through steels (**figure 3**)[18-20, 30-32]. Ledeburite are those eutectic crystals composed at 1135°C by 52% of cementite and 48% austenite.

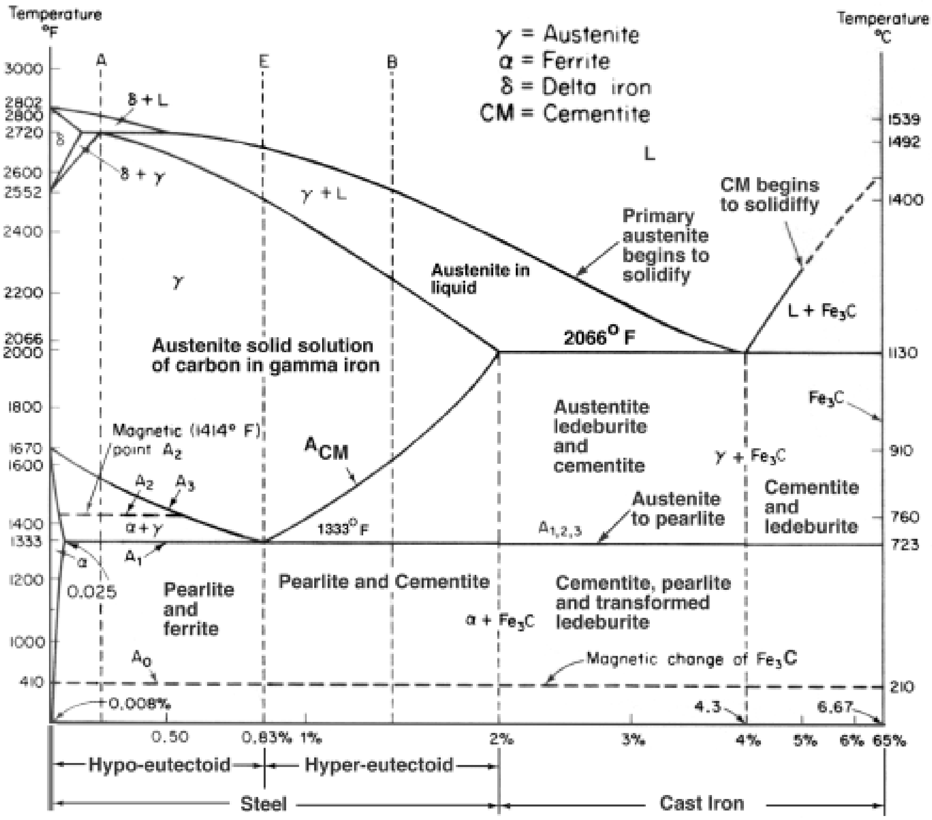

Figure 3. Phase diagram of steel.

Steel corrosion is directly related to mineral acids. The three principals acids are H_2SO_4 (this acid and the sulfamic one exhibit about the same corrosive behaviour), HNO_3 and HCl.

In the isocorrosion chart in **figure 4** it can be seen that the corrosion of steel is influenced by the concentration of strong H_2SO_4 and the temperature. The curves in **figure 4** are iso-corrosion or constant-corrosion lines, defining regions where corrosion rates of 0 to 5, 5 to 20, 20 to 50, 50 to 200 and over 200 mpy[*] can be expected. Above concentrations of H_2SO_4 of 70 % steel can be used as container for depending on the temperature, as long as it does not pass 80°C.

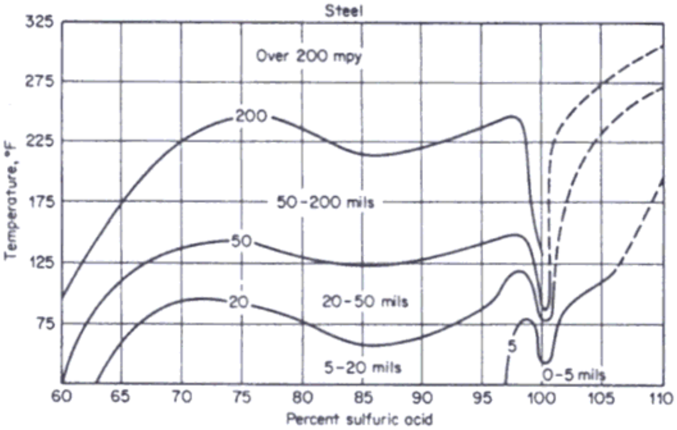

Figure 4. Corrosion of steel in H_2SO_4 as a function of its concentration and temperature[33].

2.1.5.3 Industrial steel making process

The production the steel implies several process phases. It requires high economical and energetic investments.

In **figure 5** the whole steel manufacturing process is schematically represented.

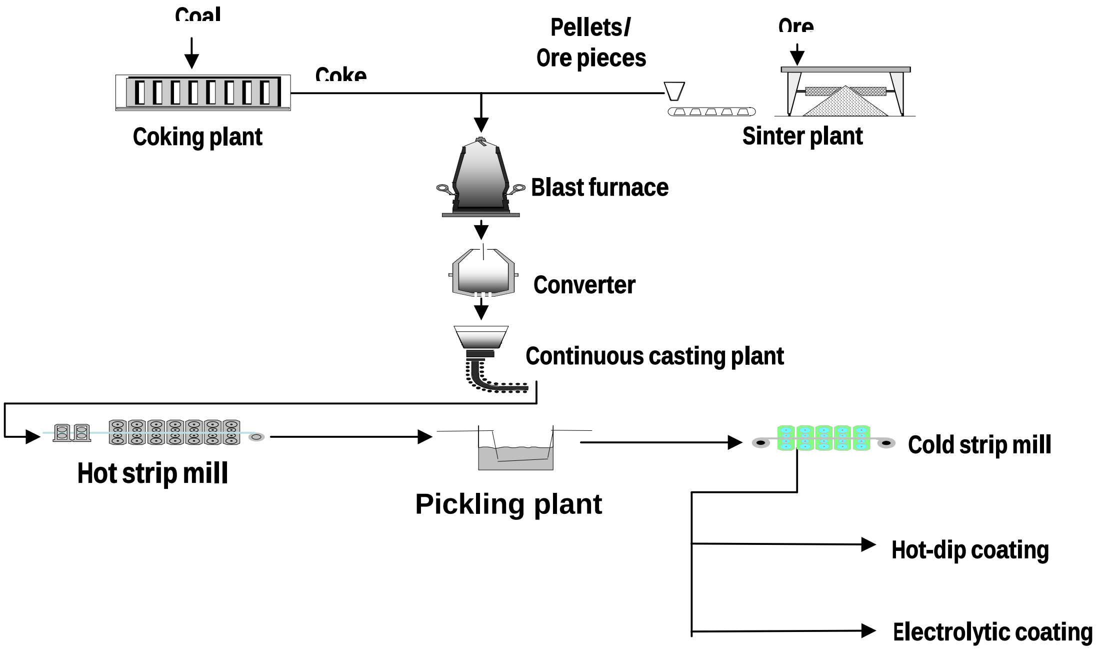

Figure 5. The steel production process.

---

[*] Abbreviation for mils (thousandths of an inch) per year penetration, being the measurement unit for the corrosion rate of a coupon[33]

The main aims pursued in the steel producing process following the initial iron production in the blast furnace are basically twofold: the removal of the unwanted metallic, non-metallic and gas-forming elements from the raw materials and the controlled addition of alloying elements with the aim to obtain a well-defined grade of steel.

The blast furnace process starts with the mixing of the iron, coke and fluxes (mainly limestone). From the blast furnace the melt is poured into the converter.

Decarburization and desulphurization to eliminate the non-desired elements (C, S, Si, or P) take place at this point. The liquid metal is brought to the continuous casting plant, where the molten steel is shaped in rectangular blocks of two by four meters and by ten centimetres.

The first shaping takes places at the hot strip mill, where the products enter in a high temperature chamber (1200°C) through several rolling mills. The latter applies a pressure to model the warm steel passing through them. The semi-finished product is entered several times to achieve its desired final shape. In this process the most external layer of the steel undergoes an oxidation due to the high temperatures and the oxygen in the atmosphere.

The material that sorts the hot-rolling is subjected to a deoxidation process called pickling. The conditions of this pickling step are determined by the surface layer on its structure, which is determined by the conditions of the hot rolling, the steel composition, the acid concentration, the temperature, the concentration of Fe(II) and the free surface available. Basically the steel is passed through a solution of hot H_2SO_4 or HCl, to get rid of the oxidized surface layer.

The last shaping of the material takes place in the cold rolling mills. Here the thickness of the steel is decreased. Therefore, the material is uncoiled, passes through rolling mills that reduce the thickness and then it is coiled again.

The importance of pickling is given mainly by two factors, namely, its direct relation to the surface quality of the produced cold rolled sheets, which will be used in the industry (e.g. automobile industry), and the corrosion resistance of the material.

2.1.5.3.1 The pickling process

In the pickling process the surface layer is chemically removed, and this is applied when metals must undergo further treatments like painting, coating, galvanizing, electroplating, cold rolling, etc, for which they must exhibit a clean surface free of salts and oxides. The oxide formation during the hot rolling can be eliminated by passing the strip band continuously through baths of HCl or H_2SO_4. This is the case for high grade steels, for which no consistent response to heat treatment and no purity requirements with respect to non-metallic inclusions are specified*. For stainless steels, which are special alloys with well determined working and application properties such as high resistance to chemically aggressive materials the strip passes through HNO_3 mixtures [9, 28, 29]. The conditions in the pickling baths will be determined by the surface layer structure, which depends on the hot rolling parameters used. The purely chemical removal of the surface layer known as "descaling", may be too long and a previous mechanical descaling[34] often is used. In an effective descaling process the scale must be broken down.

During pickling the steel strips are passed through baths with 20-25 % of H_2SO_4 at 95-100°C or 15-20 % of HCl at 60-70°C. It must be considered that aqueous solutions of acids are among the most corrosive media and their corrosion power increases with the temperature. The time for descaling therewith depends on the conditions used for the hot rolling process, the temperature, the acid concentration and the properties as well as the content of iron (II) salt in the solution, which increases as the pickling progresses. The corrosion rate depends also on the amount of carbon contained in the steel although the chemical composition is always of mayor importance for the corrosion speed. The scale structure consists of three layers as represented in **figure 6**[35].

The scale consists of an extremely thin layer of hematite Fe_2O_3 (iron (III) oxide), an intermediate layer of magnetite Fe_3O_4 (iron (II, III) oxide) and an inner layer of wustite FeO (iron (II) oxide), which lies directly on top of the bulk material. Normally a defined border in between the layers cannot be observed. The scale originally is formed from the oxidation of iron. The volume of the formed scale is larger than the volume of the original metal, as the scale is porous and highly brittle.

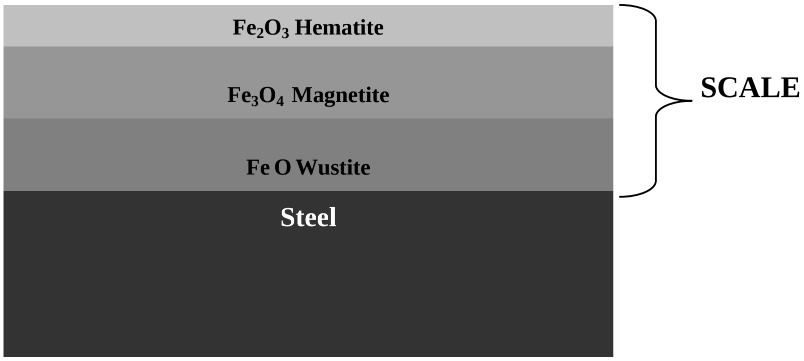

Figure 6. Scale structure

---

* according to EN 10 020 (system for classifying the types of steel as issued by the International Standards Organization (ISO) and the European Committee for Iron and Steel Standards (ECISS))

When the ferrous oxides are dissolved in the acid, ferrous salts and water are formed. The formation of H_2 is not insignificant. Most of the H_2 gas escapes to the atmosphere but part of it will be captured by the steel and can lead to a formation of defects in the finished products (embrittlement).

Pickling reactions include two simultaneous processes, namely a dissolution of the metallic iron and the dissolution of the rust, during the following reactions:

- In H_2SO_4:

Dissolution of hematite: $Fe_2O_3 + Fe + 3\ H_2SO_4 \longleftrightarrow 3\ FeSO_4 + 3\ H_2O$ **(7)**

Dissolution of magnetite: $Fe_3O_4 + Fe + 4\ H_2SO_4 \longleftrightarrow 4\ FeSO_4 + 4\ H_2O$ **(8)**

Dissolution of wustite: $FeO + H_2SO_4 \longleftrightarrow FeSO_4 + H_2O$ **(9)**

Dissolution of bulk iron: $Fe + H_2SO_4 \longleftrightarrow FeSO_4 + H_2$ **(10)**

- In HCl:

Dissolution of hematite: $Fe_2O_3 + Fe + 3\ HCl \longleftrightarrow 3\ FeCl_2 + 3\ H_2O$ **(11)**

Dissolution of magnetite: $Fe_2O_3 + Fe + 8\ HCl \longleftrightarrow 4\ FeCl_2 + 4\ H_2O$ **(12)**

Dissolution of wustite: $FeO + 2\ HCl \longleftrightarrow FeCl_2 + H_2O$ **(13)**

Dissolution of bulk iron: $Fe + 2\ HCl \longleftrightarrow FeCl_2 + H_2$ **(14)**

The dissolution process and the hydrogen recombination can be described with the:

- $Fe_{steel} \longrightarrow Fe^{2+}_{dis} + 2e^-$ **(15)**
- $2\ Fe^{3+}_{ox} + 2e^- \longrightarrow Fe^{2+}_{dis}$ **(16)**
- $2\ H^+_{dis} + 2e^- \longrightarrow 2H_{ad+dis}$ **(17)**
- $2\ H \rightarrow \xrightarrow[\text{Recombination}]{\text{Diffusion}} \rightarrow H_2^{germ}$ **(18)**

- $H_2^{germ} \longrightarrow H_2^{gasbubble}$ **(19)**

The metallic iron dissolves until a critical electron density is reached. Then these electrons are used to reduce the iron oxide covering the steel, by which the scale dissolves and the protons in the solution recombine on the steel surface to form hydrogen gas and to be released[36].

From the three oxides composing the oxide scale wustite is the not soluble one and an optimus surface is achieved when the rolling conditions lead to a scale with large amounts of this oxide. Hematite turns out to be the oxide with the lowest solubility in H_2SO_4[37].

The pickling time decreases when the free iron surface increases until a minimun is reached: in the case of H_2SO_4 it is at about 2 % and for HCl at about 15 %. This is not the only difference in pickling with the two acids as they have different mechanisms and the pickling with the H_2SO_4 is more aggressive than with HCl[38].

Pickling can be seen as a process consisting of electrochemical acid dissolution of steel and chemical reduction of the ferrous oxides by atomic hydrogen, with a subsequent dissolution of the metals in acid.

It is important to take into account the diffusion of hydrogen into metal during the acid pickling. The penetration of hydrogen into metals occurs when the metal dissolution is accompanied by hydrogen evolution and is known to lead to hydrogen occlusion or pick-up. The process depends on the metal properties, temperature and pressure and it is highly influenced by adsorption phenomena occurring on the metallic surface. This process process leads to a high damage and deterioration of the mechanical properties of the material, known as hydrogen-brittlement or pickling-brittlement. It has been shown to diminish at higher temperatures. It is due to the reduction of hydrogen ions coming from the electrolyte to the metallic surface, where they recombine to form diatomic hydrogen which escapes under the form of bubbles. A retardation of the formation of molecular hydrogen may take place for any reason and this would lead to the penetration of the hydrogen ions into the metal and its adsorption on it. Any form of the hydrogen is capable to be adsorbed by the metallic surface as it is contains enough electrons to convert the atoms in molecules. A part of these atoms dissolves into the steel, diffusing through the crystal lattice and deforming it. The problem is that the recombination of atoms to hydrogen molecules not only takes place at the steel surface but that it also can occur in internal micropores of the metal (microcavities) which leads to an accumulation of hydrogen in these microcavities, and causes lattice brittleness. The pressure into the lattice can reach high values which causes high internal strain. When the cavities of the metal are small the hydrogen formed can find an easy way to escape but if they are large its removal is more difficult. It is known that atomic hydrogen has more facilities to diffuse through the metal than molecular hydrogen, because the diffusion rate is proportional to the surface area of the metal on which it is occluded. As a result of this hydrogen pick up blisters may be formed on the surface metal, which considerably reduces the efficiency of the pickling process in terms of the quality of the finished products. The diffusion rate of hydrogen through the metal increases linearly with the concentration of the acid and it is much higher in H_2SO_4 than in HCl. It can also be observed that the effect of hydrogen brittlement is much more noticeable in the case of strong acids (like H_2SO_4 or HCl) than in the case weak ones (H_3PO_4 or acetic acid). Considering the effect of the temperature on this phenomenon two processes have to be taken into account: at higher temperatures the dissolution of metal considerably increases and also the total quantity of hydrogen produced does. On the other hand at higher temperatures the conversion of atomic hydrogen into molecular hydrogen increases. The H_2 molecules have lower diffusion rate into the metallic lattice but forms bubbles to escape from the solution. The overall result is a decrease of the metal damage in the case of HCl as compare with other acids.

Electrolytic pickling is one variant of this process, which is mainly used in the stainless steel production. It is used as a pre-treatment for the acid descaling to speed up the removal of oxide layers. This process is highly advantageous as it is environmentally friendly, provides fast pickling rates, reduces over pickling, allows a control of the pickling velocity by adjusting the current and has low maintenance and operating costs. Normally this pickling is carried out in neutral electrolytes, which turns out to be one of its main disadvantages, as the indirect polarization method gives very poor current efficiencies (30 %) and this step limits the speed in pickling and annealing lines[39].

2.1.5.4 Pickling inhibitors

According to the ISO norm **8044**:1999 a corrosion inhibitor can be defined as a chemical substance that effectively decreases the corrosion rates, when added in small concentration to an environment without having the concentration of the corrosive agent unchanged

One concrete example of corrosion inhibitors are those used in the pickling baths and known as pickling inhibitors. They are used in order to avoid the metal dissolution due to the corrosiveness and aggressiveness of the acid solutions in pickling baths limiting the acid consumption (and so they prolong the effectiveness of the pickling bath) and also to reduce fumes and spray production due to hydrogen formation.

Pickling inhibitors have been used since the middle ages to protect the steel during the scale removal and, to prevent a corrosive attack on the metallic material. At the beginning some oils, vegetable or animal extracts where used. Later synthetic additives were used and some other inorganics discovered. The best inhibitive results were achieved by mixtures. These mixtures are characterized by the synergic effect of their components: the protective power of the mixture usually is higher than the sum of protection when inhibitors are used separately. In many cases these inhibitive mixtures inlcude not only the inhibitors but also so-called pickling additives, like foaming agents. They should allow the formation of a foam layer on top of the pickling baths, which avoids the formation and escape of fumes. This clearly improves the working conditions in the plants. Also the addition of halide ions to inhibitory mixtures is known to retard the corrosive effect. One proposed mechanism for this bases on the interaction of the halide ion with the metal surface, which changes its charge and increasing its negative potential favouring the adsorption of the inhibitors on the metal surface.

Organic S^{2-} also act as corrosion inhibitors for metals in acids and for example SO_4^{2-} do in the same way in HCl solutions[40].

The action of the inhibitors has been found to be selective. Inhibitors retard the dissolution of metallic iron but the rate of dissolution of the scale or other compounds present like carbonates remains unchanged. The action of inhibitors affects only the reaction that takes place between the acid and the metal. However, an inhibitor which is very effective in protecting the metallic surface in one type of acid can be highly ineffective in the case of another acid. This is the case e.g. for amines, which are shown to be highly effective corrosion retardants in HCl while their effectiveness in H_2SO_4 is much lower. Further aldehydes are poor corrosion inhibitors in H_2SO_4 and sulphur containing compounds like thioureas have a higher effectiveness in H_2SO_4 than in HCl[40]. It can be said that the effectiveness of inhibitors greatly depends on the particular process that takes place and on the specific conditions used. Decisive factors to be taken into account when selecting the best inhibitor for a process are the kind of acid used and its concentration, the temperature, the flow rate, the presence of large or small amounts of organic or inorganic substances and the composition of the metallic phase.

Pickling inhibitors must fulfil several requirements in order to be effective under severe conditions. The protective effects of these compounds must be remained in the aggressive pickling environment and their efficiency has to be high also in the presence of large amounts of iron salts, which are know to stimulate the pickling attack onto the metallic surface. The properties required can be summarized as follows:

- effective inhibition of metal dissolution,
- no overpickling in the presence of higher iron salt contents,
- no delay of the pickling process,
- effective at low concentrations,
- effective at higher temperatures,
- thermally and chemically stable,
- effective inhibition of hydrogen up-take by the metal,
- good surfactant characteristics,
- good foaming characteristics

To fulfil all these requirements for the prevention of metal dissolution, mostly mixtures of inhibitors must be used. Substances such as wetting agents, detergents and foaming components are added to these commercial mixtures as the properties of inhibitors in this respect often are poor. Wetting agents normally facilitate the scale to flake off as the penetration of the acid in cracks or fissures is enhanced but their inhibitive effect is normally very poor or absent. These agents and detergents mostly help to clean the surface and therefore make the adsorption of the real inhibitor compounds to the surface easier so that a synergic effect is obtained with the commercially available mixtures. They also help the acids to drain off the surface and to rinse them from the pickled components. The foaming agents fulfil also two functions: they form a foam layer which eliminates much of the steam released by the solution and it therefore avoids health hazards for the workers and helps in heat preservation. These additives must be stable within a wide range of temperatures and salt and acid concentrations. Due to the large requirements to the properties, which can not be fulfilled by one single substance, several compounds are added to the inhibiting commercially available mixtures in order to achieve a good inhibitive action. Normally they are made up of active inhibitory substances, wetting and foaming agents and detergents and normally a solvent and a co-solvent if necessary. Normally the active substances are nitrogen-containing compounds, acetylenic alcohols and sulphur-containing compounds and for their easy application these commercially available formulas are normally sold in solution. Their efficiency is usually expressed in percentage of protection but the absolute corrosion rates (in $g\ m^{-2}\ h^{-1}$ or mm/y) should be mentioned in any case[40, 41].

A general mechanism for the inhibition can not be given although some steps seem to be followed by all these chemical compounds. The general pickling inhibitors form a protective layer on the metal surface. Many investigations explain the interaction of the inhibitors with the metal like a physical adsorption. Therefore it is very easy to cause desorption by bringing the metal with the formed layer in a medium without inhibitor. The formed film of the inhibitor on top of the steel surface is almost inert to the acidic environment. This film not only protects the metal to be dissolved but in many cases directly influences the hydrogen brittlement, even though the inhibitors do not diminish the dissolution rate of the metal and the diffusion rate of hydrogen into the metallic lattice. Strong inhibitors, however, have been found to have such an effect on both processes.

It is not necessary to cover the total surface to realize a good inhibition and it even has been observed that the addition of large amounts of inhibitor in the corrosive medium may lead to higher corrosion rates.

Ionic adsorption depends on the charge and the magnitude of the surface charge at the metal-electrolyte interface. When pickling the metal surface is charged negatively with respect to the solution which favours the adsorption of positively charged colloidal particles. Accordingly, the dissolution of iron in pickling baths is slowed down in the presence of amines or large heterocyclic compounds which form cations[40].

The protective power of inhibitors can be expressed by an empirical equation, which is very similar to the Freundlich[*] equation:

$$z = ac^{b} \qquad \textbf{(20)}$$

z is the protective power of the inhibitor and can be also calculated from the following equation: $(\rho_0-\rho)/\rho_0$, where ρ_0 is the corrosion rate in the medium without inhibitor and ρ the rate in the presence of the inhibitor; c is the concentration of the inhibitor in the acid and *a* and *b* are empirical constants depending on the inhibitor used.

The mechanism of the inhibitors relates to two processes. The primary process would be the adsorption and formation of the protective layer by the metal, the inhibitor and the ions present in the medium and the second process comprises all electrochemical phenomena (cathodic and anodic polarization, changes in the hydrogen overvoltage, resistance at the metal electrolyte interface,…) depending on the characteristics of the film formed.

The activity of inhibitors can be explained by a mechanism in which inhibitors adsorb on both anodic and cathodic parts of the material increasing the hydrogen overpotential and the potential of the oxidation of iron in the anode.

The action of inhibitors by the suppression of anodic, cathodic or both electrochemical reactions can be studied by polarization measurements (see **section 2.2.3**) and their effectiveness evaluated by electrochemical impedance spectroscopy (**section 2.2.4**). For example, a high ohmnic resistance has been found at the interface electrode-electrolyte in the case of inhibitors where the formed film is easily visible.

Inhibitors can be classified based on their chemical composition and structures, and their chemical or electrochemical behaviour. The classification based on their structure is quite useful but it must be taken into account that many known inhibitory substances act only as protective substances due to a structural transformation taking place in the corrosive medium. An inhibitor substance often only is the starting material for building up the real inhibitor. The most extended classification in the literature referrs to the retardation of the electrochemical reactions, which characterize most of the corrosion processes. According to that classification

---

[*] The Freundlich isotherm is one of the first equations proposed to relate the quantity of adsorbed substance to its concentration in the solution[42-44].

inhibitors can be anodic, cathodic or mixed, depending on which reaction is slowed down: the anodic, the cathodic or both simultaneously. It is not possible anyway to establish a sharp border between anodic and cathodic inhibitors as most corrosion inhibitors affect more or less both of them.

Anodic inhibitors include oxidizing inorganic anions (as chromate or nitrite) which can form ionic bonds with the surface to protect it from the acid attack. They move the potential into a noble region, where the passive film (either the one they formed or an intrinsic one) is stable. Those inhibitors may not be so useful in the case of steels where the corrosion rate of iron, even though it is passivated, is quite high. Other anodic inhibitors require oxygen to be effective. It is important to ensure that the concentration of such compounds is high enough, as a deficiency can cause pitting corrosion[40].

Cathodic inhibition takes place at surface deposits where the cathodic reactions are avoided. An important example is the reduction of dissolution of oxygen. A deficiency in the concentrations of cathodic inhibitors does not lead to excessive pitting corrosion, as in the case of the anodic inhibitors but normally the last ones are better surface protectors. In the case of cathodic inhibitors the corrosion rate decreases with their increasing concentration.

One very commonly used kind of cathodic inhibitors is the organic species. Their effectiveness depends on the alloy used and several factors influence their activity. The latter is improved by the presence of polar groups containing for example sulphur (e.g. thioamides), nitrogen (e.g. amines) or hydroxyl groups which can attach to the metal surface. Also the presence of longer chains, asymmetry, a larger molecular weight, a higher electron density and the presence of benzene rings may play a role. The number of organic compounds that can be used as pickling inhibitors is large and they have complex structures. Some examples are given in **figure 7**.

Compounds containing sulphur, such as mercaptans and derivatives are highly effective inhibitors in H_2SO_4 solutions. Most common in pickling processes is the use of thioureas and some of their derivatives, which lead to a great retarding of the corrosion rate at low concentrations. Thiourea partially decomposes to hydrogen sulphide which even in small amount favours the hydrogen diffusion through the steel lattice[40]. The decomposition can release health hazardous compounds which can attack the eyes. Hydrogen sulphide acts differently to other inhibitors and normally lowers their action or in some cases enhances it. It also affects the hydrogen uptake.

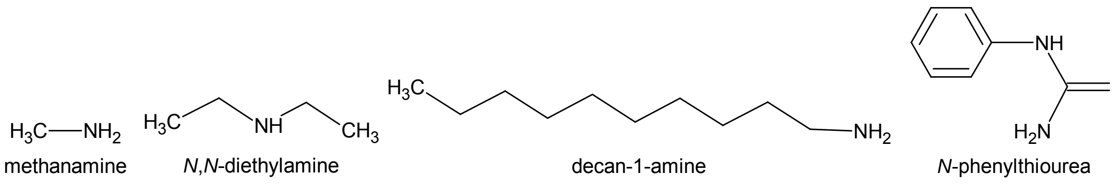

Figure 7.-Some organic compounds used as pickling inhibitors.

Further halide ions are highly effective in this medium. Of chloride, bromide and iodide, iodide is the most effective one followed by bromide and chloride. No inhibitory effect is observed when fluoride ion is used. Also aldehydes have been reported to be weak inhibitors in H_2SO_4 solution. N-containing compounds have an optimum effect in HCl solutions and are quite useless in H_2SO_4, unless certain anions, like halides (except F^-) and pseudo-halides are present to promote a synergistic effect which increases in the sequence $Cl^- < Br^- < I^-$. They are widely used in inhibitor formulations. This effect is also observed with acetylenic alcohols, where higher concentrations are required than for HCl when no halide or pseudo halide ion is present in H_2SO_4.

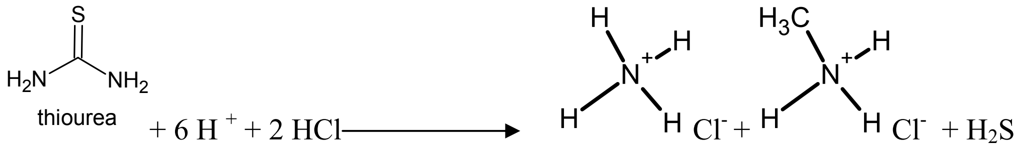

Figure 8. Decomposition of thiourea in acid solutions[40].

Many inhibitors for ferrous metal corrosion used in H_2SO_4 can be also used in HCl: amines, aldehydes and sulphur containing compounds. In HCl nitrogen-containing compounds and aldehydes have a stronger inhibitory power than in H_2SO_4 and they have the highest inhibitory effect among all inhibitors. The protective effect of amines increases with their molecular weight. Among aldehydes, formaldehyde has the highest efficiency. Hexamine, which is a compound obtained by the reaction of formaldehyde with ammonia (**Figure 9**), is a common cheap inhibitor used in HCl.

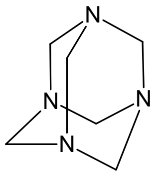

Hexamine

Figure 9. 1,3,5,7-tetraayatrcicyclo[3.3.1.1^{3,7}]decane, one of the most frequently used compounds to inhibit metallic corrosion in HCl.

N-containing compounds are normally accompanied by derivatives of acetylene, for example acetylenic alcohols of general formula $R^1\text{-C}\equiv\text{C-}(CH_2)_m\text{-}CR^2R^3\text{-OH}$ which have excellent characteristic in terms of efficiency at temperatures up to 100°C[25, 27, 29, 40, 41].

2.1.5.4.1 Pickling inhibitors studied

The inhibitor which is currently used at the pickling plants, ADACID VP1140, is a commercial product which is used mainly to prevent the corrosion of steel in the pickling baths. It can be used both in HCl and H_2SO_4.

This commercial formula is made of several components, listed in **table 2**.

Formula	**IUPAC name**	**Abbreviation**
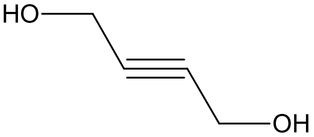	but-2-yne-1,4-diol	BD
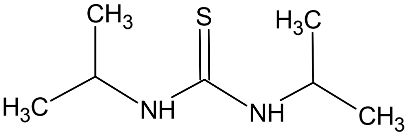	*N*,*N*'-diisopropylthiourea	DITU
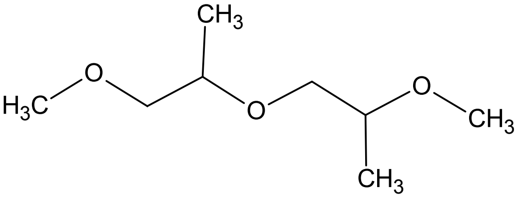	2-methoxy-1-(2-methoxy-1-methylethoxy)propane	DPGDME
KI	Potassium iodide	KI
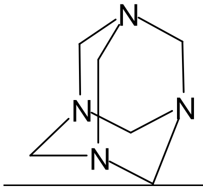	1,3,5,7-tetraazatricyclo[3.3.1.1]^{3,7} decane	Hexamine

Table 2. Individual components constituting the commercially available inhibitor ADACID VP1140.

The commercially available inhibitor ADACID VP1140 is given the abbreviation CI.

The individual components were also studied by means of several methods (*section 2.2*) in order to evaluate their individual activity as corrosion inhibitors.

Furthermore, three analogues of DITU have been used also in this study in order to evaluate the influence that the lateral chain of the molecules has on the inhibitor activity (**table 3**).

Formula	IUPAC name	Abbreviation
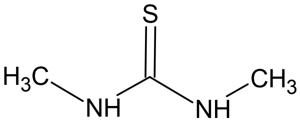	*N*,*N'*-dimethylthiourea	DMTU
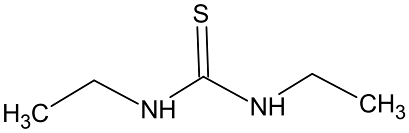	*N*,*N'*-diethylthiourea	DETU
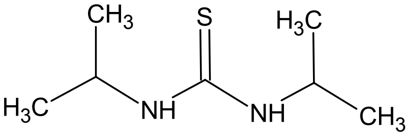	*N*,*N'*-diisopropylthiourea	DITU
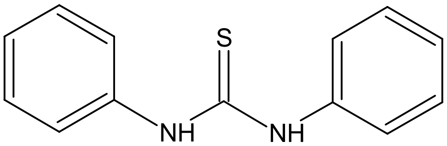	*N*,*N'*-diphenylthiourea	DPTU

Table 3.-Thiourea series used to determine the influence of the lateral chain in the corrosion inhibition, molecule of DPGMME is an analogue DPGDME and KBr an analogue of KI.

2.1.5.4.1.1 Chemical and Physical Properties

In **tables 4** and **5** [45-51] the main characteristics of the compounds mentioned in **tables 2** and **3** are described.

Parameter	KI	DPGDME	Hexamine	BD	DITU
Empirical formula	KI	$C_8H_{18}O_3$	$C_6H_{12}N_4$	$C_4H_6O_2$	$C_5H_{12}N_2S$
Molecular weight/(g/l)	166.00	162.23	140.19	86.09	160
Boiling point/°C	1330	175	-	238	200
Melting point/°C	680	-	280	58	68-78
Density	3.1300	-	-	1.1	1.0
Molar solubility from pH=1 to pH=10	-	-	-	very soluble	soluble at pH=1 and slightly soluble at all others
pK_a	-	-	-	12.7±0.1	13.9±0.7
pK_b	-	-	-	-	1.5±0.5

Table 4. Chemical and physical properties of inhibitors in **table 2**.

Parameter	DPTU	DETU	DMTU
Empirical formula	$C_{13}H_{12}N_2S$	$C_5H_{12}N_2S$	$C_3H_8N_2S$
Molecular weight/(g/l)	228.32	132.23	104.18
Boiling point/°C	-	169	122
Melting point/°C	150-153	75-78	58-62
Density	1.320	0.99	1.03
Molar solubility from pH=1 to pH=10	-	very soluble at pH=1 and soluble at all others	very soluble
pK_a	-	14.5±0.7	15.0±0.7
pK_b	-	2.1±0.5	1.6±0.5

Table 5. Chemical and physical properties of inhibitors in **table 3**.

2.1.5.4.1.2 Applications and inhibitive behaviour

A brief description of some characteristics and behaviour as corrosion inhibitors for a number of compounds belonging to the same chemical family or structurally analogues is given next:

- *KI→ I^- (effective inhibitor)*: The effect of the iodide ion on the corrosion of Fe in H_2SO_4 solutions was studied by means of electrochemical measurements. It was found to be an inhibitor of the corrosion reaction as the presence of KI in a pure H_2SO_4 solution reduces the corrosion potential E_{corr} and the corrosion current density I_{corr} regarding the non inhibited reaction. By means of corrosion measurements it was determined to be a synergistic substance which promotes the inhibitive effect of other compounds such as thiourea. This is explained by the change that ion adsorption induces in the potential and of the surface which determinates the adsorption of molecules. The addition of KI decreases i_{corr} is as compared to the value when it is absent in the thiourea solution, while E_{corr} is slightly changed about 5 mV towards a more negative value. The effect of I^- is explained by *Ammar* and *Darwish*[52] to be a consequence of its deformability and its capacity of forming surface compounds by covalent linkages. Its desorption is known to be promoted by O_2 when dipping the electrode in an inhibitor free solution[53]. A study made by *Murakawa et. al.* [54] on the differencial capacity as a function of the electrode potential when adding I^- in the treatment of iron in $HClO_4$ solution showed a suppression of peaks attributed to adsorption of HO^-, ClO_4^- or the precursor of hydrogen evolution and leads to the conclusion of a low reversible adsorption. This study also indicates the existence of a corrosion retardation as a consequence of the adsorption of the ions on the steel surface. A chemisorption on the steel surface is found also in this case but tis is non-reversible adsorption. This study also mentions that a competitive adsorption takes place when two kinds of ions are present. *Rawat* and *Udayabhanu*[55] also found that I^- has a synergistic effect and promotes the effect of an organic substance as protector of mild steel in dilute sulphuric acid. While other halides where found to act as corrosion promoters, the presence of I^- at certain concentrations reduced the corrosion rate. This synergistic effect was explained in terms of co- and overlap adsorptions of I^- and the inhibitor molecules or cations. In contrast to these findings, they also found that a high halide concentration increases the corrosion rate as explained by the following reactions:

$Fe + X^-_{(aq)} \leftrightarrow (FeX^-)_{(ad)}$ **(20)**

$(FeX^-)_{(ad)} + H_2O \leftrightarrow (FeOH^-)_{(ad)} + H^+ + X^-$ **(21)**

$(FeOH^-_{ad}) \rightarrow (Fe\ OH)_{ad} + e^-$ **(22)**

$(Fe\ OH)_{ad} \rightarrow (Fe\ OH)^+ + e^-$ **(23)**

$(Fe\ OH)^+ \leftrightarrow Fe_2{}^+_{(aq)} + OH^-$ **(24)**

$OH^- + H^+ \leftrightarrow H_2O$ **(25)**

The speed controlling step is the first reaction. This means that the reaction depends on the halide ion concentration. It is known that the lower the concentration of $(FeOH^-)_{(ad)}$, the better the halide anion adsorbs on the surface. The adsorption of anions is found to be higher for the halide ions Br^- and I^- than for Cl^-. There are two main effects which are important for the protection of the surface by the halides[55]:

- The deformability of the anion: this property promotes the displacement of other adsorbed species. When the deformability is large enough surface compounds can be formed and this enables inhibition. This property increases in the order: $Cl^- < Br^- < I^-$.
- The corrosion process is enhanced by the formation of soluble metal complexes. The ability of the anion to form these complexes will determine their protection grade.

I^- can form surface compounds while Cl^- is known not to have this ability. When the adsorption is strong enough to avoid the desorption showed in the above reaction scheme proposed by *Rawat* and *Udayabhanu*[55], inhibition takes place.

In the same study the synergistic effect of I^- with benzyl amine was studied and an increase in the inhibitive effect in presence of this halide was found. This is explained by a joint adsorption of I^- ions and inhibitor cations or molecules. A reversible chemisorption of the I^- ions is proposed in contrast to the work of *Murakawa et al.*[53], where a non reversible adsorption was proposed. The halide ion would enter the metallic part of the double layer and a stable covalent I^--metal bond would be formed. The charge of the metallic surface is modified by the adsorption of the I^- ions and therefore the cations will be attracted more to the surface.

The high efficiency of I^- is explained by its larger ionic size, the strong adsorption due to the easy polarizability of its electron shells and the possible formation of a surface layer with the amine on the metal.

- *DPGDME*: this compound is an esterified dimer of propylene glycol (**figure 10**).

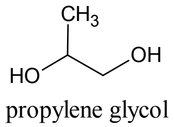

Figure 10. Structure of propylene glycol.

They can be structurally related to ethylene glycol (**figure 11B**) which polymerizes to polyethylene glycol (PEG, **figure 11B**). This is known to be a corrosion inhibitor of steel in acidic environment. *Ashassi-Sorkhabi et al.*[56] studied different PEG polymers, which are water-soluble and contain atoms which are known to have an effect on the protection of corrosion by adsorption (oxygen), as a function of their mean molecular weight and their concentration in HCl. The studies by means of polarization curves in HCl revealed a positive shift of the corrosion potential in the presence of the different PEGs. This means that the anodic process is much more affected by these compounds than the cathodic one and therefore they can be considered to be anodic inhibitors.

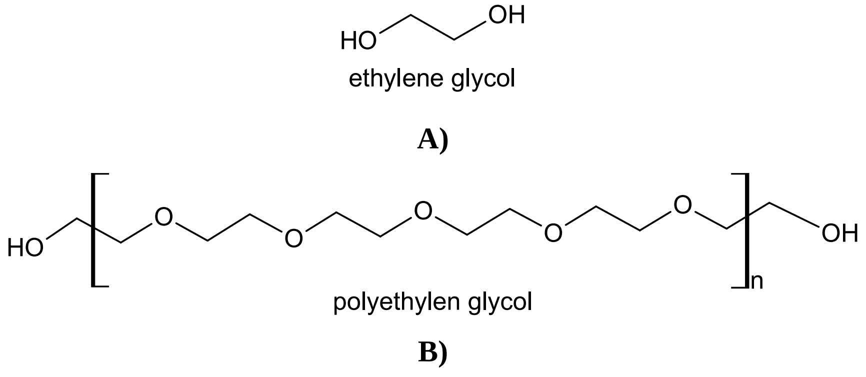

Figure 11.-Structure of **A)**ethylen glycol, **B)** and poly ethylene glycol.

The density of the corrosion current was found to depend on the mean molecular weight of the polymer and on its concentration. Electrochemical impedance spectroscopy measurements lead to the conclusion that a protective layer covering the electrode surface is formed. However one could not distinguish between a solid film, a film of some inhibiting species or both. The behaviour is proposed to depend on the relationship between the degree of coverage and the monomer (or oxygen atoms number). For polymers with lower mean molecular weights an increase in the concentration becomes more effective than in the case of polymers with a high mean molecular weight, which have more oxygen atoms. Another reason might be the shape and size of the molecules. PEG molecules with a number of monomers $n<11$ are zigzag-shaped while those which a number of monomers $n>>11$ are shaped as meanders. The weight loss assays made at T=25°C again showed an increase of the inhibitory efficiency with the concentration and the polymer mean molecular weight, which is due to the higher surface coverage. The latter leads to a higher inhibitory efficiency. The obtained values for this parameter from the different methods used are comparable within the three cases. The adsorption of an organic molecule on a metal/solution interface is described by these authors as a substitution of the adsorbed water molecules on the metallic surface $H_2O_{(ads)}$:

$$Org_{(sol)} + x\ H_2O_{(ads)} \leftrightarrow Org_{(ads)} + x\ H_2O_{(sol)} \qquad \textbf{(26)}$$

$Org_{(sol)}$: organic molecule in solution, $H_2O_{(sol)}$: water molecule in solution, $Org_{(ads)}$: adsorbed organic molecule and $H_2O_{(ads)}$: adsorbed water molecule. x is the size ratio representing the number of water molecule replaced by one molecule of organic adsorbate.

In this study it was shown that the mentioned molecules adsorb at the interface according to the Langmuir adsorption model and by a study of the isotherms obtained it could be concluded that no interaction between the adsorbed molecules takes place.

From this study it was concluded that the effectiveness of different PEGs in HCl depends on their concentration and molecular weight according to a Langmuir model[56].

The structure of the polymers has been found to have an influence on their inhibitory activity[57]. In H_2SO_4, polarization curves have shown thin compounds to behave as anodic inhibitors. The corrosion current density was shown to depend on the molecular weight of the polymer as well as on the kind of acid used. Remarkable is that a dependence on the mean molecular weight can shown in HCl but that the effectiveness of the inhibitors is independent on the mean molecular weight in H_2SO_4[57]. An explanation could lie in the formation of metal-polymer complexes until all active sites of the specimens are covered. Then a protective layer is supposed to cover the surface of the electrode. Experiments at high temperatures showed that the corrosion rates increase with the temperature and the efficiency of the low molecular weight polymers was shown to decrease with the temperature. This behaviour might be related to the weakness of the polymer adsorption onto the metallic surface at higher temperatures and suggests the existence of physisorption. At the tested conditions the carbon steel surface becomes negatively charged (rich in electrons) and an interaction with a positively charged species would be possible. It would be possible that the molecules could be placed on the surface in such a way that the $-CH_2-CH_2-O-$ groups are oriented towards the surface with the carbon atoms, which constitute the positive part of the dipole and then the oxygen atoms would be oriented towards the solution.

Ethylene glycol was used as a co-solvent to determine the corrosive effect of Cl^- ions for the case of magnesium alloys and a protective effect on the material could be observed[58]. Ethoxylates [$R-O-(CH_2-CH_2-O)_nH$, $n=C_{10}-C_{18}$] are also known to be surface active compounds (wetting agents, detergents and foaming agents) and are preferred over the ionic compounds when the precipitation of iron salts is not desired[40, 59].

Mircheva and Tabakova[60] also studied the use of multi-block polymers of ethylene glycol (EG) and propylene glycol (PG), which are suitable wetting agents in pickling processes. Polymers normally have advantages as compared to molecules with a low molecular weight such as a lower toxicity, lower volatility, chemical stability in acidic environments at high temperatures, and an easy elimination from the sewage.

PEG and the three block polymers composed of PEG and polypropylenglycol which is a non-toxic, non-ionisable surface active substance, are added to the inhibitive commercially available mixtures used in pickling and acidic cleaning baths as surfactants. They act as surface active compounds and help to wet the products and to make it easier to remove the oxide scale. The three block polymer PEG-PPG work in water in an analogous way as the classic non-ionisable tensides (**figure 12**). Micelles with a hydrophilic crown are made out of the block of ethylene glycol and a hydrophobic nucleus is made of propylene glycol blocks[61]. The molecular mass of the polymers again could be shown to influence the grade of surface protection.

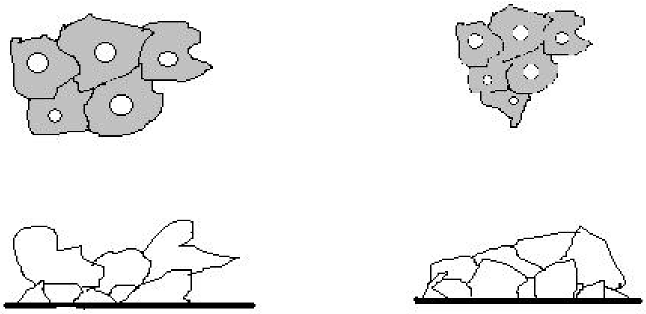

Figure 12. Adsorption model proposed for the three-block and multi-block polymers (top and lateral views).

- <u>HMTA</u>: (also known as urotropin) was mentioned as pickling inhibitor in *section 2.1.5.4*. It is an effective inhibitor in the prevention of steel corrosion in HCl baths, as many other nitrogen-containing compounds are. When using this substance, precautions for health hazards must be taking because of its slow decomposition in HCl (**figure 13**), to small amounts of chloromethyl ether and bischloromethyl ether which are volatile and highly carcinogenic products.

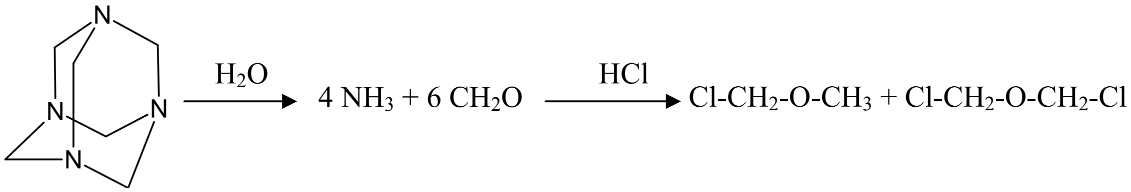

Figure 13. Decomposition of HMTA to carcinogenic chloromethyl and bischloromethyl ethers.

HMTA is used for the removal of acid-soluble sulphide-containing scales from metal surfaces in industrial plants (like refineries). The cleaning solutions consist of a 14 % HCl solution containing 33-37 g/l of HMTA. It is known that at 65°C sulphide scales are decomposed under the evolution of H_2S, which is trapped by the formaldehyde produced by the thermal decomposition of HMTA.

N-containing inhibitors are frequently accompanied in the commercially available products by acetylenic derivatives with the formula $R\text{-}C{\equiv}C\text{-}(CH_2)_m\text{-}CR^2R^3\text{-}OH$. The synergistic effects of HMTA and potassium iodide (see *KI section*) when added to 4-phenoxy-butyn-1-ol (**figure 14**) are well known[40, 59].

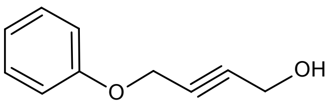

Figure 14. Structure of 4-phenoxy-but-2-yn-1-ol.

A study carried out by *Hackerman and McCafferty*[62] on the mechanism of the adsorption and corrosion inhibition with flexible organic diamines in HCl, which up to now was never studied, showed that they can adsorb at the metal/solution interface in different ways. In the vertical position only one of the two end-groups are adsorbed with the hydrocarbon chain perpendicular to the surface and in the flat position when both end-groups are adsorbed with the hydrocarbon chain parallel to the surface. If the molecule is long enough to be flexible, the hydrocarbon chain can be buckled between both adsorbed end groups (**figure 15**).

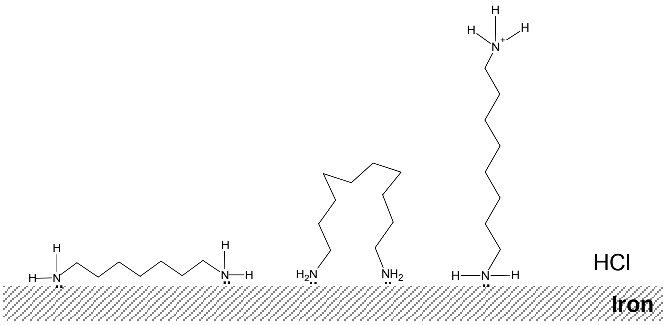

Figure 15. Possible adsorption for poliamines with different length chain.

The effect of the amines can be explained on the base of their pK_a values. The larger the pK_a value, the higher the basicity and hence more effective electron donors which would justify the inhibitory power. The larger the lateral chain, the larger pK_a value as long as the solubility is comparable. This would explain the experimentally found better inhibition of propylenediamine as compared to ethylenediamine[62].

Already in the late twenties amine compounds were known as corrosion inhibitors. *Pirak* and *Wenzel*[63] in their work referred to several amines and heterocycles as protectors of iron in an acidic environment.

- *BD*: BD is an acetylenic (**figure 16**) derivative with two terminal alcohol groups and is an important pickling inhibitor (see *section 2.1.5.4*). It is a useful synthetic intermediate as it is a precursor in the synthesis of oxacyclopentane (or tetrahydrofurane, **figure 16**) being one of the most used solvents for Grignard reactions or organolitics[64].

The use of acetylenic compounds as effective corrosion inhibitors was discovered in the mid-1940 but the detailed study of their properties would start in the following decade[65].

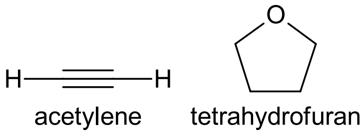

Figure 16. Structures of acetylene (ethyne) and tetrahydrofuran.

Acetylene derivatives can be used with N-containing compounds in order to promote their action in HCl solutions. Different studies proved that propargyl alcohol, 1-hexyn-3-ol and 1-iodo-3-methyl-1-butyn-3-ol are the most effective hydroxyl acetylenes in this medium.

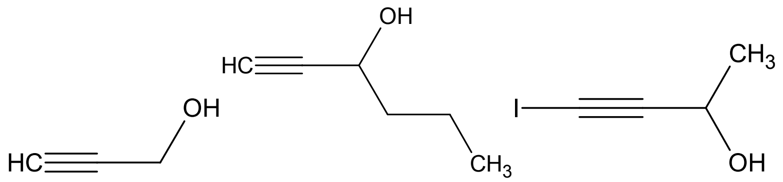

prop-2-yn-1-ol hex-1-yn-3-ol 4-iodobut-3-yn-2-ol

Figure 17. Structures of propargyl alcohol (prop-2-yn-1-ol), 1-hexyn-3-ol (hex-1-yn-3-ol) and 1-iodo-3-methyl-1-butyn-3-ol (4-iodo-3-yn-2-ol).

Acetylenic alcohols have been proved to have protective effects in H_2SO_4 as well but their efficiency is less than in HCl. In H_2SO_4 an enormous synergistic effect with halide ions occurs. These compounds have and, especially 1-hexyn-3-ol (**figure 17**), are valuable inhibitors at high temperatures. Their efficiency is excellent at temperatures up to 100°C and therefore they are normally added to commercially available formulas to be used in acids at high temperatures. Propargyl ethers are also known to give good results for the protection of metallic surfaces from acidic mediums. The stability of propargyl compounds can be explained by the catalysis of a Fe-complex in the formation of protective polymer films which is favoured at higher temperatures[40, 59].

The mechanism of the inhibitors of acetylenic alcohols in the corrosion of iron in acid solutions was described by *Bockris et al.*[66] Their model includes the effect of a competitive adsorption of water dipoles and organic molecules. The dissolution of iron takes place according to the mechanism described in *section 2.1.5.3.1.* In the regions where the organic molecule is adsorbed, a consecutive transfer of electrons in which no more than one is involved in each step occurs and the rate determining step would be the first electron transfer. When the concentration of the acetylenic alcohol studied increased in the solution, it could be shown that the orientation of the adsorbed molecule changed from flat to partly upright and finally to upright after which by a continuously growing multilayer polymer film is formed (**figure 18**).

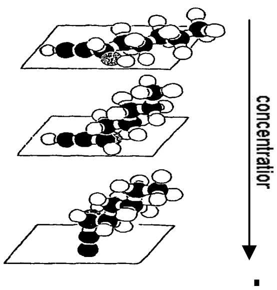

Figure 18. Orientation of the acetylenic alcohol molecules as a function of the concentration[66].

The speed of the process increases with the temperature and a upright position is reached inside the film during the “layer by layer” growing of the film[66].

A study has been made by *Growcock et al.*[65] on the inhibitive effect of 1-octyn-3-ol for steel (**figure 19**) in a HCl environment.

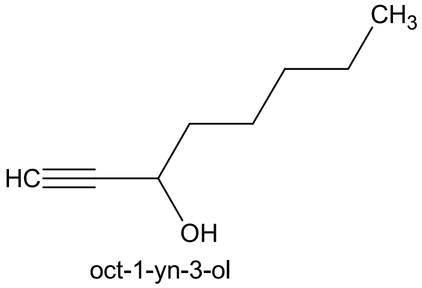

Figure 19. Structure of 1-octyn-3-ol.

These authors proposed a three-step mechanism involving an activation of the inhibitor followed by an adsorption according to Langmuir and oligomerization[65]:

Octynol + H_3O^+ ↔ P (P =activated product of octynol with HCl) **(27)**

$Fe[Cl^-][H_2O] + P \leftrightarrow Fe[Cl^-][P] + H_2O$ **(28)**

$Fe[Cl^-][P]$ + x octynol → $Fe[Cl^-][P][Film]$ (film formation) **(29)**

Alternatively a combined step for reactions **(27)** and **(28)** where adsorption and oligomerization may occur in the same step also is proposed:

$Fe[Cl^-][H_2O]$ + j octynol ↔ $Fe[Cl^-][octynol]_j + H_2O$ **(30)**

In the work of *Utaka et al.*[67] a transformation of BD in the easily polymerizable intermediate hydroxymethyl vinyl ketone (**figure 20**) has been proposed.

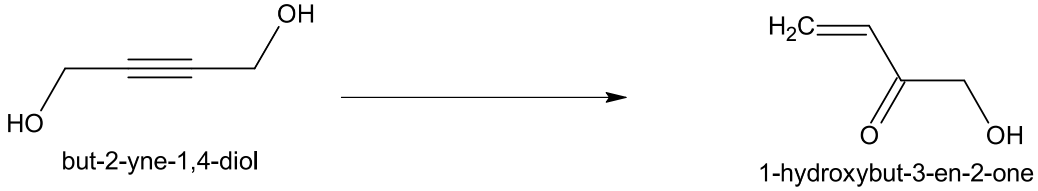

Figure 20. Polymerization of BD through the conversion into a easily polymerizable hydryomethyl vinyl ketone (1-hydroxybut-3-en-2-one).

However *Tedeschi et al.*[68] have proposed an alternative mechanism. They argue that the polymers derived from 1-hydroxybut-3-en-2-one or any other product obtained by the reaction of BD in acid environment have no effect as inhibitors. They postulate an interaction of the acetylenic compounds with the iron surface as shown in **figure 21**.

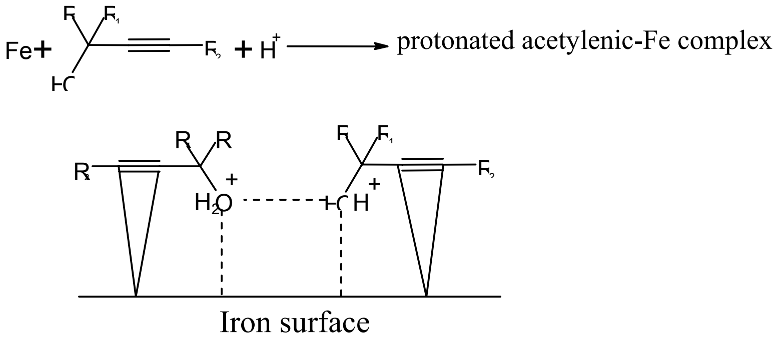

Figure 21. Reactions of alkynol in strongly acidic medium.

This kind of interaction explains the effectiveness of the acetylenic compounds in preventing an oxidation of iron to the ferrous ion in the anodic zones.

The synergistic effect observed among alkynols and amines can be explained by the formation of hydrogen bonded complexes. Amines can be present (in HCl) as amine hydrochloride or bonded with alkynols and the metallic surface. The dominant bonding forces are supposed to lead to the formation of a complex together with the triple bond-metal attraction and must be compared to the amine-metal attraction. Polyamines give better results than mono-amines because of their superior polarity and therefore they are more effective as a result of the stronger attractive forces in the multilayer (**figure 22**). This multilayer (**figure 23**) can be explained to be an inhibitor barrier because of its two main characteristics: site charge inhibition and film forming inhibition.

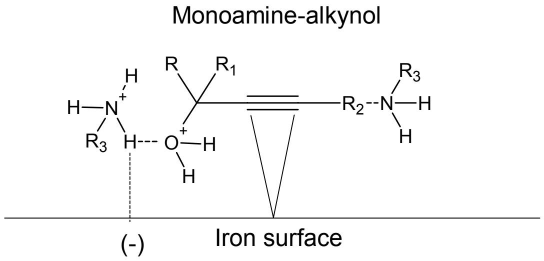

Figure 22. Interactions of a monoamine in the presence of an alkynol with an iron surface.

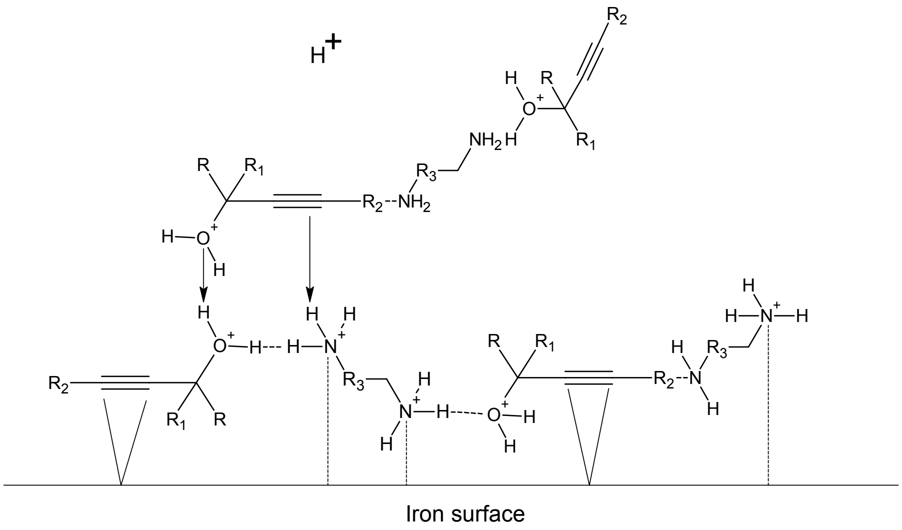

Figure 23. Formation of a multilayer by the interaction of alkynols and amines

The addition of surfactants to such mixtures improves the solubilization of less soluble components, the contact of the molecules with the surface and the formation of hydrogen bonds in the barrier[68, 69.]

The use of hydroxyethyled 2-Butine-1,4-diol (HEBD) (**figure 24**) as corrosion inhibitor was studied by *Mircheva and Tabakova*[60]. This compound was proved to be an inhibitor by its direct addition to a corrosive solution.

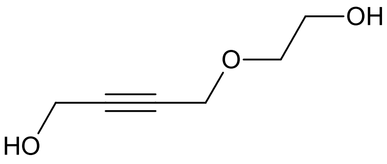

4-(2-hydroxyethoxy)but-2-yn-1-ol

Figure 24. Structure of hydroxyethyled 2-Butin-1,4-diol (4-(2-hydroxyethoxy)but-2-yn-1-ol).

- <u>*DMTU, DETU, DITU, DPTU*</u>: *Hoar and Holliday*[70] made an study about the inhibitive power of thioureas and quinolines on the acidic dissolution of mild steel. They have proved that thiourea and some of its derivatives, such as methylthiourea, ethylthiourea and *o*-, *m*- and *p*-tolylthiourea (see **figure 25**) inhibit the steel dissolution in sulphuric acid. These molecules are shown to be increasingly effective in the order given above. The obtained results are interpreted by the authors on the base of a modified adsorption theory.

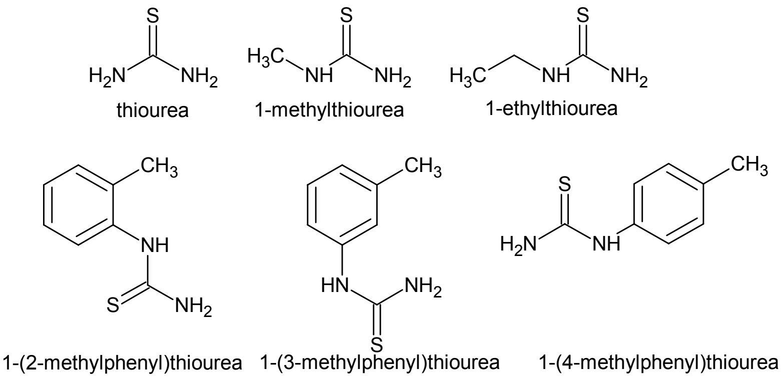

thiourea 1-methylthiourea 1-ethylthiourea

1-(2-methylphenyl)thiourea 1-(3-methylphenyl)thiourea 1-(4-methylphenyl)thiourea

Figure 25. Chemical structure of the thioureas studied by *Hoar and Holliday*[70]. [1-(2-methylphenyl)thiourea = *o*-tolylthiourea; 1-(3-methylphenyl)thiourea = *m*-tolylthiourea; 1-(2-methylphenyl)thiourea = *p*-tolylthiourea]

Thioureas are much more effective as inhibitors than quinoline or its derivatives. This is due to the fact that the group 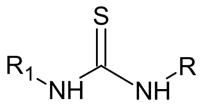 more strongly is adsorbed onto the steel surface than the :N-R group of the quinolines. Both thioureas and quinolines show a better inhibitory effect with increasing molecular weight and hydrocarbon chains in the molecule. This improvement of the inhibitory effect is due to an enlargement of the non-polar part of the molecule and consequently related with an increase of its molecular weight and of its thermal stability and spatial block properties. These characteristic increase the time between adsorption and desorption and allows the molecules to stay longer at the metallic surface and to enlarge the covered area during this time. In this work it is assumed that inhibitors adsorb as a monolayer onto the steel surface and randomly cover an homogeneous part of the metal. This allows it to treat the data according to a Langmuir adsorption model. The behaviour of *o*-tolyl-thiourea was found to be contradictory as its inhibitory efficiency decreased at lower temperatures. This fact was explained on the basis of the large time required to reach the adsorption equilibrium because of two possible factors: the non-negligible adsorption activation energy or the difficult diffusion of the molecules through the solution due to their fairly large size. A modification of the commonly accepted adsorption theory therefore was proposed in order to explain the obtained results. It is suggested that the adsorption of the molecules to a different extend depends on the nature of the surfaces and therefore a different influence in the anodic and cathodic processes is found. It is also suggested that results with molecules with the same adsorbable group correlate as it is the case with substituted thioureas. The adsorbability of the molecules at any of the existent anodic or cathodic sites, which vary in importance and number depending on the type of iron and steel, is supposed to depend on factors such as the size, shape, dipole moment and deformability of the surface-active group, and the hydrocarbon part of the molecule is thought to determine its quantitative behaviour. Experiments show how both kind of molecules, quinolines and thioureas, are far less effective inhibitors for pure iron in 5 % (w/v) H_2SO_4 at 70°C than they are for steel. This fact strongly suggests that the inhibition is due to the blockage of the anodic sulphur-activated sites which are not present in pure iron. It was also observed that thiourea and ethylthiourea molecules accelerated the corrosion reaction in pure iron which is explained on the base of a creation of sulphur-activated sites by these molecules, which are not present in pure iron but are already present in steel as a result of the sulphur impurities of the alloy. This lowest accelerating effect of thioureas is easily overcome just by avoiding lower concentrations. When an inhibitor is adsorbed to either an anodic or a cathodic site one avoids both the dissolution of bulk iron and the evolution of hydrogen. Therefore the adsorption of the inhibitor can be related to a decrease in the number of active sites or in the free electrode area, leaving fewer sites where the corrosion reaction can take place. Nevertheless, it is possible that sites adjacent to those where the molecules are adsorbed can be influenced and therefore no exact and quantitative equation can be established due. The explanation for the predominance of anodic inhibition is a function of the free space between the adsorbed molecules. When a monolayer covers the largest part of the surface, only small gaps remain due to the irregularity of the packing and here it is easier to enter and discharge H_3O^+ than to form of $Fe\cdot xH_2O^{++}$ from $Fe^{++}_{lattice}$ and xH_2O which would need bigger gaps.

As it was explained in *section 2.1.5.4*, it is essential that an inhibitor retains its inhibitive properties under the conditions at which it will be used. In this case it means that molecules should be specifically adsorbed in acidic conditions but should not interfere with the action of the acid or anything else. The functional group in the thioureas, (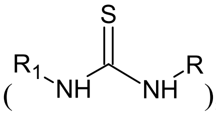), seems to be strongly adsorbed when corroding steel and even stronger under cathodic conditions. These molecules since long have been used for the protection of iron or steel subjected to pickling and are known to be good inhibitors. Other substances containing similar functional groups are thought to give similar results. As it is expected, the activity of the inhibitors changes with the temperature and they are more effective at 70° than at 40°C[70].

Kaesche[71] reported on the inhibitive behaviour of phenylthiourea (PTU, **figure 26**) in the case of sodium perchlorate ($NaClO_4$). In this work an inhibitive effect of this molecule both in anodic and cathodic reactions was shown to exist.

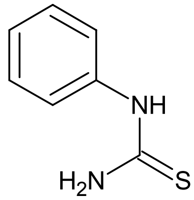

1-phenylthiourea

Figure 26. Chemical structure of phenylthiourea.

Studies made by *Sykut and Saba*[72] showed that thiourea is an effective inhibitor for the corrosion of iron in H_2SO_4 solutions. The adsorptive behaviour of this inhibitor can be described with a Frumkin isotherm accepting lateral repulsion. The adsorption was found to take place with the molecule placed vertically and through the S atom. As in the work of *Hoar and Holliday*[70], thiourea was found to be a mixed type inhibitor. Phenylthiourea was also studied by these authors, and it could be shown to be an effective corrosion inhibitor for mild steel, as a marked decrease in corrosion rates accounting to both partial reactions and a shift of the corrosion potentials to higher values was found.

Thioureas are known as effective pickling inhibitors but their promoting degradation in the pickling process is also known. As it was explained previously, *Hoar and Holliday*[70] proposed the creation of sulphur-activated sites where corrosion would easily take place. There is another theory, supported by *Schmitt*[40,59] or *Frignani et al.*[73], which proposed the decomposition of the molecules releasing H_2S, which promotes hydrogen penetration into the metal and causes hydrogen embrittlement, and N-mustard compounds, which are eye-damaging. The presence of formaldehyde, which could come from the degradation of HMTA; prevents the uptake of hydrogen by the metal in the presence of H_2S[40, 59]. *Frignani et al.*[73] studied the inhibitory behaviour of thioureas on iron in 1M H_2SO_4. They proposed three reasons why the presence of an inhibitor can yield higher corrosion rates in an acidic medium, namely:

- the decomposition products of the inhibitor could act as stimulators,
- the stimulation can occur through preferential paths of partial electrochemical reactions in the corrosion process,
- the inhibitor could directly promote metal dissolution.

Thioureas can be considered as an example of the first case. Here as a result of the descomposition corrosion stimulating products are formed. Other studies on thiourea and its derivatives DMTU, DETU and DITU performed in 5N HCl at 30°C and steel powder showed that these compounds are corrosion accelerators. The effect is explained by the formation of H_2S through a reduction of the thio-compounds (**figure 27**).

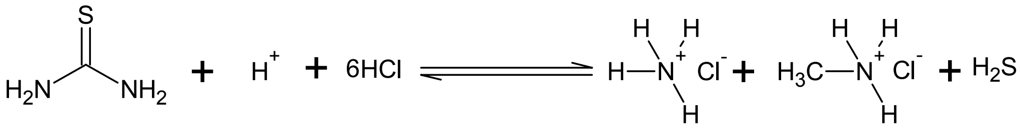

Figure 27. Decomposition of thiourea yielding hydrogen sulphide (H_2S).

The S^{2-} ions present at the interface may facilitate a passing of ferrous ions from the lattice to the solution, probably through the formation of ferrous sulphide as an intermediate which would dissociate in the acid medium yielding S^{2-} ions. The presence of even small amounts of that ion at the interface could greatly increase the corrosion velocity. This effect is also reported for the case of PTU in sodium perchlorate where lower concentrations than the critical one will bring a faster dissolution of iron. Studies with acidified solutions of Na_2SO_4 have shown the formation of pitting corrosion on iron electrodes when PTU is present and this was explained by a deficient surface coverage. This and other mentioned examples are explained on the basis of the decomposition reaction given in **figure 27** where HS^- ions at the interface and amino derivatives are formed. This allows the following postulation: thiourea or thiourea derivatives, or their decomposition products, only act as corrosion inhibitors when a proper relationship between the content of H_2S, the inhibitor and the pH of the environment exists. Nevertheless, it is pointed out that many substances containing the C=S group, such as thioureas, are able to effectively prevent corrosion. However they can stimulate the penetration of hydrogen into the metal lattice and promote an embrittlement of the metal. This is explained by the admission of a reduction of thioureas on the cathodic zones, where H_2S can be liberated and penetrate into the metal[73].

2.2 Methodologies used for the study of the inhibitors and their effect

In this section the different methodologies used for the investigation of inhibitor effects as well as the theoretical models used are briefly described.

2.2.1 *Weight loss measurements.*

A very commonly used method to quantify somehow the effect of the inhibitors is the gravimetry with which the corrosion rate in the presence of an inhibitor (ρ) and in its absence (ρ_0) can be measured. It is important to be careful when carrying out the experiments and interpreting them. A sufficient number of determinations has to be made for ρ and ρ_0 in order to ensure analytical validity of the results. *Putilova*[29] recommends a number of repetitions between three and ten, depending on the reproducibility of the experiments, while *Mercer*[41] "Test Methods for Corrosion Inhibitors", prepared for the European Federation of Corrosion and Working Party on Inhibitors, mentions that at least two but preferably more specimens should be exposed for each set of conditions. The recommendation made in the ASTM norm G: 31-72 is that at least duplicated specimens should be used for each test[74]. It has to be taken into account also that not all metals and alloys respond alike to the many factors that affect corrosion.

The gravimetric method consists of the determination of the loss in weight, $\Delta\rho$, for a sample of which the area after its immersion during a certain time, *t*, in the corrosive medium with certain inhibitor concentration is known. If the reactions generate corrosion products, they should be removed before weighting.

In these immersion tests, the shape of the specimens would be optimal when square or round coupons of a minimal thickness and with a minimal edge surface to total surface ratio and a large surface to mass ratio are used. The experimental conditions will be determined by the purpose of the test, and should be reproducible. The scattering of the results for a couple of specimens should not exceed 10 % of the average, when the attack is uniform. The concentration of chemicals should be given in weight percentage but molarities and molalities can also be useful. Preferentially, only one type of metal should be used for a single test. The temperature of the corrosion solution should be controlled within ±1°C and the time should be adapted to the nature and purpose of the immersion test. The volume of the solution used should follow the ratio of the specimen area of 20 ml/cm^2 or 40 ml/cm^2 to the specimen surface. The supports used to hold the samples in the solution can be of different kinds and materials: glass, ceramic, fluorocarbon, insulated or coated metallic supports.

All data should be reported in detail and all pertinent information as well as all initial and final masses and the mass losses for each specimen should be properly recorded in order to make the experiments traceable [28, 41, 74].

2.2.2 *Electrochemical methods:*

The mechanism and processes occurring during corrosion can be understood from the electrochemical processes taking place. Electrochemical methods are normally used for studies in liquid systems, and less appropriate for studying vapour phase systems[38].

2.2.2.1 Concepts

As it was mentioned previously in *section 2.1.4* corrosion is an electrochemical process as a result of the electron transfer occurring during this chemical reaction.

Indeed, both oxidation and reduction simultaneously take place at a surface. By definition, the oxidation reaction generating electrons take place at the anodic areas (rich in electrons) and the reduction reaction at the cathodic areas (poor in electrons). The basic law in electrochemistry is the maintenance of neutrality by means of an equal rate of anodic and cathodic reactions.

The corrosion of steel in acid solution was explained in *section 2.1.5.2*, will be used as an example. Corrosion takes place because of the behaviour of the system like an electrochemical cell. Both anodic and cathodic areas can be found on the surface of the corroding metal. In **figure 28** it is shown how electrons are produced at the anodic sites, where the oxidation reaction takes place, and flow towards the cathodic areas where the reduction reaction proceeds and where they are consumed.

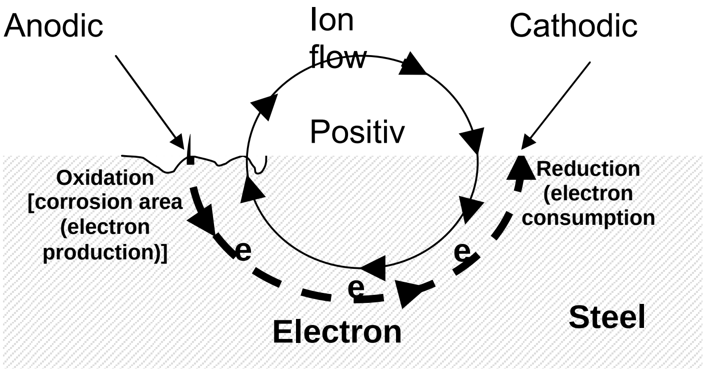

Figure 28. Electrochemical process occurring on a metal corroding in an acid.

The conventional current flows opposite to the electron flow, which goes from the anodic to the cathodic areas. The positive current flows through the electrolyte by ionic conduction completing the circuit in the metal. The potential difference between anodic and cathodic sites is the driving force for the electron movement.

The total number of electrons flowing delivered by the oxidation reaction must be equal to the total number of electrons consumed in the reduction reaction.

The resistance of the cell determine the magnitude of the current at a certain potential. Potential (V), current (A) and resistance (Ω) are the primary controlling parameters in the corrosion cell and constitute the essence of the electrochemical methods, where one or more of those parameters are applied while measuring the other ones.

The measurement of current and potential is of primary interest in corrosion studies due to their direct correlation with the quantity of iron oxidized and of hydrogen ions reduced. The value of the current is a directly relates to the rate of the reaction taking place.

The potentials as driving forces of electrochemical reactions are determined by thermodynamics, while the currents as a measure of the rate of electrochemical processes are governed by kinetics.

- *Thermodynamic principles of corrosion*:

One of the basic thermodynamic principles is that a material always looks for its lowest state of energy, and that an oxidation will take place when it is necessary to reach this state.

The energy of a system can be measured in terms of Gibbs free energy (G). For a spontaneous process like corrosion the change in Gibbs free energy (ΔG) must be negative. For most common metals $\Delta G < 0$ in the natural environment and corrosion is thermodynamically favoured.

The complete corrosion process forms an electrochemical cell, which can be considered as built up by two half cells, in which an oxidation and a reduction, respectively, takes place. These reactions can occur at adjacent places or at widely separated parts of the metal.

The free energy for each of the reactions is related to a reversible electromotive force or electrode potential E through the equation:

$$\Delta G = -|n|FE \tag{31}$$

Here n is the number of electrons exchanged in the reaction and F is the Faraday constant. This formula directly relates the potential E with the driving force ΔG.

- *Kinetic principles of corrosion*:

During the corrosion process current flows between the anodic and the cathodic areas, the potential of the anode increases to more positive (noble) values and the potential of the cathode decreases to more negative (active) values.

Polarization can be defined as the difference of the electrode potential from the corrosion potential as a result of the current. It is measured as over-potential and it is always accompanied by a net current flow.

In metal corrosion one type of very commonly observed polarization is the so-called activation polarization. In this case the rate of corrosion is limited by the electron transfer reaction at the metal surface. This electron transfer has an activation energy which is exponentially related to the free energy change which also is related to the potential. Further the corrosion rate is related to the electrical current and so the relationship becomes:

$$\Delta I \propto e^{\eta / RT} \tag{32}$$

Here I is the corrosion current, R is the gas constant, T the absolute temperature and η the symbol indicating the polarization.

The other type of polarization commonly observed is the concentration polarization, which can be defined as the part of polarization produced by concentration changes resulting from the current through the electrolyte. It is normally associated with the reduction reaction.

The recording of polarization curves can be used to measure the corrosion rate. It provides the corrosion potential, the corrosion rate and the corrosion current.

The corrosion potential (E_{corr}) is defined as “the electrode potential spontaneously acquired by a corroding material in a particular environment” (IUPAC). It can also be defined as the potential for which the rates of oxidative electrochemical processes occurring on the metal surface are balanced by the rates of reductive processes so that the net exchange of electrons equals zero. Indeed, all electrons liberated by the oxidation of the metal must be consumed by the reduction reactions. The corrosion rate (V_{corr}) is the amount of substance transferred per unit time at a specific surface. The use of Faraday's law allows to obtain the corrosion current (I_{corr}), which is the current flowing at the corrosion potential. Faraday's law has the form:

$$I = nFV \quad \textbf{(33)}$$

Here n is the number of the electrons exchange and F the Faraday constant. When the V_{corr} is used, the I_{corr} is obtained[75].

2.2.2.2 Open circuit potential (OCP)

The open-circuit potential is also called the zero or the rest potential. It is the potential measured when a high impedance voltmeter is placed across an electrolytic cell. A high impedance voltmeter has such a high internal resistance that no appreciable current flows through it during the measurement[76].

The measurement of this magnitude provides information but its use is not completely reliable[75]. The metal ennoblement is indicated by an increase of the OCP. This potential informs on the driving force for the corrosion reaction.

2.2.2.3 Current density – potential or polarization curves

Polarization curves are plots of the current to or from the working electrode surface *vs*. the electrochemical potential of the electrode surface. By varying the potential of the electrode, different oxidation conditions at the electrode surface can be examined. The corresponding current provides a measure for the rate of the reactions at each potential.

The current associated with the equilibrium potential for each reaction is referred to as an exchange current i_0. It is important to remark that the exchange current is highly dependent on the type and nature of the surface where the corrosion is taking place.

The slopes of the anodic and cathodic lines are referred to as Tafel slopes. In general, the anodic and cathodic Tafel slopes are different.

Evans diagrams or polarization diagrams are obtained by plotting the variation of the potential (Y axis) against the logarithm of the current response (X axis). The current is plotted with the corresponding sign, namely the cathodic current down and the anodic current up. In some cases it is better to plot both currents as positive[4, 27, 38, 41, 77].

2.2.2.4 Electrochemical impedance spectroscopy (EIS)[7, 50, 51]

This is an electrochemical technique where the impedance of the cell or of the electrode is plotted *versus* the frequency. During the measurements the system is perturbed with an alternating current (ac) and the response observed. The measurements are made over a wide range of frequencies, namely from: 10^{-1} to 10^6 Hz.

The impedance, *Z*, is defined by the IUPAC in its Compendium of Chemical Terminology as the complex representation of a potential difference divided by the complex representation of the current[21].

To facilitate the understanding of the concept, the impedance (Z) can be said to be the ac analogue of the direct current (dc) resistance. For a dc system the resistance is related to the current and the voltage by means of Ohm's law: V=IR.V is the voltage over the resistor, I is the current and R is the resistance in ohms. For ac signals it would be translated into V=IZ. Here Z is the impedance of the circuit and the impedance depends on the frequency of the signal applied.

In this method one applies an ac signal to an electrode, in this case to a corroding metal and measures the response. The perturbing signal normally is a small voltage and the measured response is the current obtained. The results are processed in dependence on time in such a manner that the impedance is obtained as a function of the frequency which delivers an impedance spectrum. The complexity of such spectra is due to the amount of parameters collected for different frequencies. Indeed, the impedance is defined by two terms depending on the output current and the input voltage, namely the amplitude of the ac current signal is divided by the amplitude of the ac voltage and the phase angle, which is proportional to the shift in time between the current peak and the voltage peaks. Sometimes these two terms are represented as real and imaginary parts of the impedance. When an ac signal is applied the behaviour of the system is much more complicated that a simple resistor.

From these spectra the low-frequency polarization resistance, which is comparable to the value obtained by dc methods, is obtained. The advantages of this method over the traditional dc methods are the following:

- Possibility to correct the polarization resistance for high solution resistances or to determine the corrosion rates in highly resistive systems like oils, painted surfaces metalbars placed in concrete.
- Possibility to examine complex corroding systems as those found in multi-phase alloys, non-aqueous solutions, fused salts and inhibited systems.

- In many cases the corrosion rates can be calculated by the use of graphical analysis based on equivalent circuits. The rates obtained in this way are highly accurate.
- The recording of the whole spectra gives confidence about the limit value of the impedance obtained for low frequencies. It also can help to choose the correct values for the coefficients which help to determine the corrosion rate from the corrosion resistance.

The polarization resistance can be determined after a subtraction of the solution polarization, but the determination of all other parameters requires some data processing. The polarization resistance can be used to obtain more confident information on the corrosion rate.

There are two kinds of data presentation: the Nyquist diagrams and the Bode plots. In Nyquist or complex plane plots one plots the imaginary part of the impedance Z'' (in corrosion studies it is conventional to plot –Z'') against the real part Z'. In Bode plots one plots impedance parameters against frequency. Most commonly one plots the logarithm of the absolute value of the impedance *versus* the logarithm of the frequency, which includes all the information obtained. By modifying these plots, information on the capacitances can be obtained when the logarithm of Z' and of Z'' are plotted against the frequency.

With this method it is possible to obtain information on parameters such as charge transfer resistance even for systems exhibiting mixed diffusion-charge transfer control and to study adsorption effects[53].

2.2.2.4.1 Simulation of equivalent circuits for the EIS data

When an ac current is applied to a corroding system in solution, its behaviour is more complicated than that in a single resistor. Besides polarization resistance (R_p, the total resistance of the system) there is a capacitance coming from the separation of the charges on the surface due to the double layer, C_{dl} (capacitance of the double layer in Faradays) and the resistance of the solution, R_s (resistance of the solution in Ω). The combination of capacitors, resistors, inductors and various forms of distributed impedances, giving the same electrical response at all frequencies, as the original corrosion cell, results in a so-called equivalent electrical circuit. The application of an alternating current allows the identification of each single electrical component by an interpretation of the impedance spectrum. At high frequencies the solution resistance can be identified while at low frequencies other processes like diffusion or adsorption/desorption can be studied. Numerical values for the capacitors and the resistors can be obtained. This approach can be useful for estimating the corrosion rate. Equivalent circuits are useful in the interpretation of the data obtained from the impedance diagrams, an enable a better understanding of impedance spectroscopy. The selection of an appropriate circuit is important for a correct interpretation of the data.

The circuit described here (**figure 29**) is the simplest one and it is present in all corroding systems in solution.

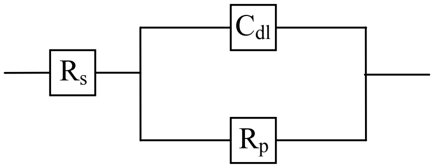

Figure 29. Representation of a single equivalent circuit for the corrosion of a metal in solution

The fact that C_{dl} and R_p are in parallel responds to the fact that current can either flow through the interface provoking the oxidation or reduction of species and the charging or discharging of the capacitance. R_p can be considered to be a Faraday impedance, which includes also the Warburg impedance. The Warburg impedance represents the part of the resistance related to mass transfer. When the process is controlled by an electron transfer process, the Warburg impedance can be neglected. For a circuit as drawn in **figure 29** systems with the Bode impedance and the phase shift diagram of **figure 30** are obtained.

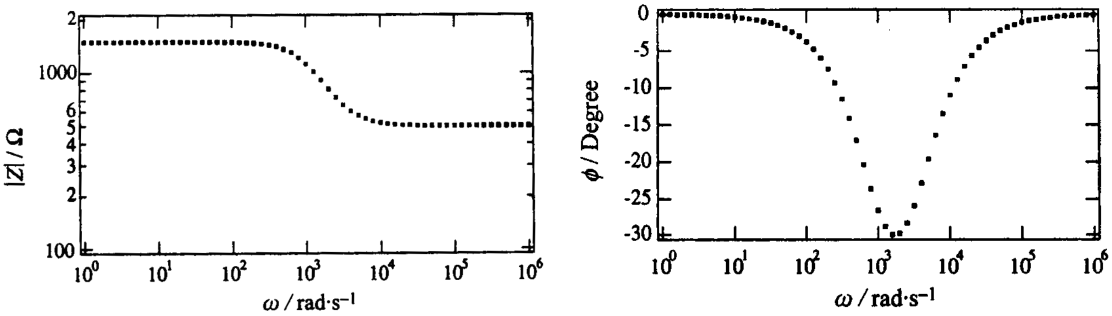

Figure 30. Bode impedance and phase shift diagrams represented by the equivalent circuit represented in **figure 29**.

There are almost an infinite number of equivalent circuits that are able to accurately reproduce the response of a given corrosion system at all frequencies and not all of them are suitable to interpret the data. An equivalent circuit must be explainable from a physical point of view. The values calculated from the electrical circuit can provide information either about the corrosion rate or the corrosion mechanism. The diagrams proposed in **figure 31** are normally used for coated metals.

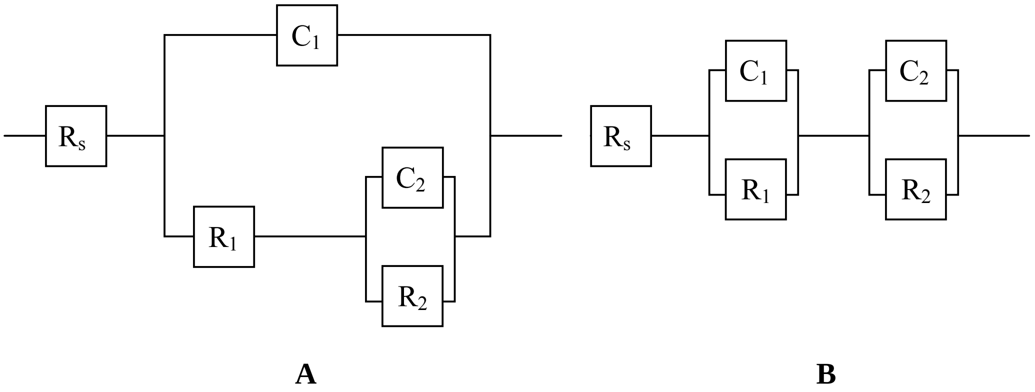

Figure 31. Circuits used to describe coated metals.

One of the RC pairs relates to the corrosion process and the other one to the coating.
Some other circuits are described in the literature when an intermediate or an electro-active species is adsorbed on the electrode surface. An example is given in **figure 32**.

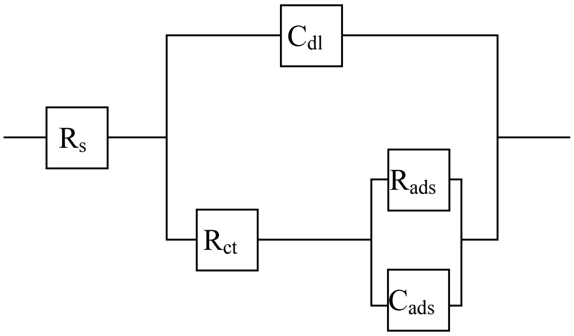

Figure 32. Electric circuit for an intermediate or electroactive species adsorbed as a monolayer on the electrode surface.

R_{ct} represents the resistance to the charge transfer, R_{ads} and C_{ADS} are components relating to the surface coverage (concentration) contribution of the adsorbed intermediate[8, 78-80].

2.2.3 Chemical methods

2.2.3.1 Infrared reflection absorption spectroscopy (IRRAS)[81-86]

This is a method to study the adsorption of substances (ultra thing layer or coatings as adsorbates) on a metal surface. The infrared radiation is reflected by the surface instead of transmitted through the sample.

Infrared radiationg can be resolved into p- and s- polarised components. The oscillation of the electric vector is parallel to the plane of the incidence in the case of p- polarised radiation and perpendicular to the plane of incidence in the case of the s- polarised radiation, as shown in **figure 33**.

(a)

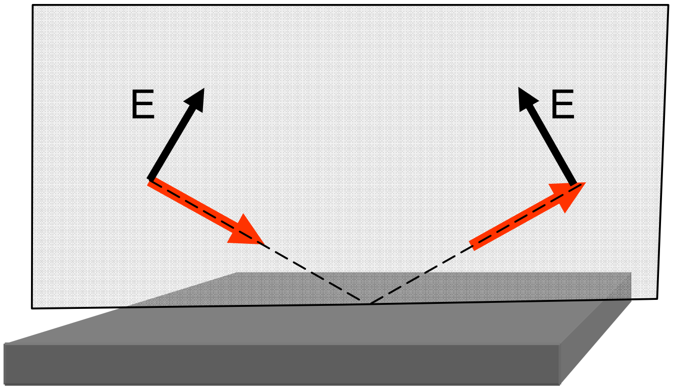

b)

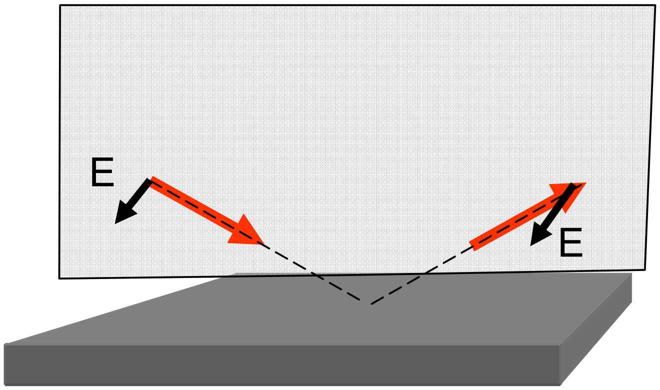

Figure 33. Behavior of the field in the case of polarized radiation. With radiation **p-polarized** **(a)** the electric field lies in the plane formed by incident and the reflected waves and has a component perpendicular to the surface and a component parallel to the surface With **s-polarized** radiation **(b)** the electric field is perpendicular to the plane formed by the incident and the reflected waves and parallel to the surface plane.

The sensitivity of this technique is very high, facilitating the investigation of very thin films like those formed by molecules adsorbed from a gaseous phase or by organic monolayers deposited onto the metal surface.

It is possible to obtain quantitative information from IRRAS spectra when the film is thin enough in comparison to the wavelength of the incident IR radiation.

In this work the infrared reflection absorption spectroscopy was used to detect a formed layer of organic compounds on the surface of the steel after the coupon was immersed in a dissolution containing the organics.

2.2.3.2 X-ray photoelectron spectroscopy (XPS)[87, 88]

X-ray photoelectron spectroscopy is a method used for surface analysis and it is also known for historical reasons as electron spectroscopy for chemical analysis (ESCA). In this method the surface is irradiated with mono-energetic x-rays and the emitted electron beam produced by the incident radiation is analysed (**figure 34**). This type of spectroscopy is useful for the identification of all elements of the periodic table with the exception of hydrogen and helium. Besides information on the chemical composition of a sample, XPS also allows on the identification of the oxidation state of the elements and of the type of bonding. Accordingly it provides useful information on the electronic structure of the molecules. It is normally applied to solids and recently it has also been successfully used for solutions and liquids. Both quantitative and qualitative information can be obtained.

The X-ray source used normally emits Mg Kα (1253.6 eV) or Al Kα (1486.6 eV) radiation. The photoelectrons normally come from a layer of 1 to 10 μm and information about the first atomic layers in solids is obtained.

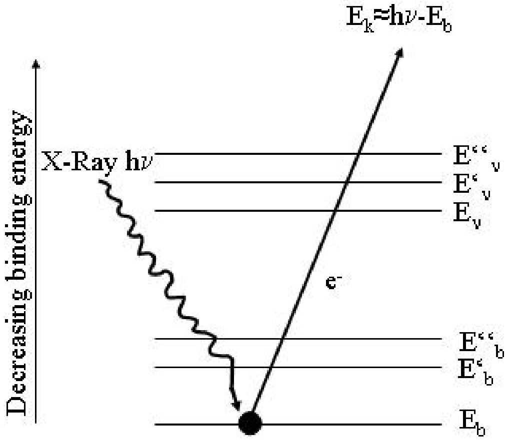

Figure 34. Principle of XPS.

X-ray photoelectron spectroscopy in this work was used for identifying the bonds of the formed layer of determined organics on the steel surface after the coupon was immersed in a solution containing the desired compound.

2.2.3.3 Glow discharge optical emission spectroscopy (GDOES)[89, 90]

Glow discharge optical emission spectroscopy is a method which provides information on the bulk composition of solids and on the distribution of elements within its surface, in coatings or at interfaces. Any solid material allowing the vacuum conditions can be analyzed by means of this method, which is extremely rapid and sensitive. Both sputtering processes and atomic emission are important to deliver the desired information.

When an anode and a cathode (normally the material to be analyzed) are separate in a vacuum chamber, a carrier gas (usually Argon) is admitted in the tube and a potential difference is applied across the plates, a glow discharge can occur. This is the case when the pressure of the gas and the potential difference reach suitable values depending on the gas used and the cathode material. The plasma is generated with dark and bright bands between the anode and the cathode. The plasma contains ionised argon atoms, which are accelerated towards the surface of the sample and sputter material form the cathode. This sputtered material enters an area in the plasma where it is excited and yields atomic emission. The emitted are spectrally isolated and by measuring the lines intensities with an attached spectrometer, quantitative and qualitative analyses of the surface are possible. Since the atomic layers are sputtered one after another a depth profile with a resolution between 0.1 μm and 100 μm can be obtained.

In this work glow discharge optical emission spectroscopy was used to characterize the steels.

2.2.3.4 Secondary sputtered neutral mass spectroscopy (SNMS)[91-93]

When high energetic primary particles like electrons, photons, ions or neutral atoms impact on a surface (generally solid) particles can be emitted, normally neutral species (atoms or molecules), atomic clusters or ions. 95% of the sputtered particles are neutral and the residual ones are ionized. When detecting the ions the method is called secondary ion mass spectroscopy (SIMS). The SIMS method has suffers from severe matrix effects, which are almost eliminated in the case of SNMS as a result of decoupling the emission and ionization processes and the determination of the emitted neutrals.

The high energies of the particles normally range from 1 to 15 keV. When they reach the sample a cascade collision takes place. The energy that the incident beam carries is transferred to the molecules on the solid sample, which collides with one another in a kind of billiard-board-hit. Some of the colliding species return to the surface, provoking the emission of particles of the surface. The emitted secondary particles have a low energy (20 eV) and for over 95 % originate from the top two layers of the solid.

The SNMS method is used normally for depth profiling and thin film analyses.

Summarizing, SNMS is a dynamic very common method for in depth profile analysis which provides elemental information of the sample. The best spatial resolution achieved is of the order of 50 μm while the sample depth of the layer studied can be up to 10 μm. A new variant is electron gas secondary neutral mass spectroscopy, which has been recently developed, to increase the common spatial resolution obtainable. The detection limits are better than 1 ppm and it is easy to quantify. SNMS is a quite popular method because the easiness in sample preparation, and use, as well as the extend of data obtained is good and all elements can be determined.

In this work secondary neutral mass spectroscopy was used to follow the compositional changes on the steel surface depending on the pickling time and the nature of pickling acid.

2.2.3.5 Time-of-flight secondary ion mass spectrometry (TOF-SIMS)[94-97]

Time-of-flight secondary ion mass spectrometry combines the analytical method SIMS with time of flight mass analysis. In SIMS, the sample is bombarded with packets of electrons, primary ions or laser generated photons under ultra high vacuum conditions ($< 10^{-7}$ bar). These pulses have normally a frequency ranging from 10 to 50 kHz and a duration of 0.25 μs. This incident beam is used to desorb and ionize species from the surface of a sample, which are accelerated by an electric field to a time-of-flight mass spectrometer. The electric field is pulsed at the same frequency but with a delay with respect to the ionization pulse. The accelerated particles enter a field free drift tube which is approximately 1 meter in length. In the ideally case all particles have the same kinetic energy when they enter the tube whereas their velocity will vary depending on their masses. Accordingly, the light particles will arrive earlier at the detector than the heavier ones. On the base of their flight time the ions can be separated according to their masses. Typical flight times are between 1 and 30 μs.

Summarizing, TOF-SIMS is a tool for the characterization of the chemical composition, for imaging and for determining the distribution of chemical species, and for depth profiling as well as for thin film characterization.

In this work the time-of-flight secondary ion mass spectroscopy was used to confirm, from detected fragments, the presence of a formed layer of determined organics on the steel surface after the immersion of the sample in a solution containing the organic compounds.

2.2.4 *Topographical studies:*

2.2.4.1 Scanning electron microscopy (SEM)[100-102]

This is a type of microscopy used for surface characterization. An image is obtained by scanning the surface with a beam of energetic electrons which generates various types of signals when focused on a solid surface. The emissions of backscattered and secondary electrons are used for imaging the surface.

The main characteristics of SEM are:

- great versatility of its various modus of imaging,
- excellent spatial resolution,
- poor requirements to sample preparation and conditions,
- direct interpretation of the obtained images is possible,
- associated spectroscopy and diffraction techniques are accessible
- a high level of automation and high throughput can be realized.

The primary beam of electrons used in SEM is obtained by thermionic emission of a tungsten or lanthanum hexaboride cathode. Through a system of lenses these electrons, are accelerated to energies ranging from hundreds of eV to 50 keV, focused on the surface in a very fine focal spot size of 1 to 5 nm with which a rectangular area of the surface can be rastered. When the primary electrons hit the solid surface they are scattered by the atoms present. They are effectively spread and form teardrop shaped volumes advancing into the material from less than 100 nm to 5 μm depth, producing backscattered and secondary electrons of which the detection allows it to the obtain an image.

In this work scanning electron microscopy was used to characterize the surface of the steel after a treatment in different acids with and without inhibitors for different time periods.

2.2.4.2 Atomic force microscopy (AFM)

In atomic force microscopy a surface is scanned in a raster modus with a force-sensing stylus placed on a cantilever. The forces between the stylus and the surface provoke deflections on the cantilever which are detected and measured optically [93, 100, 102, 103]. The function of the instrument is shown in **figure 35**. A piezoelectric piece is used to obtain topographical information, resulting from the upwards and downstairs motions caused by the fact that the force between the stylus and the surface is held constant.

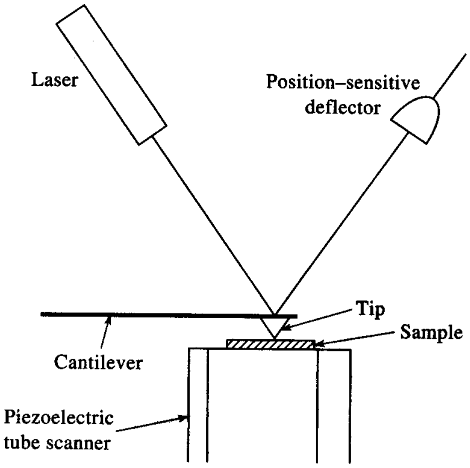

Figure 35. Principle of AFM.[102]

This technique was used to study the dependence of the topography of the steel surface on the nature of the used acid and the pickling time

2.2.4.3 White light interferometry (WLI)

With this method a three dimensional image of reflecting surfaces from cm^2 to mm^2 is formed. The vertical resolution is of 0.1 nm and the lateral resolution 0.3 to some µm.

In the interferometer the sample is placed on a vibration-damped table to eliminate the vibrations, which are highly inconvenient in topographic measurements. In **figure 36** the principle of the WLI is shown. The light is emitted by a tungsten halogen lamp and is divided by means of a beam splitter into two beams. One of the beams incises on a reference mirror while the other one is projected on the sample surface. Both beams are reflected from their respective surfaces and recombined. The pattern of the formed new beam is studied. The relative position of the sample and the mirror can be changed by means of a piezo actuator.

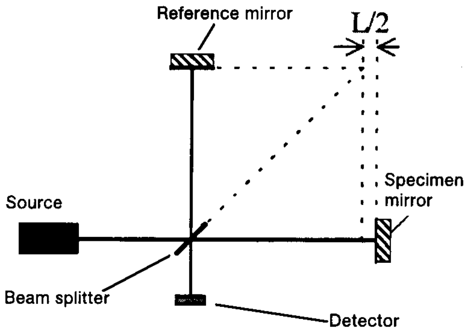

Figure 36. Optical path in a Michelson interferometer.

2.2.5 Theoretical studies

2.2.5.1 Parameters for the measurement of the inhibitive action

The transformation of the data obtained from the experiments is crucial for the evaluation of the inhibitive action. Some of the most used parameters are described below.

The corrosion rate (ρ) is one magnitude normally used to quantify the inhibitive action. It can be expressed in terms of the mass loss:

$$\rho = \frac{\Delta\rho}{tA} \qquad \textbf{(34)}$$

t is the time and A represents the surface area of the sample. Normally the corrosion rates are given in grams per square metre per hour or also by the distance the corrosion penetrates into the metal (mm/year or μ/year).

An evaluation of the inhibitor can be expressed by two ratios: the retardation coefficient or inhibitive effect γ and the protective power of inhibitor efficiency IE:

$$\gamma = \frac{\rho}{\rho_0}, \; IE = \frac{\rho_0 - \rho}{\rho_0} x100\% \qquad \textbf{(35)}$$

The inhibitor efficiency is the percentage decrease of the corrosion rate when the inhibitor is added.

Both quantities γ and IE are related by:

$$\gamma = \frac{100}{100 - IE} \qquad \textbf{(36)}$$

The retardation coefficient and the protective power of inhibitors are closely related to the material composition. In the case of steels, they greatly depend on the carbon content[23, 33].
In this work the efficiency of inhibitors will be calculated also from some other parameters:

$$IE = \frac{M_0 - M}{M_0} x100\% \qquad \textbf{(37)}$$

Here M_0 is the initial value of the parameter, like corrosion rate, corrosion potential or corrosion current density, and M the value of the parameter at the conditions selected.

2.2.5.2 Isotherms

2.2.5.2.1 Langmuir isotherm

This is a model typical for chemisorption. This model assumes that:

- The adsorbed molecules behave as an ideal gas in the vapour phase.
- The molecules adsorb on the surface until they form a complete monolayer (saturation) and then the adsorption ends.
- The surface is homogeneous, uniform (the surface is perfectly flat at the microscopic scale) and therefore all sites are equivalent. The affinity of each binding site for gas molecules is the same, which often is a gross simplification.
- The ability of a molecule to adsorb at a given site is independent of the occupation of neighbouring sites; or in other words there are no lateral interactions between adsorbate molecules.
- The adsorbed gas molecules are localized; they do not move around on the surface.

Most of the assumptions for the Langmuir model are valid for ideal systems. They apply at low pressures in real systems. As the gas pressure approaches the saturation pressure, the vapour condenses. Further the surfaces of most solids are not uniform but heterogeneous, and the desorption rate depends on the location of the adsorbed molecule. The affinity for gas molecules on different crystalline faces is also different, and differences in binding site are introduced by edges, cracks, and crystal imperfections. Heterogeneity leads to a decrease in the binding energy as the surface coverage increases. Further the force between adjacent adsorbed molecules often may be substantial. There is much evidence that adsorbed molecules can move around on the surface. This mobility is much greater for physically adsorbed molecules than for chemisorbed molecules and increases with *T*. In physical adsorption multilayer adsorption is common. In some systems the physisorption is the predominant process at low temperatures, while the chemical adsorption is found at high temperatures.

A deduction of the Langmuir isotherm expression can be made thermodynamically, just by considering the equilibrium between the gas molecules (G), the free superficial centres (S) and the adsorbed molecules (A):

$$\boldsymbol{G + S \leftrightarrow A} \qquad \textbf{(37)}$$

with K_e, equilibrium constant:

$$K_e = [A]/([G][S]) \qquad \textbf{(38)}$$

Taking into account that: $[A]= \theta$, $[S]=1-\theta$ and $[G]=n/V=P/(RT)=aP$, (θ: coverage degree, R: ideal gas constant, T: temperature in K, P: pressure, a: proportionality constant), the following expression is obtained:

$$K_\text{e}=\theta/[(1-\theta)aP] \qquad \textbf{(39)}$$

This expression is the same as the previously deduced one, just making $K=K_\text{e}a$ results in c as equilibrium constant. The formula can be rearranged to:

$$\theta=KP/(1+KP) \qquad \textbf{(40)}$$

This isotherm well describes many systems. However, the experimental points at low pressures are more or less uncertain. The reason then is the hetereogenity of the surface. At the beginning, the molecules will occupy the more active centres, and those which adsorb subsequently (at higher equilibrium pressures) will adsorb onto centres which are less active, with a different K value. In liquid systems the concentration of the adsorbate in the liquid is the parameter used instead of the pressure in the gas systems[21-23,108, 109].

2.2.5.2.2 Frumkin isotherm

This is a more refined form of the Langmuir isotherm. It takes into account the lateral interaction between the adsorbed molecules as well as the linear relation between the free adsorption energy and the degree of coverage. This model takes into consideration the effect of surface heterogeneity and the saturation of the coverage degree. This model is also valid for the case of multilayer adsorption.

The following expression applies:

$$|\Delta G_{ads}| = |\Delta G_{ads}^{0}| + RTg\theta \qquad \textbf{(41)}$$

where $|\Delta G_{ads}|$ is the absolute value of the free adsorption energy, $|\Delta G_{ads}^{0}|$ is the absolute value of the free adsorption energy when the value of θ tends to zero and g is a constant representing the influence of the increasing degree of coverage on the free adsorption energy. It shows that the free adsorption energy would be increasing when attraction is taking place among the lateral chains of the adsorbed molecules and decreasing if a repulsion would take place between the lateral chains of the adsorbed molecules:

- g > 0: there is attraction between the lateral chains of the adsorbed molecules and therefore an increase in the absorption Gibbs energy with θ.
- *g* = 0: there is no interaction between the lateral chains and the model is comparable to the Lanmguir one.
- *g* < 0: there is repulsive interaction between the lateral chains, resulting a decrease of the adsorptive free energy.

For any adsorption process:

$$\Delta G^{0}_{ads} = -RT\ln K \tag{42}$$

where *K* is the adsorption equilibrium constant.

$$K = e^{-\frac{\Delta G^{0}_{ads}}{RT}} \tag{43}$$

Substituting the expression **(41)** into **(43)** the following equations are obtained:

$$K^{'} = e^{\frac{\Delta G^{0}_{ads}+RTg\theta}{RT}} \tag{44}$$

$$K^{'} = e^{\frac{\Delta G^{0}_{ads}}{RT}+g\theta} \tag{45}$$

$$K^{'} = e^{\frac{\Delta G^{0}_{ads}}{RT}}\, e^{g\theta} \tag{46}$$

When combining equations **(43)** and **(46)** a new expression is obtained:

$$K^{'} = Ke^{g\theta} \tag{47}$$

and the of Frumkin isotherm is described by:

$$\frac{\theta}{1-\theta} = K^{'}C \tag{48}$$

$$\frac{\theta}{1-\theta} = Ke^{g\theta}C \tag{49}$$

$$\frac{\theta}{1-\theta}e^{-g\theta} = K\ \ C \tag{50}$$

When plotting $\ln\frac{(\frac{\theta}{1-\theta})}{C}$ *vs*. q a linear function should be obtained, where the ordinate (or angular coefficient) is given by ln *K* and the slope is *g*. As it was mentioned before:

- *g* > 0 describes an attraction between lateral chains

- $g = 0$ describes a case where no interaction with lateral chains of the adsorbed molecules applies and therefore a Langmuir model is found to apply
- $g < 0$ means that repulsion between the lateral chains take place[109].

2.2.5.2.3 Tempkin isotherm

Normally, lateral interactions between adsorbed molecules and heterogeneity occur at real surfaces, which can be accounted for by introducing a coverage-dependent interaction energy term.

It can be considered that the adsorption energies depend on the heterogeneity of the surface. The surface must be considered as made of a distribution of patches. At each of these patches the Langmuir isotherm rules apply independently, with a characteristic local standard free energy for the patch distribution.

Tempkim propose an isotherm based on the supposition of a linear variation of the adsorption enthalpy ΔH_{ads} and the free adsorption energy ΔG_{ads} with the degree of coverage.

$$|\Delta G_{ads}| = |\Delta G_{ads}^{0}| + RTg\theta \qquad \textbf{(60)}$$

Here $|\Delta G_{ads}|$ is the absolute value of the free adsorption energy, $|\Delta G_{ads}^{0}|$ is the absolute value of the free adsorption energy when the value of θ tends to zero. This is the same equation as the one used in the Frumkim model.

The suppositions are based on the formation of more than an adsorbed monolayer. However, the non-availability of the already covered active sites is not taken into account.

When the degree of coverage is low, the model of Temkin applies, which bases on the Henry model:

$$\theta = K^{'}C \qquad \textbf{(61)}$$

Substituting *K*' by *K* $e^{g\theta}$ delivers:

$$\theta = Ke^{g\theta}C \qquad \textbf{(62)}$$

$$\frac{\theta}{e^{g\theta}} = KC \qquad \textbf{(63)}$$

$$\theta e^{-g\theta} = KC \qquad \textbf{(64)}$$

When potting ln (θ/*C*) *vs*. q a linear function should be obtained where g is the slope and ln *K* the intersection. Further, *C* is the inhibitor concentration, *g* the lateral interaction parameter, θ the fraction of the covered surface and *K* the adsorption equilibrium constant[108, 109].

2.2.5.2.4 Flory-Huggins isotherm

In the model of Flory-Huggins one relates the concentration of the adsorbate with the degree of coverage. It is assumed that a molecule of adsorbate displaces a number of solvent molecules adsorbed on the adsorbent surface, while taking into account the relative volumes of the molecules. It can be considered to be a correction of the Langmuir model and can be expressed by the equation:

$$\frac{\theta}{x(1-\theta)^x} = KC \qquad \textbf{(65)}$$

$$\frac{\theta}{C} = Kx(1-\theta)^x \qquad \textbf{(66)}$$

θ is the fraction of the surface covered, C is the concentration of the inhibitory substance, x is the relative size of the adsorbate molecule as compared to the solvent molecules and it gives an idea of the number of solvent molecules displaced by an inhibitor molecule. When $x=1$, the Flory-Huggins model reduces to Langmuir adsorption model.

When plotting $\log(\theta/C)$ *vs*. $\log(1-\theta)$ a linear function should be obtained, where x is the slope and $\log xK$ the intersection.

Which isotherm should be used depends on the experimental systems considered. The application of the adsorption isotherms is useful for understanding the behaviour of corrosion inhibitors in the case of practical applications and technology. However, none of the chemisorption models is entirely satisfactory[108].

3. Experimental description

In this section the experimental details and the conditions used during the measurements and sample preparation with the different methods applied are given.

3.1 Samples preparation

For the polishing of samples cold rolled steel A sheets of 15 mm x 15 mm x 1 mm are used and mechanically polished with silicon carbide paper of diminishing grade: 180, 240, 500, 800. Subsequently, one uses a diamond paste and then a spray of particles with the size of 15, 3 and 1 μm. Finally cleaning is done with water and ethanol.

3.2 Glow discharge optical emission spectroscopy

For GDOES a vacuum simultaneous emission spectrometer (Fa. Spectruma) was used. The type GDA 750 (1996, Andechs, Germany), operated at (ca. 10^{-3} bar), was used.
The anode had a diameter of 4 mm was used. The voltage was kept constant at 800V and a pressure of ca. 3 mbar applied so as to obtain a constant current of 20 mA.
The wavelengths of the lines used for each element were: Fe 371.994 nm, Mn 403.449 nm, Al 396.152 nm, Cu 327.396 nm, C 156.143 nm, O 130.27 nm, S 180.731 nm, Cr 425.433 nm, Si 288.157 nm.

3.3 Secondary neutral mass spectroscopy

With SNM the analysis of conductive and non-conductive thin layers is possible. A solid sample in vacuum is bombarded with low energetic ions (0-2 KV) from a low pressure plasma (10^{-3} mbar) in such a way that atomic layers are removed. The removed particles are ionised in the plasma by means of electron bombardment. For the detection of the ions formed a quadrupole mass spectrometer is used.

3.4 White light interferometry

For these experiments a Wyko NT330 (Veeco, Woodbury, USA) interferometer was used. The interferometer was used in the VSI modus with a 2.52 times magnification using a Michelson objective. The resolution of the pixels was 3.33 μm. The measured area was of 4.64 mm^2.

Steel B was used for these measurements.

3.5 Scanning electron microscopy

For the investigations of the surface morphology by SEM a Cambridge Instruments Cam Scan 44 microscope equipped with an Oxford SiLi detector for the energy eispersive X-ray (EDS) analysis was used. Before the analysis the surface of the samples is made electrically conductive, mostly by covering with gold, silver or carbon.

The analyses with FE-SEM were made with the field emission scanning electron microscope model LEO 1530 (Fa. Carl Zeiss NTS GmbH). Secondary electrons were detected using an acceleration voltage of 1 kV.

3.6 Atomic force microscopy

The AFM images were obtained in the contact mode in fluid with a Dimension3100/NanoScope IIIa instrument (Digital Instruments, Santa Barbara, USA). Commercially available silicon nitride probes (Olymen) were used, having a pyramidal shape and a tip height of 2.9 μm, a tip radio <20 μm and a tip angle <70°. A total of 216x216 points were collected for each scan at a scan rate of 1.5 Hz. All experiments were carried out at room temperature and humidity.

As liquids a commercially available pH=1 (Titrisol® buffer solution pH=1.00±0,02 (20°C) glycine- HCl solution, Merck) and the same solution with 3.0g/L of BD were used. As substrate polished steel A of dimensions (1.5 X 1.5 X.~ 0.1 cm) was selected. Images were taken first before bringing the subtract in contact with the fluid and then after 13, 24, 30, 45, 52 and 72 minutes of contact.

3.7 Infra-red spectroscopy

The FTIR spectroscopic experiments were carried out with a type 510P FTIR-spectrometer. For the measurements in liquids the attenuated total reflexion technique (ATR) was used. Measurements were made with a ZnSe crystal. For experiments with solids a KBr optical blank was used.

3.8 Weight loss studies

For these experiments steel samples with a thickness of about 1 mm and squares of 50 mm length were used. They were cleaned by immersion in *n*-hexan, rinsing with 1,3-isopropanol and drying with N_2. After these exposures, the pieces were weighted with an analytical balance. All weight loss experiments were performed in a 600 mL beaker with 400 mL of a stirred aerated solution of 20 % H_2SO_4 and 50 g/L $FeSO_4$ in distilled water. The solution contained the different commercially available inhibitors. The immersion time was 3 minutes. The pieces were removed from the pickling bath, rinsed with 1,3-isopropanol and dried with N_2. Then they were placed in a vacuum chamber for 3 hours to ensure their complete drying and weighted again.

The concentrations of the inhibitors used ranged from 0.1 g/L to 3 g/L. The temperatures used were similar to those used in pickling (95ºC ± 3). In tests at different temperatures with 2-Butin-1,4-diol the same experimental procedure were used.

3.9 Electrochemistry

For all experiments in 0.5 % $FeSO_4$ the measured area was selected to be 14.6 cm^2 and 12 cm^2 for those made at pH=1. However for CI the samples brought in this solution were untreated 14.6 cm^2 specimens. The experiments were carried out at room temperature in naturally aerated media using an electrochemical cell containing 0.5 % $FeSO_4$ in distilled water and a commercial solution at pH=1 (Titrisol® glycine-HCl buffer solution pH=1.00 (20°C), Merck) as electrolytes. Between 0.1 g/L and 3 g/L of the test compounds were added. An Ag/AgCl reference electrode was used. The potential of the standard hydrogen electrode (SHE) against the Ag/AgCl electrode was 207 mV, and all the given potentials are referred to this SHE reference electrode. The steel sample is used as the working electrode.

These samples used for the experiments in 0.5 % $FeSO_4$ were cleaned with *n*-hexane followed by rinsing with isopropanol and drying with air. The electrolytic cell was asembled before starting the measurements and all the recordings were started when the metal was in contact with the solution.

These samples used for the experiments at pH=1 were cleaned with *n*-heptane followed by rinsing with isopropanol and finally with acetone for at least three minutes Ultrasound treatment was performed with each one of the solvents. The cleaning using ultrasound was determined to be the most effective after several experiments. An area of 12 cm^2 was covered with magnetic foil and the piece immersed in a corrosion protective lack. To start the measurement the magnetic foil was taken away, leaving a fresh flat area to be exposed to the corrosive environment. The piece of metal was connected and once the electrode is ready the system is prepared and the potentiostat started. Then the piece was put into the solution.

For all electrochemical measurements as computer controlled potentiostat the electrochemical workstation IM6 (Zahner Electrik GmbH & Co. Kronach, Germany) was used. The open circuit potential was recorded for 10 minutes. For the potentiodynamic experiments a cyclically varying potential is applied from the cathodic zone to the anodic one (from - 800 mV to 0 mV). A scan rate of 4mV/s is used and the electrochemical impedance spectroscopy data are presented in the form of Bode diagrams. They were recorded within a frequency range from 100 KHz to 100 mHz, with an applied sinusoidal potential equalling the open circuit potential ± 5 mV. The impedance data were analyzed under the use of the Zview software (version 2.8d) and for all measurements steel B was used.

3.10 Infra-red reflection absorption spectroscopy

For the sample preparation polished specimens of steel A (1.5 x 1.5 x ~ 0.1 cm) in a 5%HCl solution at room temperature to remove the residual oxide followed by rinsing with water. Then, they were submerged for 72 minutes in solutions of 1.5 g/L DITU, DETU and DMTU in DPGDME and rinsed with DPGDME.

The IRRAS measurements were performed with the aid of an Excalibur Spectrometer (Fa. Bio-Rad, Cambridge, USA). The spectra were recorded with a PbSe detector, 256 scans were made, a resolution of 1 cm^{-1} as well as beam incidence angle of 80° realized.

3.11 X-ray photoelectron spectroscopy

For sample preparation the polished specimens of steel A (1.5 x 1.5 x ~ 0.1 cm) were immersed in a 5% HCl solution at room temperature to remove the residual oxide followed by rinsing with water. Then they were brought for 3, 30, 60 and 120 minutes in solutions of 1.5 g/L DITU, DETU and DMTU in DPGDME and rinsed with DPGDME.

The XPS spectra were recorded with a commercial Quantum 2000 system (Physical Electronics, Chanhassen, USA). A monochromatic Al k (Alpha) (1486.7eV) source at a power of 25W and 15 kV was used. The pressure in the vacuum chamber was 5.0 x 10^{-9} mbar. The emitted electrons were detected by a hemispherical analyzer at fixed pass energy of 117.4 eV for the survey spectra and 46.95 eV for the multiplex spectra. The angle between beam and sample surface was 45°. The survey spectrum was taken in the range of 0-1400 eV with steps of 1eV. For energy calibration the main C 1s peak at 284.8 eV was used. For spectral deconvolution mixed Gaussian-Lorenzian curves were used and iterate Shirley background subtraction applied. Sputtering with argon ions was applied and acquisition times ranged from 10 to 20 minutes.

Experiments under N_2 atmosphere were carried out at the Max Planck Institute für Eisenforschung in Dusseldorf. The experiments were performed in a glove box under nitrogen atmosphere (water < 2 ppm, oxygen < 1 ppm). The XPS data were obtained with a (PHI) Quantum 2000 Scanning XPS (Physical Electronics, Chanhassen, USA) with Al k(Alpha)X-ray excitation. The typical background pressure during the experiment was better than 10-9 Torr. The emitted electrons were detected with the aid of a hemispherical analyzer at fixed pass energy of 93.90 eV in the case of the survey spectra and 29.35 eV in the case of the high resolution spectra. The X-ray emission energy was 25W, the accelerating voltage 15 kV and the spot size 100 micron.

3.12 Time-of-flight secondary ion mass spectrometry

The steel A (1.5 x 1.5 x ca.0.1) cm polished samples were subsequently rinsed with EtOH, *n*-heptane, deionised water, 5% HCl (30 seconds, afterwards few corrosion visible), and with deionised water, then dried in an air stream and immersed for 35 minutes in solutions containing 1.5g/l of DMTU, DETU and DITU in DPGDME. Afterwards they were rinsed with DPGDME and stored under vacuum over night in the load lock of the TOF-SIMS instrument.

A TOF.SIMS 5, ION-TOF GmbH (Münster, Germany) equipped with a bismuth liquid metal primary ion source was used for all measurements. The pulsed primary ion beam consisted of 25keV Bi^{3+}, a target current of 60 fA average, a cycle time of 100 µs, an area (128 x 128 pixel random scan) of 500 x 500 µm² and a duration of the signal acquisition of 30 sec were selected as measurement conditions.

4. Results and discussion

4.1 Effects of pickling on the steel surface

4.1.1 Characterization of used steels

Through this work cold rolled steels are used. The presence of scale, which is most of the time non-homogeneous, would have lead to much error. Cold rolled steels, therefore, has a homogeneous surface where the effects of pickling can be directly seen and the effect of inhibitors directly tested.

The main steels used for the studies have been characterised by means of chemical bulk analysis and the surface composition was studied by GDOES and by means of SEM images.

The two different main steels used were:

Steel H180Y (Steel A): cold rolled continuously annealed steel. With this steel atomic force microscopy measurements as well as investigations by infra-red reflection adsorption spectroscopy, x-ray photoelectron spectroscopy and time-of-flight secondary ion mass spectrometry were performed.

Steel H260Y (Steel B): cold rolled non-continuously annealed steel. This steel was used for experiments with white light interferometry, field emission scanning electron microscopy and weight loss assays.

The selection of these steels responded to the availability of the material at the time the experiments were made. For this reason another kind of steel was also used in the pickling experiments: **steel H143906 (Steel C)**, which is a non-continuously annealed cold rolled steel. The elemental composition of the cold rolled annealed steels is seen in **table 8**. They were obtained by means of optical emission spectroscopy.

Elements	**Mass %**			**Elements**	**Mass %**		
	Steel A	**Steel B**	**Steel C**		**Steel A**	**Steel B**	**Steel C**
C	0.06	0.045	0.049	**Cr**	0.036	0.026	0.026
Si	0.133	0.012	0.006	**Ni**	0.022	0.022	0.016
Mn	0.74	0.33	0.222	**V**	0.004	0.002	0.003
P	0.02	0.022	0.009	**Mo**	<0.002	0.002	0.004
S	0.001	0.007	0.016	**Ti**	0.004	0.002	<0.002
Al	0.036	0.034	0.034	**Nb**	0.029	0.022	0.003
N	0.0033	0.003	0.0070	**B**	<0.0004	<0.0004	<0.0004
Cu	0.027	0.012	0.028	**Fe**	98.88	99.46	99.4306

Table 6. Elemental bulk composition of the cold rolled steels A and B.

The three cold rolled steels A, B and C are low alloyed steels. The presence of the alloying elements is slightly lower in the case of steel B.

The results of GDOES are shown in **figure 37**. The spectra of GDOES for steel A shows how the steel surface mainly consists of Fe and at the very outermost surface an O layer is found, which decreases, disappearing within the first µm. The concentrations of elements like Mn, Al and Cr increase with depth, but their concentrations are always very low. The bulk concentration values for Mn, Al and Cr are in good agreement with those obtained from elemental determinations. For steel B, the results of elemental analyses and the values resulting from GDOES in the bulk, agree quite well. When comparing the spectra of GDOES steel A and steel B it can be recognized that both steels went through a different kind of annealing. Steel B is a non-continuously annealed steel, which went through a longer annealing process at high temperatures. This gives the elements enough time to diffuse to the surface, and therefore higher concentrations of Mn, Cr and Al are found in the first nanometres in the case of steel B.

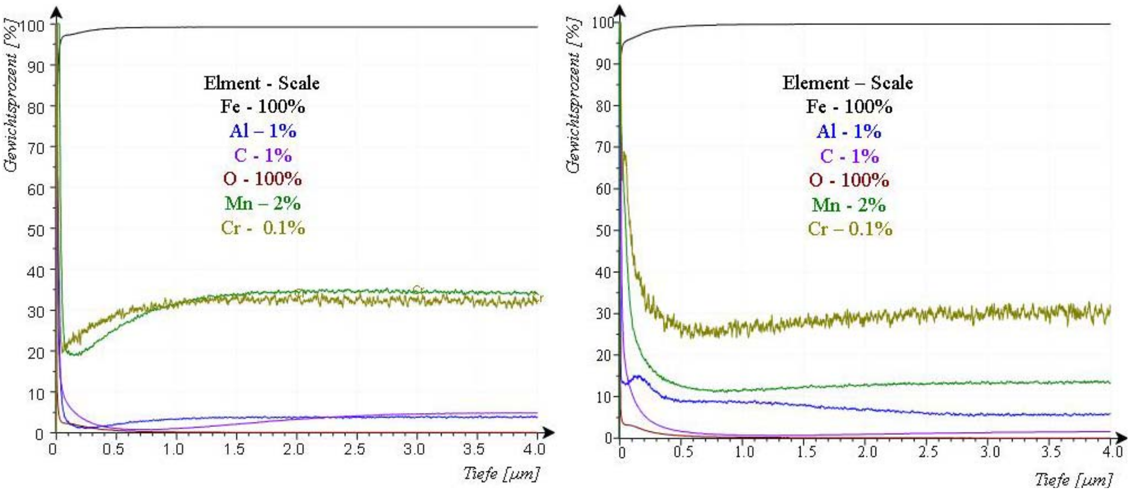

A **B**

Figure 37. GDOES depth analysis results for steels A and B.

In **figure 38** results of the investigation of the steels by means of SEM is shown. The images show the existence of a structure formed by bright and dark crystals. The bright crystals are ferrite and the dark ones are pearlite, which are located at the grain boundaries. The crystalline structure for steel A shown in **figure 38** is typical of so-called low carbon steels[19]. The grain size according to the American Society for Testing and Materials (ASTM) norm is 11-12 (4.5-3.2 µm^2)[83]. From the microstructure for steel B shown in **figure 38** it can be concluded to have a matrix of ferrite. In the matrix little globular structures or white spots are observed. It can be concluded that these spots are metallic carbides (Ti, Nb, …). The elemental composition of steel B is comparable to that of steel A but the microstructure is different: in steel A pearlite is present in the grains and at the grain boundaries while steel B has metallic carbides mainly in the grains. This difference in microstructure can be attributed to the annealing process. The grain size of steel B according to ASTM is 7-8 (1000-500 μm^2). The microstructure and the grain size mainly depend on the cooling temperatures applied[9, 19, 111, 112].

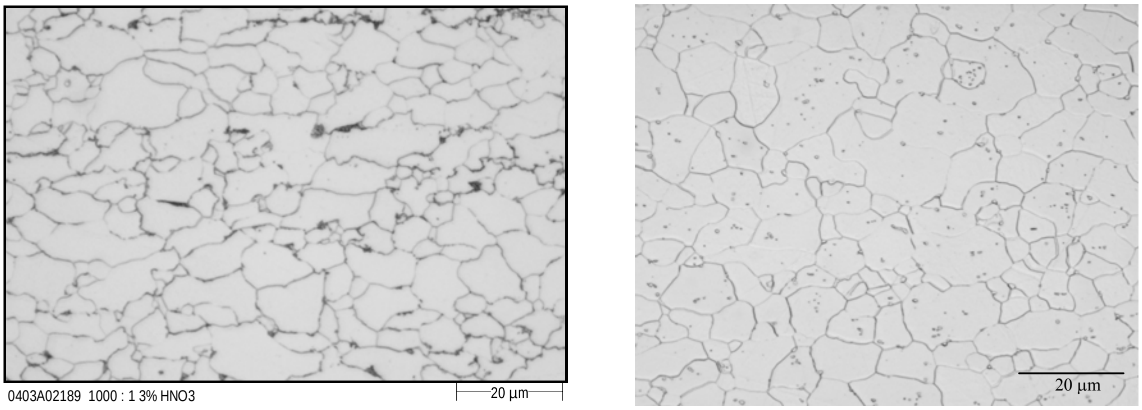

A **B**

Figure 38.-Microstructure of the low alloyed cold rolled strips A and B.

4.1.2 Effects of acid treatment in steel

An investigation ofto the effects of pickling was made in the case of cold rolled steel (steel B) by using HCl at a concentration of 7 % and 20 % and H_2SO_4 20 % (**figure 39**) at room temperature. The concentrations were chosen on the basis of the experimental conditions at the pickling plants. Hydrochloric acid is used in a gradual pickling starting through a bath of 7 % HCl and finally through a bath of 20 % HCl. The pickling with sulphuric acid is carried out at a concentration of 20 %.

The effects of acids were tested for a duration from 5 to 50 minutes to see how the surface was affected by increases in time.

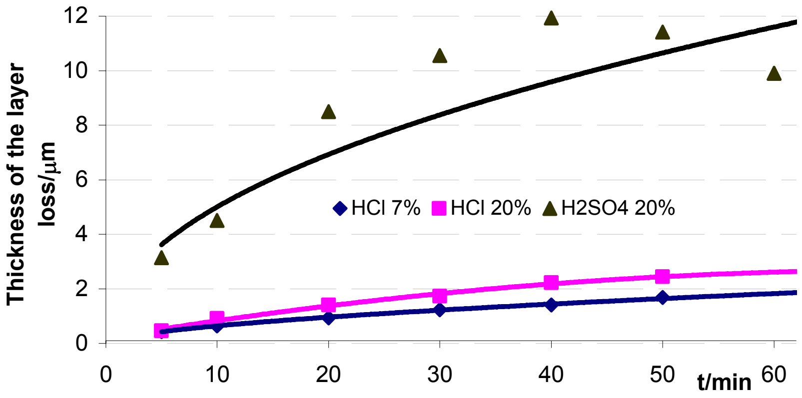

Figure 39. Thickness of the layer lost when pickling with HCl at different concentrations *vs*. the pickling time.

In **figure 39** it is shown how at both concentrations the thickness of the lost layer increases with time. It is found to be larger in the case of the higher concentration (20 % HCl). The more the pickling takes place, the more the difference between the acidic concentrations.

It can be seen that the effect of H_2SO_4 is higher than the effect of HCl. The increase of the lost layer with the pickling time lasts until 40 minutes and then from the 40 to 70 minutes. The latter could be due to the formation of a passivation layer during this period. It could be thought that corrosion products are formed on the surface. SNMS results (following) lead to the conclusion of the formation of a layer made out by elements which are increasing on the surface with time and oxygen, which is higher in the treated samples that in the non-treated sample. Most likely insoluble oxides are being formed and passivating the surface.

Some of the pieces pickled with 20 % H_2SO_4 were analysed by means for SNMS in order to determine the changes in depth composition of the samples. In **figure 40** the change of the concentration of Cu with the time of immersion in the acid solution is shown.

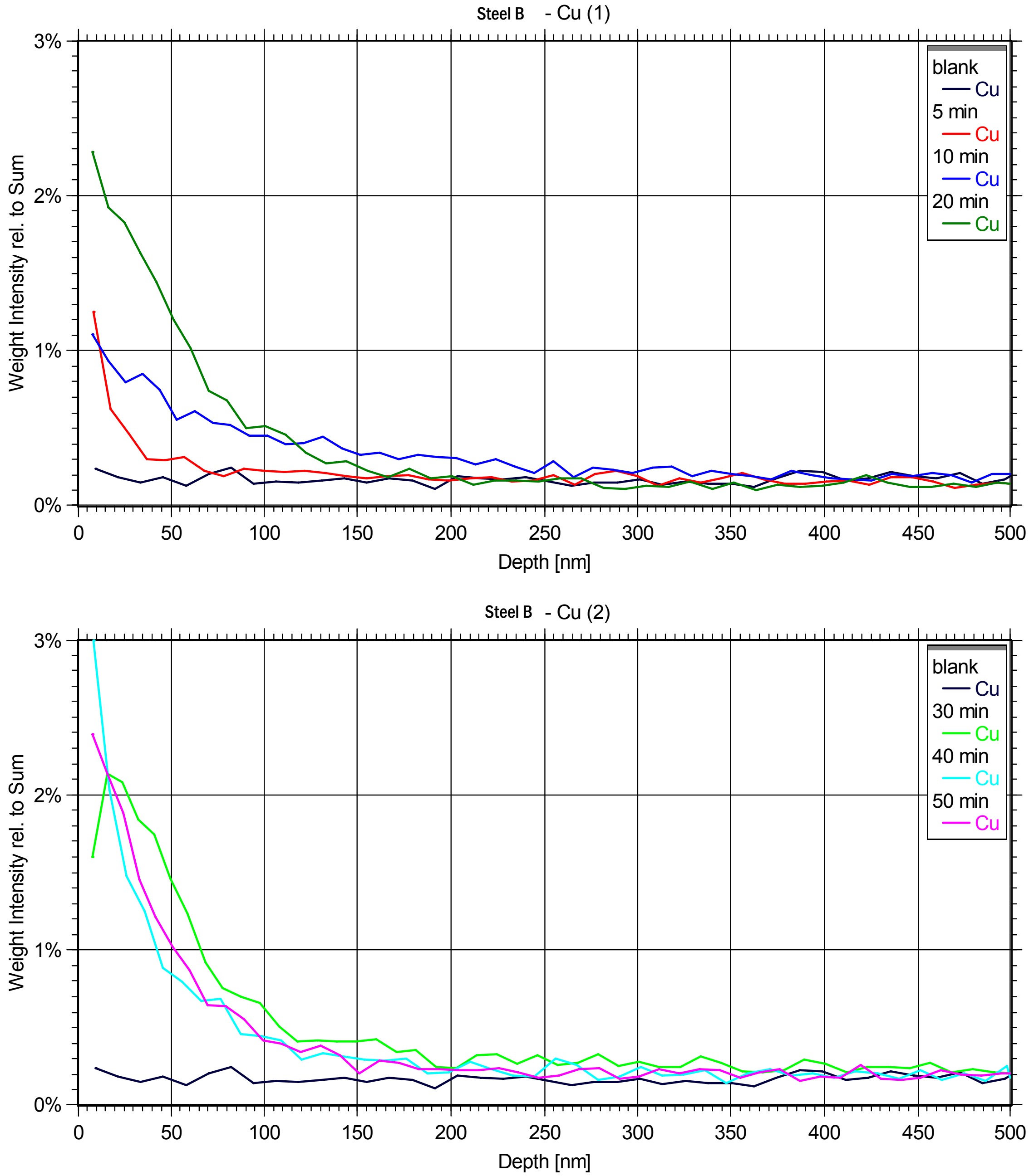

Figure 40. Results of SNMS for steel B samples, which have been immersed during different times in a solution of 20 % H_2SO_4.

It can be seen how the concentration of Cu at the surface increases at short pickling times and that it behaves irregularly at long ones. The concentration of Cu at the sample surface after treatment is always higher than in the non-treated sample. This might be due to the high nobility of copper, being the highest of all alloying metals studied.

In **figure 41** the change of the concentration of Mn with the immersion time is shown.

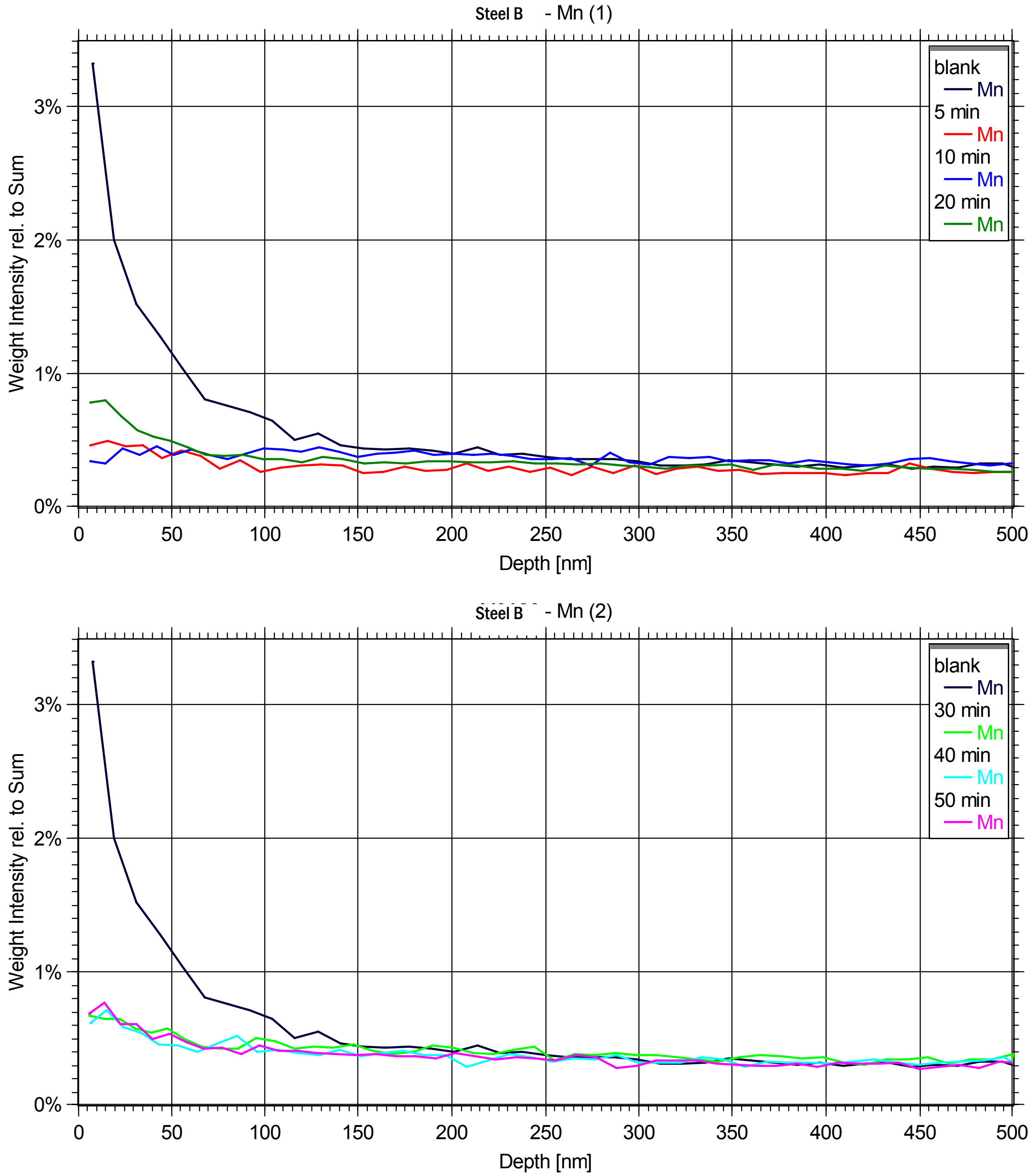
Steel B - Mn (1)

Steel B - Mn (2)

Figure 41. Results of SNMS obtained for a couple of steel B after immersion during different times in a solution of 20 % H_2SO_4.

The concentration of Mn on the surface has been found to decrease when the sample is immersed in a solution of 20 % H_2SO_4 as compared to the non-treated sample. The change with time increases slightly up to medium immersion times but after 30 minutes the change is almost constant.

The trends for these other elements analyses are given:

- aluminium concentration at the surface increase with the pickling time as compared to the non-treated sample,
- chromium concentration as compared to a non-treated sample has the tendency of increase at the surface with the immersion time until medium values then it is nearly constant,
- the concentration of iron at the surface decreases as compared to a non-treated sample,
- the concentration of oxygen is higher at the surface as compared to a non-treated sample confirming the formation of corrosion layers in the pickling experiments,
- the concentration of sulphur at the surface compared to a non-treated sample was found to be higher and to increase with the immersion time,
- the concentration of silicon as compared to a non-treated sample decreases but remains almost constant at different pickling times,
- the concentration of titanium at the surface as compared to a non-treated sample is considerably higher and increases with immersion times.

The increase of the concentrations of Cu, Al and Cr on the surface during the first 30 minutes of immersion only leads to the conclusion that a passivation layer is formed on the surface. This can be confirmed by the visually observed thin black layer that covers the steel sample.

4.1.3 Study of the topography of the surface after acidic treatment

The effects of acidic attack on the steel surface were studied using several methods and the results of these experiments described below.

4.1.3.1 White light interferometry

White light interferometry and field emission scanning electron microscopy were used to study the morphological changes of steel B during pickling. Pickling at room temperature using 20 % H_2SO_4 and 7 %HCl was performed during different times. Further the surface of the steel has been examined after it was exposed during 3 minutes to a real pickling solution (20 % H_2SO_4 + 50 g/l $FeSO_4$) at 95°C. The high temperatures chosen are to reproduce the real conditions used in the pickling plants (*see section 2.1.5.3.1*)

In **figure 42** the pictures corresponding to the white light interferometry for a blank sample and for a sample which was exposed 50 minutes in the acid solution are shown.

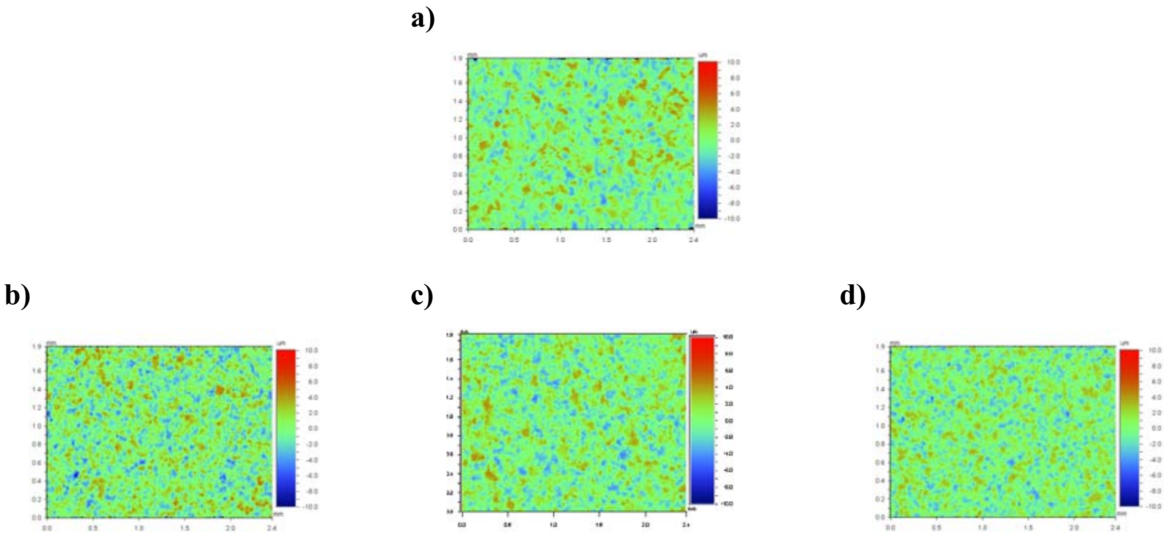

Figure 42. Images of the surface of steel B without pickling (**a**) and pickling during 50 min in 20 % H_2SO_4 (**b**), 7 % HCl (c) and 20 % HCl (**d**).

In **table 7** results of measurement of the roughness of the surface after these treatments are given.

Pickling time/min	H_2SO_4 20%	HCl	
		20%	7%
0	1.4	1.4	1.4
5	1.4	1.3	1.4
10	1.2	1.2	1.5
20	1.6	1.4	1.4
30	1.6	1.3	1.2
40	1.4	1.5	1.5

Table 7. Evolution of roughness as a function of the pickling time.

R_a is the two-dimensional *roughness average*, which is the arithmetic mean of the absolute values of the surface departures from the mean place[84].

From the results showed it can be seen how at low immersion times the roughness of the surface seems to be lower than the one of the blank sample. That means that the acids first flatten the surface by reacting with its outer parts and that then the roughness starts to increase again.

It is remarkable to see that HCl is more aggressive at a concentration of 7 % than at a concentration of 20 %. The parameters, which are a measure for the roughness, are normally higher at a concentration of 7 % and also the erosion at the surface was found to be higher (**figure 42**).

In **figure 43** planar views of the steel surface after a three minutes pickling s (T=95°C, H_2SO_4 20% + $FeSO_4$ 50g/l) are shown.

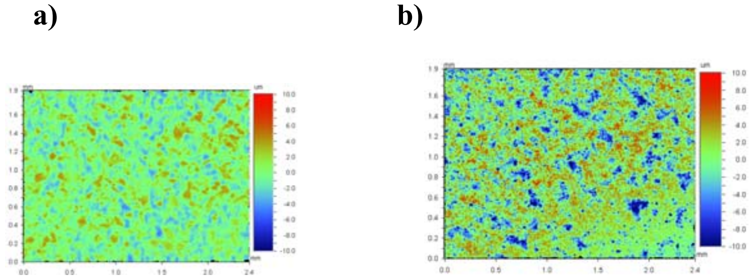

Figure 43. Planar views of a piece of steel B. Blank sample (**a**) and sample after a three minutes pickling in H_2SO_4 20 % + $FeSO_4$ 50 g/l (**b**).

When comparing the results for the treated sample with those of the blank it can be seen how the surface is much more damaged when the treatment is carried out at 95°C and how the roughnessn then greatly increases. The values of the measured roughness are given in **table 8**:

Pickling time/min	**R_a/μm**
0	1.4
50 (T=22°C)	1.6
3 (T=95°C)	2.6

Table 8. Roughness of the surface for steel B after treatment of the samples in H_2SO_4 at different conditions.

When subjecting the sample to pickling at room temperature during 50 minutes the roughness was found to be by 18 % longer than in the case of the non treated sample. Therefore a sample treated during only 3 minutes at 95°C shows an increase of the roughness by 88 %. This testifies that the pickling at high temperature is a very aggressive process.

4.1.3.2 Scanning electron microscopy and field emission scanning electron microscopy

Scanning electron microscopy and field emission electron microscopy were used so as to investigate the effects of pickling on the surface morphology.

The steel used for these experiments was steel B. Pickling at room temperature was carried out with 20 % H_2SO_4, 7 % HCl and 20 % HCl during different times and pickling at 95°C was performed during 3 minutes with a mixture of 20 % H_2SO_4 and 0.5 % $FeSO_4$. After treatment the samples were examined with the aid of scanning electron microscopy.

In **figure 44** a comparison between the different surfaces is made ate the hand of the SEM images obtained after different pickling times with the three different mentioned environments.

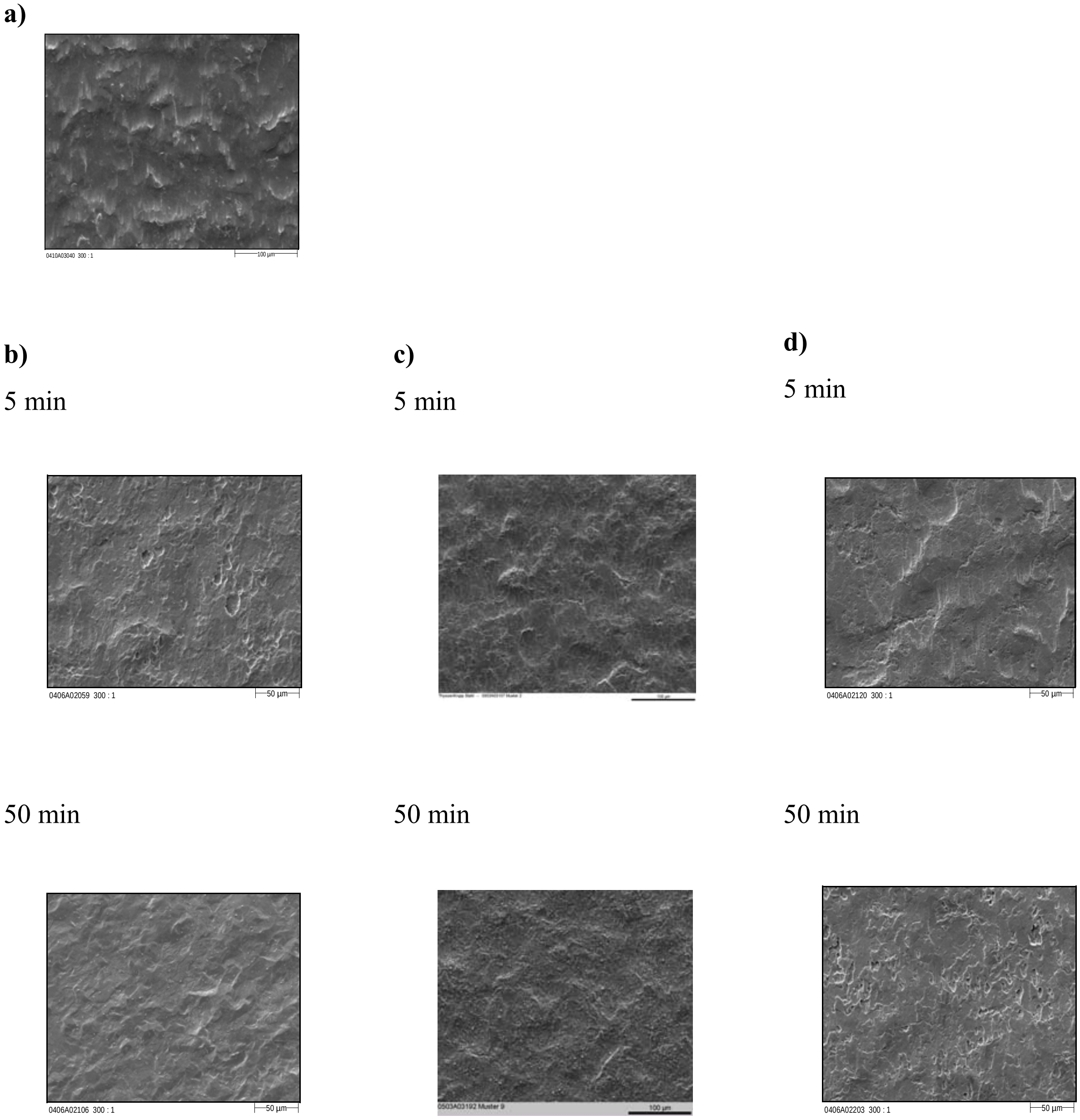

Figure 44. SEM pictures made for sample without treatment (**a**) and samples after different pickling times of steel B in 20 % H_2SO_4 (**b**), 20 % HCl (**c**) and 7 % HCl (**d**).

The surface of the non-treated sample is mostly finely constructed but thrust faults. In addition there are smooth risers recognisable at the surface.

When using a 20 % H_2SO_4 solution, it can be seen how the attack directly takes place at the ferrite grains at the surface, which are completely removed. The longer the pickling time, the more the surface changes. The surface also displays pickling residues, the first grain layer is partially pickled and the original topography is no longer visible.

When performing pickling with 20 % HCl the SEM image obtained after 5 minutes pickling was similar to the one for the case of 20 % HCl during 3 minutes. Pickling attacks were mainly found at the grain boundaries and very little at the grain surface. The original topography here is still recognisable. After 50 minutes of pickling a strong attack to the grain surfaces is observable and no free grain boundaries can be seen. Dry residues of the pickling reagents could also be detected locally and the original sample topography is practically no longer found.

In the case of 7 % HCl, as well as with 20 % HCl the main attack takes place at the grains boundaries. When the acid is less concentrated the attacks seem to be deeper at high pickling times but only few grain surfaces seem to be affected at longer pickling times.

In case of H_2SO_4 the thickness of the lost layer seems to be one order of magnitude larger than for HCl (*section 4.1.2*). This can be explained by the SEM results: in case of H_2SO_4 almost a complete layer of ferrite grains is lost while HCl seemed to attack mainly at the grain boundaries and not so much material is lost. From the images in **figure 44**, a mechanism of dissolution for the case of HCl can be proposed: at low concentrations or short pickling times the material dissolves at the grain boundaries. When increasing the pickling time or at high concentration, the grains themselves are being removed, so it would be reasonable to accept that the dissolution starts at the grain boundaries and then dissolves the ferrite grains.

In **figure 45** the cross sections of the samples after 50 minutes pickling times with 20 % H_2SO_4, 20 % HCl and 7 % HCl are shown. The samples were cut lengthwise in order to showe the effect of pickling on the cross section topography. These images were obtained by means of light microscopy. A pickling with 20 % H_2SO_4 seems to be the more aggressive one. Here the surface is damaged and the holes left after pickling show that complete grains have been removed.

When pickling with 20 % HCl, the pickling causes already shown by white light interferometry pores and defects, and some of them are recognisable the result of a complete removal of grains.

Pickling with 7 % HCl seems to be the less aggressive. However, also here some holes are found as a result of a complete removal of grains.

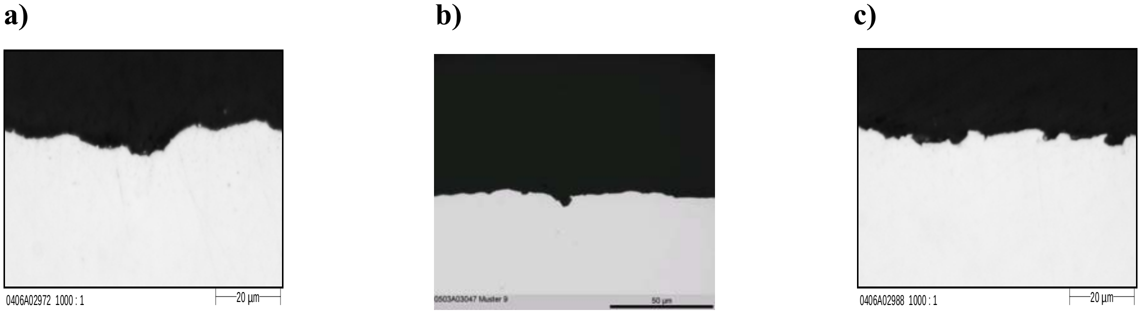

Figure 45. Cross sections after pickling with 20 % H_2SO_4 (50 min) (**a**), 7 % HCl (50 min) (**b**) and 20 % HCl (50 min) (**c**).

In **figure 46** the cross section obtained by means of light microscopy and a SEM image of the surface of a sample of steel B after pickling during 3 minutes at 95°C with a mixture of 20 % H_2SO_4 and 0.5 % $FeSO_4$ are shown.

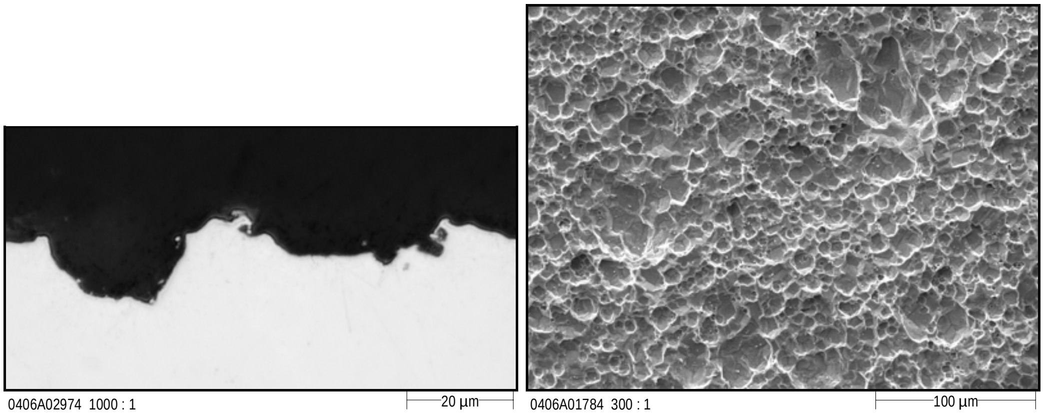

Figure 46. Light microscopic image of the cross section and SEM image of the surface of a steel B sample after 3 minutes pickling with a mixture of 20 % H_2SO_4 and 0.5 % FeSO4 at 95°C.

From **figure 46** it can be seen how deep is the damage caused by pickling at the mentioned conditions is. The cross section shows that the damage is larger than in the case of the images shown in **figure 45**. Here the holes are bigger and the erosion is larger.

The topography reflected by the SEM image shows that a honeycomb structure is formed as a result of the removal of complete grains. The weight loss in the case of pickling at 95°C is a some higher than the double of that obtained after 50 minutes of pickling at room temperature. The thickness of the lost layer can be calculated to be around 25 µm. In *section 4.1.1* it was mentioned that the grain size for steel B was between 10 and 20 µm. This means that by pickling at high temperature at least more than one whole layer of grains (between 1 and 3 grain layers) were removed.

By FE-SEM more detailed images of the surface after pickling could be obtained. In **figure 47** FE-SEM images at two different magnifications obtained from steel B after pickling in 20 % H_2SO_4 at room temperatures during different times as well as an image of the blank material are shown.

Without treatment the sample shows a relative flat surface with only few defects. After pickling the samples show a rough surface with compact inclusions at some places. After increasing pickling time the surface becomes rougher and the quantity of inclusion due to the acid attack rises. According to the SNMS analysis (*section 4.1.2*) these inclusions mainly consist of Cu, Al, Cr, S and Ti, which are the elements found at the surface after increasing pickling times.

It can also be observed how at longer pickling times cracks are formed (see **figures 47 d** and **e**) and how they become deeper the longer the contact with the H_2SO_4 solution.

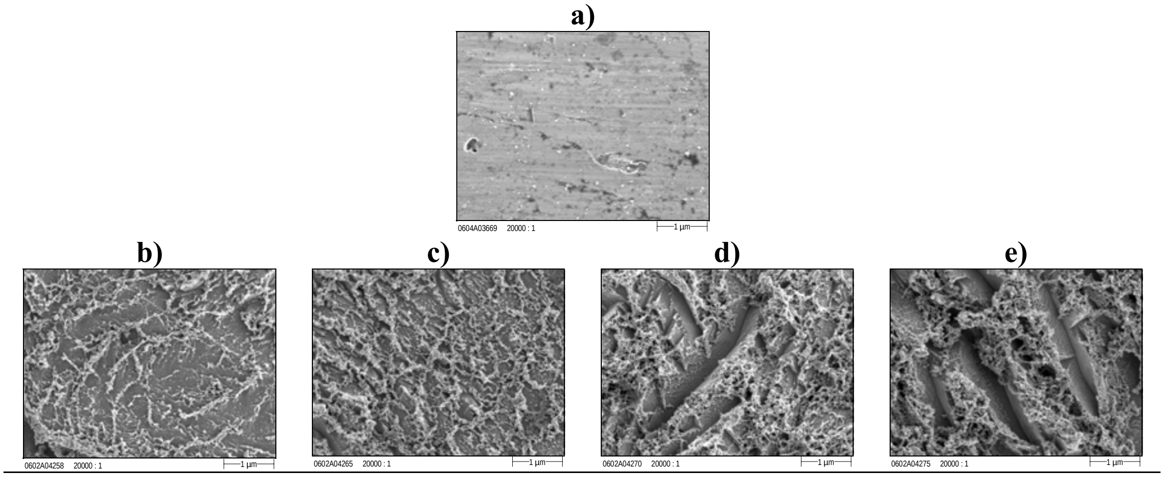

Figure 47. FE-SEM images of samples of steel B after acidic treatment with 20 % H_2SO_4 (scale 20000:1). Sample without treatment (**a**), and samples treated for 5 (**b**), 10 (**c**), 20 (**d**) and 30 min (**e**).

4.1.3.3 Atomic force microscopy

The effect of a commercially available solution of pH=1 (500ml buffer solution, pH=1±0.02 (20°C) Tritrisol®, glycine-HCl, Merck) on the steel A was studied by means of *in-situ* atomic force microscopy in the liquid. The use of a buffered solution is required a minimal change in the composition of the liquid during the measurement would be affecting the pH and this again would affect the further dissolution of the material.

In **figure 47** records of the blank sample made in contact modus are shown. They visualize the structure and roughness of the surface. At a decrease of the scale more details are visible. The topography is shown to be irregular enough to recommend the use of polished samples for these measurements, when one considers that the AFM stylus can measure differences in height of 6 µm.

Scale	Three-dimensional image	Two-dimensional image
1µm	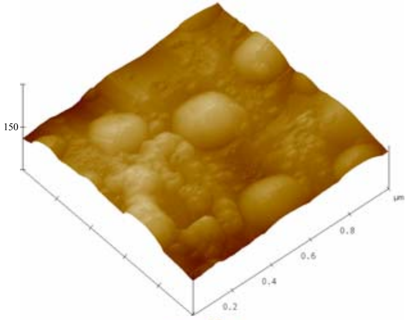	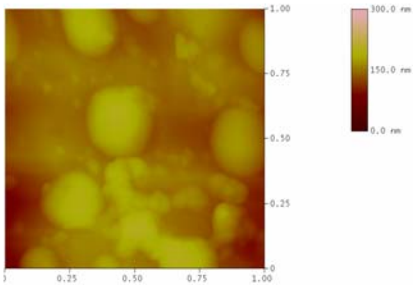
5 µm	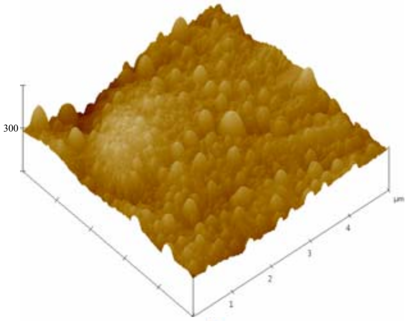	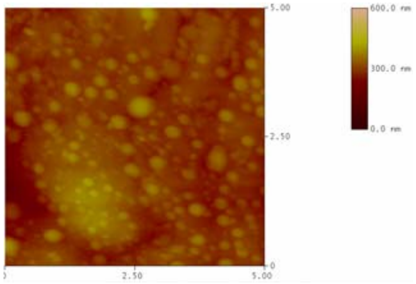
10 µm	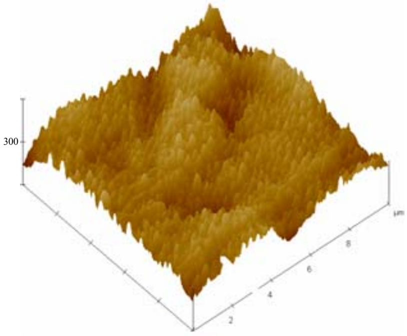	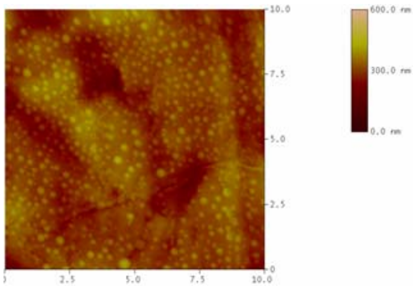
50 µm	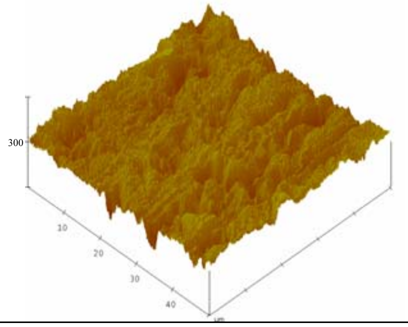	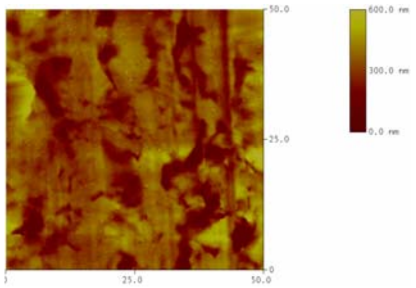

Figure 47. Different images of the steel A blank sample made with AFM.

In **figure 48** three-dimensional AFM images of a surface of steel A are shown. When comparing these images to those of a non-polished sample the difference can be clearly seen. In the case of the polished samples the surface is much more homogeneous and smoother and the roughness is significantly lower. The natural metal roughness would make it very difficult to monitor the corrosion process, especially from in its first steps, where the roughness mainly increases. Accordingly, all AFM measurements in liquids were made with polished samples..

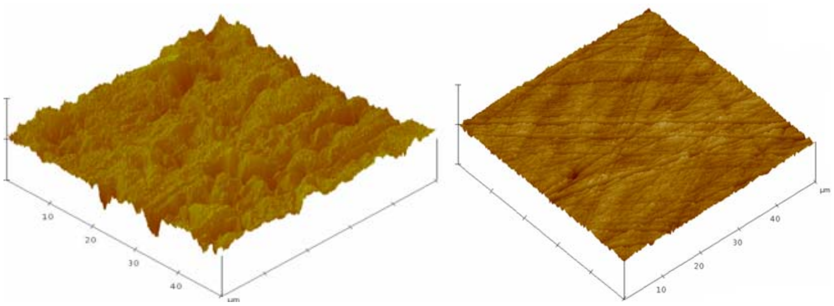

Figure 48. Comparison of three-dimensional AFM images for non-polished and polished samples of steel A (scale: 50µm).

The effects of a commercially available solution of pH=1 (Tritrisol®, Merck) on the steel could be visualised by means of records for samples which were immersed during different times in the solution. In that way the corrosion could be evaluated as a function of the surface roughness. The results of the experiments are shown in **figure 49**.

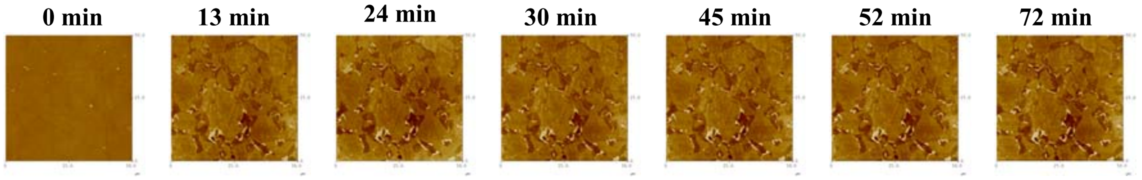

Figure 49. AFM images (50 x 50 µm) taken of steel A in contact with the commercial buffer solution Titrisol pH=1.

These pictures show the corrosive effect of the solution on the steel surface. The holes shown are those left by the dissolution of the material grains. A remarkable fact is that localised corrosion can be observed. Indeed, only certain parts of the surface are corroded which are mainly at the grain boundaries and not the whole surface. This could be related to the presence of chloride ions (from the HCl) in the buffer solution. Indeed, it was seen in the SEM images that pickling in HCl mainly occurred at the grain boundaries.

These conclusions from the results in **figure 49** can be confirmed by the graph in **figure 50**. The roughness can be used as a measure for the advance of the corrosion. It can be seen how the roughness greatly increases to up to 13 minutes of immersion but from this time onwards it practically remains stable.

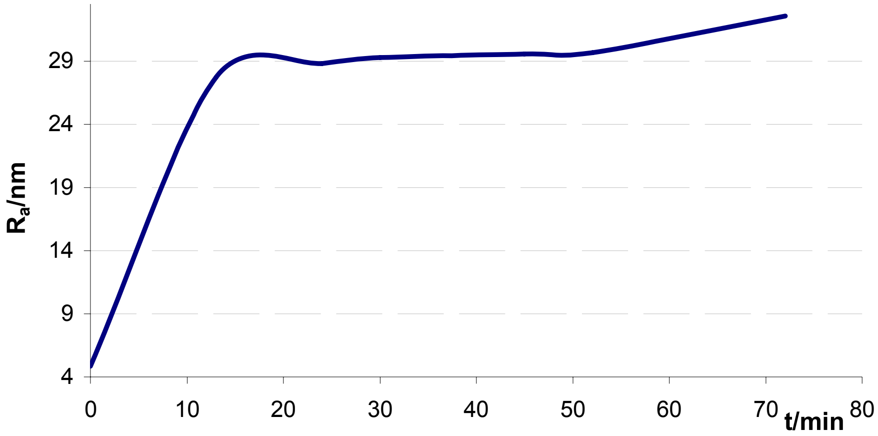

Figure 50. Evolution of the roughness with the immersion time for a sample of steel A in a buffer solution of pH=1.

From the AFM images and the evolution of the roughness it could be concluded that a passive layer is formed on the surface. It is reasonable to think that the soluble elements on the surface are dissolved and that the non-soluble ones would form a layer which would avoid a progression of the corrosion. This would be in agreement with the results of SNMS, where the concentrations of elements like Cr, Al, Cu, S and Ti were found to increase at the surface with the pickling time for a solution at low pH.

4.1.4 Summary

A solution of 20 % H_2SO_4 could be shown to be more aggressive and to cause more damage than a solution of 20 % HCl. From the results of the SEM images this difference could be explained in terms of differences in the dissolution mechanism: 20 % H_2SO_4 could be shown to directly dissolve the ferrite grains while in the case of 20 % HCl the dissolution of the material starts at the grain boundaries first and then the ferrite grains are dissolved.

The results of white light interferometry show that at low pickling times the pickling with HCl at low concentrations is more aggressive than with HCl at higher concentrations.

The final material damage observed with atomic force microscopy made in a buffer solution at pH=1 could be explained by the formation of a passivation layer. This would be in compliance with the increase of the concentrations of some elements at the surface, as shown by SNMS. The formation of inclusions on the steel surface, as observed with FE-SEM could be confirmed by SNMS, which shows that they are consistent.

4.2 Study of pickling inhibitors

4.2.1 Characterization by infrared spectroscopy

First the IR spectra of the substances present in the commercially available inhibitor were recorded and compared to the spectra obtained from the commercial formula.

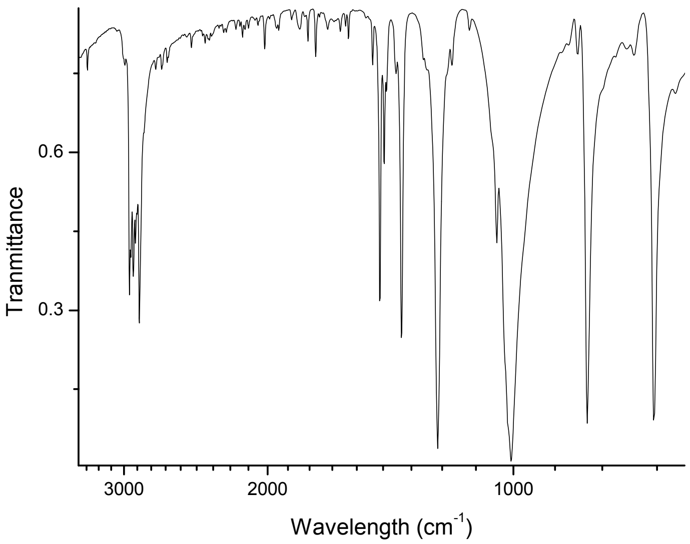

Figure 51. IR spectrum of HMTA.

In the spectrum of hexametylentretaamine (**figure 51**) there are three main bands: two medium bands correspond to the vibration of the bonds CH_2 and one strong band corresponds to the vibration of C-N bond. The multiple bands between 2953-2872 cm^{-1} corresponds to the stretching frequencies of CH_2 and, in secondary amines, of CH_2-N, $\nu_{as(scissors)}(CH_2\text{-}N)$ 1458cm^{-1} (m), $\nu_{as(scissors)}(CH_2)$ 1439cm^{-1} (w), $\nu_{s(wag)}(CH_2)$ 1371cm^{-1} (m), $\nu(C\text{-}N)$1238cm^{-1} (s), $\nu_{wag}(CH_2)$ 1047 cm^{-1} (w), $\nu_{stretch}(N\text{-}C)$ 1007cm^{-1} (s), $\nu_{stretch}(N\text{-}C)$ 812cm^{-1} (s). This molecule possesses high symmetry, which can lead to a displacement on the wavelengths of the bands respect to the literature[113, 114].

The spectrum of but-2-yne-1,4-diol (**figure 52**) contains as bands: $\nu_{stretch}$(OH) 3279-3163 cm^{-1} (s, b), $\nu_{stretch}$(-CH$_2$-) 2928 cm^{-1} (m,sh), $\nu_{scissors,bend}$(-CH$_2$-) 1443cm^{-1} (m). As the alkyne is symmetrical the stretching frequency due to the C≡C bonding may be absent. In this case a rather weak peak is detectable and it could not be clearly assigned to the C≡C bond.

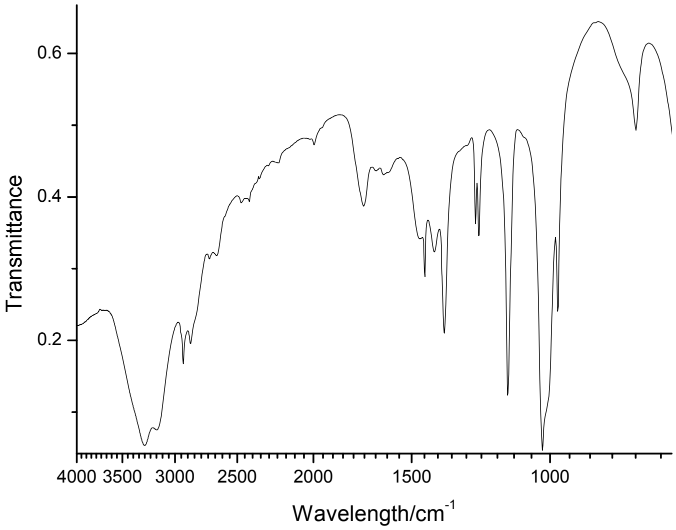

Figure 52. IR spectrum of BD.

The spectrum of *N*,*N*'-diisopropylthiourea (**figure 53**) was made using the spectra of allylthiourea and ethylthiourea as a guide and containing the bands[115]: ν(NH) 3285-3221 cm^{-1} (s, b); ν_s(CH) 3018 cm^{-1} (s); ν_{as}(CH$_3$) 2970 cm^{-1} (s); ν_s(CH$_3$) 2873 cm^{-1} (s); ν(CN), δ(NCN), ν(CS) 1562 cm^{-1} (vs, b), 1517 (vs) cm^{-1}; ν_{as}(CN) 1409cm^{-1} (m); δ_{as}(CH$_3$) 1384 cm^{-1}(m); δ_s(CH$_3$) 1313 cm^{-1}(s); δ(NH) 1263cm^{-1}(s); ν(CN), ν_s(CN) 1169cm^{-1}(s); mainly skeletal vibrations 982 cm^{-1}(s), 930 cm^{-1}(m). The peaks at 743cm^{-1}, 650cm^{-1}, 596cm^{-1}, 573 cm^{-1}, 480 cm^{-1} and 453cm^{-1} could be due to different CS, CNC, SCN, CN and NH vibration modes. The bands due to the symmetric and anti-symmetric NH stretching are broad and not completely resolved in the region of 3300-3000 cm^{-1}, which could be due to intermolecular hydrogen bridges.

The spectrum of dipropylene glycol dimethyl ether (**figure 54**) was found to contain[116]: ν(CH$_3$-, -CH$_2$-, -CH-) 2974-2822 cm^{-1} (s), ν(CH$_3$-, -CH$_2$-, -CH-) 1452-1352 cm^{-1}(s), ν_s(C-O-C) 1109 cm^{-1} (vs, b), ρ(CH$_3$-, -CH$_2$-, -CH-) 906-817 cm^{-1}. The fact that the alkyl peaks are found between 2974 and 2822 cm^{-1} and below 3000 cm^{-1} confirms the absence of C=C or aromatic carbons. These peaks are normally strong and multi-banded due to symmetrical and asymmetrical stretching as well as to differences between primary, secondary and tertiary carbons. The peaks due to the presence of ether function are normally prominent like the one found at 1109 cm^{-1}. The peak found at 1173 cm^{-1} is probably due to the methyl groups.

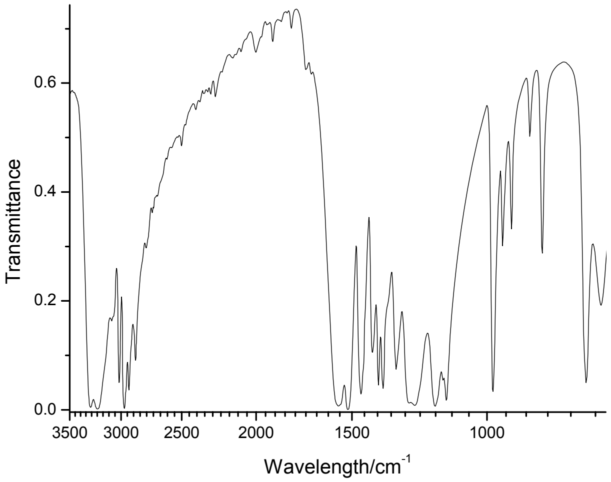

Figure 53. IR spectrum of DITU.

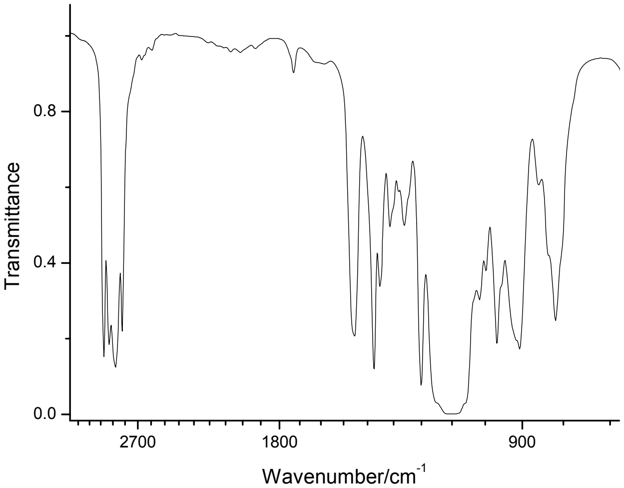

Figure 54. IR spectrum of DPGDME .

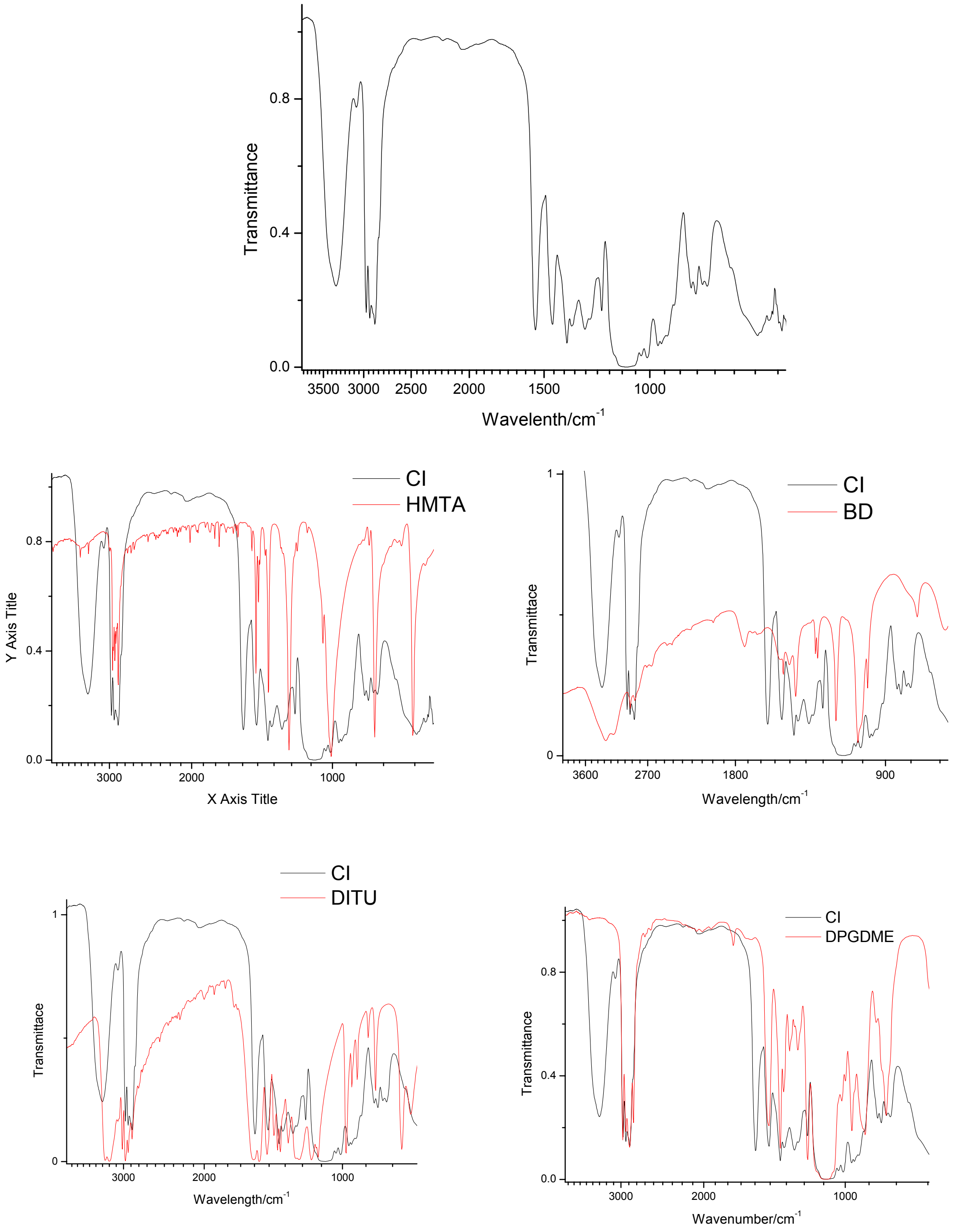

Figure 55. IR spectrum of CI and superposition of the IR spectra of the individual components.

In **figure 55** the spectrum of CI is shown as well as the superposition of the IR spectra obtained from each of the individual compounds to compare it with it.

The bands observed in the spectrum of CI are usually very broad and not very well resolved. This may be due to the superposition of several spectral bands at the same time, due to the different compounds present in the sample.

The bands in the spectrum of CI in some cases seem to be displaced in wavenumber from the bands found in the spectra of the compounds. This may be due to the interactions between the different components in the commercially available mixture. Also the very broad bands observed in the spectra of CI make it difficult to relate to the peaks found the other spectra.

4.2.1.1 Summary

In **table 9** the contribution of the different molecules to the bands found in the IR spectrum of the CI is shown.

CI	HMTA	BD	DITU	DPGMDE
3337		OH	NH	
2970-2873	CN	CH_2	CH_3, CH_2	CH_3, CH_2, CH
1551			CS, CN, NCN	
1425	CH_2	CH_2	CH	CH_3, CH_2, CH
1375	CH_2			CH_3, CH_2, CH
1350				Alkyl chain
1253	CH_2		NH	
1101				COC
1034	CH_2			
1009	CN			
968-957			CH	
852-837			CH	
813				CH_3, CH_2, CH
659			CN	

Table 9. Bands in the spectrum of CI resulting from the different individual compounds.

4.2.2 Weight loss experiments

Weight loss experiments have been carried out in order to study the effects of the use of inhibitors under real pickling conditions in the case of H_2SO_4 bath at 95ºC.

The first experiments were carried out with hot rolled (HR) steels and the pickling inhibitor HMTA. In **figure 56** the results obtained with hot rolled and cold rolled steel are shown. Therefore the corrected corrosion rates are plotted versus the inhibitor concentrations selectd.

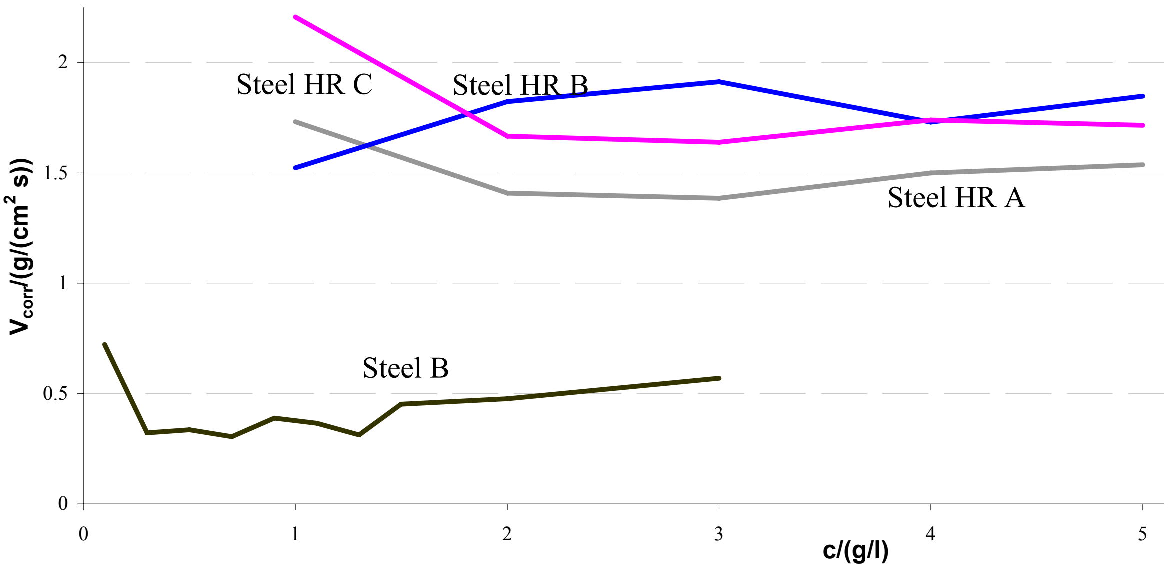

Figure 56. Pickling experiments carried out with HMTA comparing the effects on hot rolled (steels HR A, HR B , HR C) and cold rolled steels (steel B).

In the case of the hot rolled materials (steels HR), it can be seen how the corrosion reaction rate is always higher than for the cold rolled steel (steel B), which shows that the inhibitor more absorbs on the steel surface than on the oxide scale.

As it can be seen in the graphic, in the case of the cold rolled steel a much lower corrosion rate is obtained. This can be understood as the inhibitor is likely to cover the steel surface better, minimizing the lost of material.

Considering these results, further experiments were carried out with cold rolled steels and the effects of inhibitors on the material weight loss will be shown. A comparison of the different inhibitors is given in **figure 57**. Pickling was done with steel C while using the inhibitors DITU, KI and CI and with steel B for the case of all other substances.

At first it can be seen from the graph that all substances tested are protecting the material from dissolution and behave as corrosion inhibitors. Only with DPGDME a slightly lower value for the inhibitory efficiency was found at low concentrations but when its concentration increases it still behave as an inhibitor.

Nevertheless in **figure 57** two groups can be distinguished. There are inhibitors with low inhibitive capacity (DPGDME, DPTU and HMTA) and inhibitors with higher inhibitive capacity (BD, DMTU, DETU, DITU, KI and CI). Especially DPGDME and HMTA have not such a big inhibitive effect as all other substances and it is even noticeable how from a concentration of 1.3 g/l onwards the effect of HMTA starts to be the opposite as desired: the inhibitory efficiency turns out slightly decreased. The case of DPTU is very particular. At concentrations lower than 1.1 g/l the effectiveness of the compound is poor and comparable to that of DPGDME but from 1.1 g/l onwards it seems to exert a high inhibitive effect.

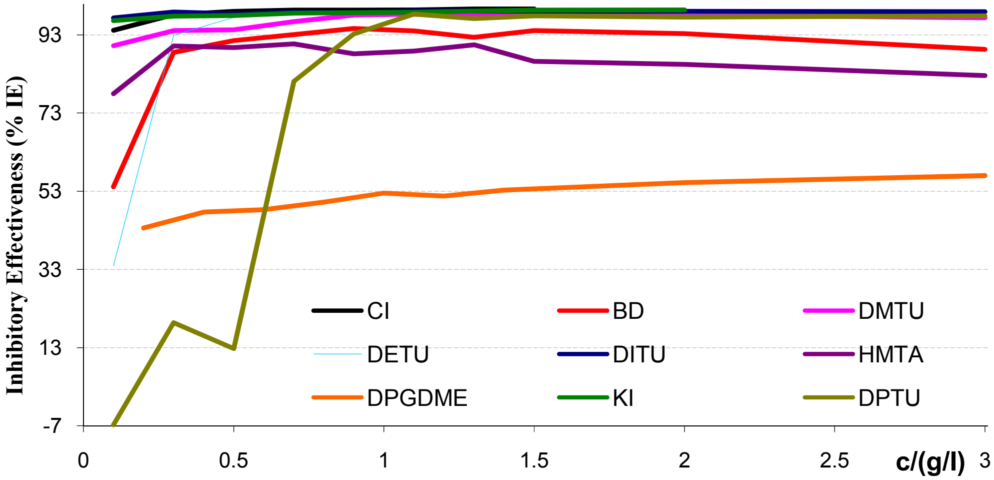

Figure 57. Results of weight loss experiments for different inhibitors in the pickling of cold rolled steels with H_2SO_4 at 95ºC.

In **figure 58** the behaviour of CI, KI, DITU, BD, DETU and DMTU is shown more in detail so that the differences in behaviour between the different substances can be evaluated more easily.

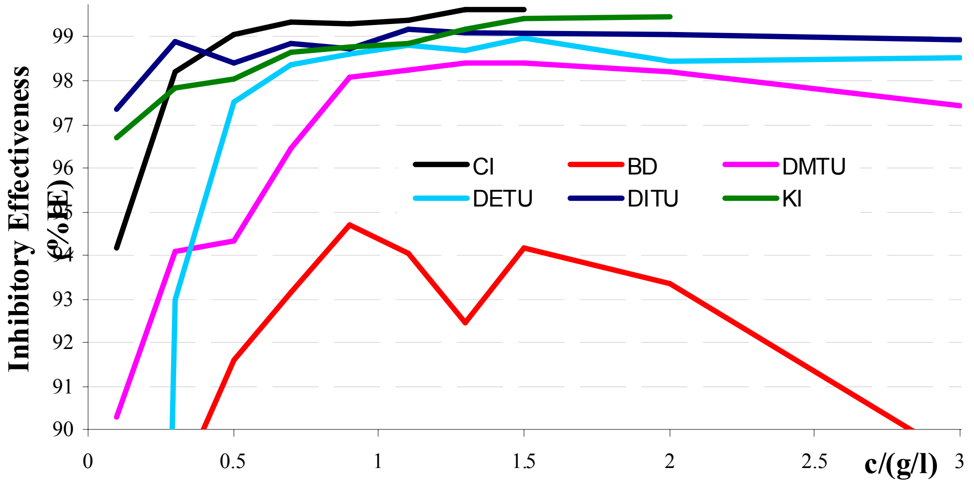

Figure 58. Curves obtained for the substances with pronounced inhibitor behaviour in the case of pickling experiments with cold rolled steels in H_2SO_4 at 95ºC.

CI has been found to be the most effective inhibitor from a concentration of 1.0 g/l onwards. The effects in the case of KI and DITU are almost comparable while BD seems to be the less effective substance of the group in the case of pickling with H_2SO_4. Nevertheless, it is generally considered to be a highly effective inhibitor.

In **figure 59** the curves obtained with the three thiourea containing substances (DPTU, DITU, DETU and DMTU) are shown. It can be seen that in the case of the aliphatic molecules the corrosion rate decreases with a longer lateral chain (DITU < DETU < DMTU). This means that when the surface is more effectively protected and less material is lost the molecular weight of the molecules increases and the lateral chain is longer. This effect was also observed by *Hoar and Holliday*[70] when the same substances were tested in the case of H_2SO_4 and with mild steel as material. They proposed, that the fact that the reaction becomes slower with the enlargement of the molecule is due to the molecule being a more stable spatial blocker of surface during the adsorption-desorption equilibrium and to its better covering the surface. The trend is not followed by DPTU. The reactivity of this substance may have been changed by the presence of the aromatic groups and its solubility in the solution is also much lower.

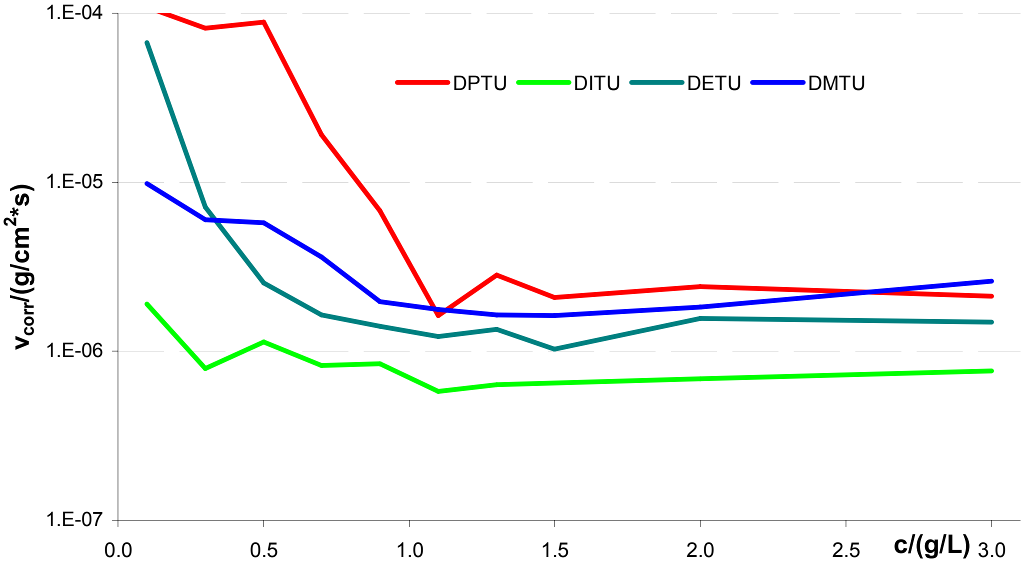

Figure 59. Corrosion rate curves when using the three thiourea containing inhibitors in the pickling of steels B (DMTU, DETU, DPTU) and C (DITU) in H_2SO_4 at 95ºC.

In **figure 60** a comparison of the picklings when using DITU, DPGDME as inhibitors and in the case of DITU dissolved in DPGDME is shown, which allows it to test if the effect thiourea can be improved by the presence of DPGDME.

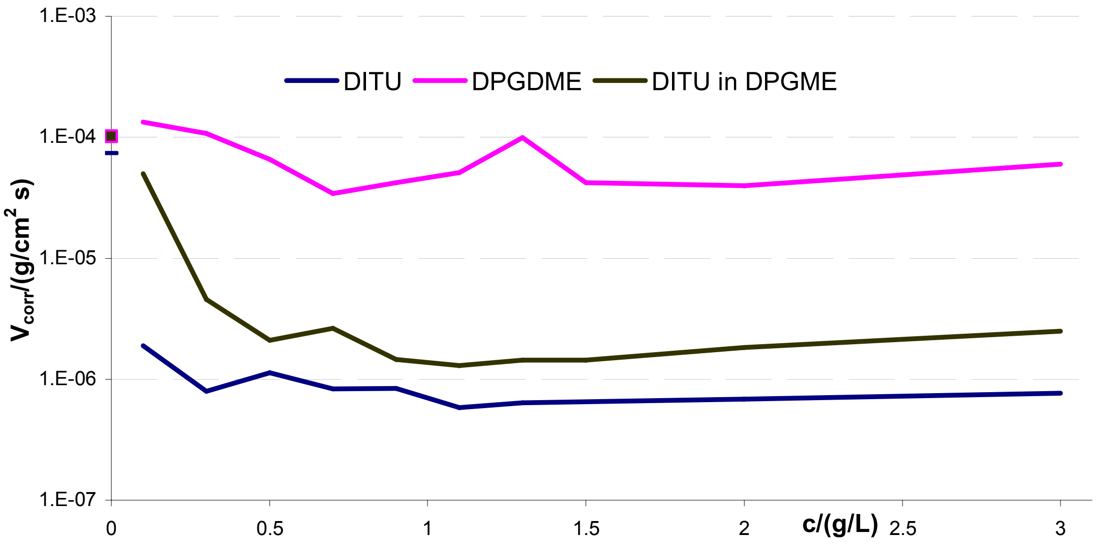

Figure 60. Comparisson of corrosion rate in the case of pickling in the presence of DITU and DPGME and of DITU dissolved in DPGDME.

In **figure 60** it is shown that the pickling with DPGDME only is higher than when DITU is added. However, it is still worse than when only DITU is used. At low concentrations the compounds mixture have a low effect on the corrosion rate but with the increasing concentration the pickling effects tend to become equal. The differences could be related also to differences in the steels used as well as with the presence of DPGDME.

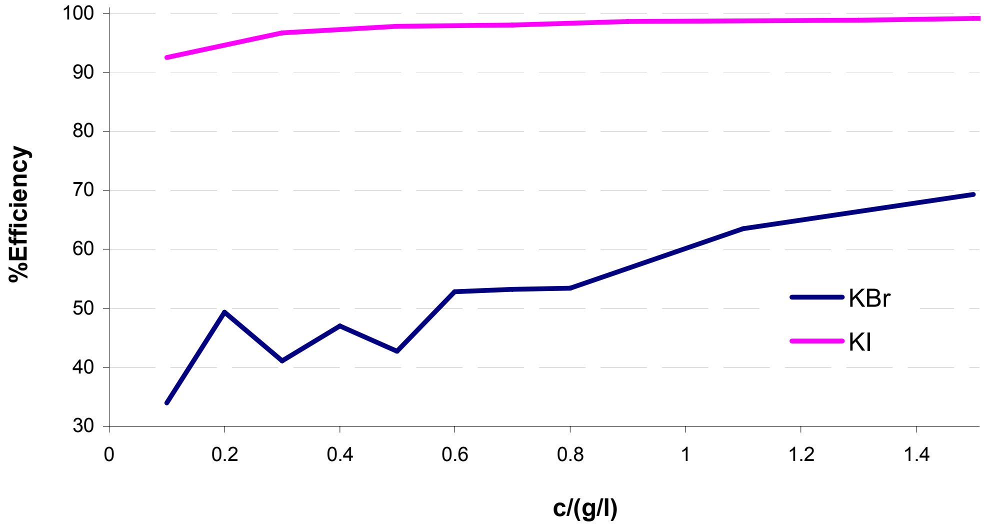

Figure 61. Inhibitory effects of KI and KBr.

In **figure 61** the effect of KBr and KI is shown on the pickling behaviour for steels in the case of H_2SO_4 acid is compared. It can be seen how the protection against corrosion is much higher in the case of KI than for KBr. This confirms the results described in *section 2.1.5.4*.
Assays using KI in the pickling with HCl for different steels at room temperature gave similar results to those found here[117].

4.2.2.1 Experiments with 2-butyne-1,4-diol but at different temperatures

In **figure 62** the effectiveness of BD as inhibitor in H_2SO_4 at different temperatures is shown. It can be observed that the effectiveness decreases slightly with the temperature. At the lowest temperature (15°C) the data obtained are very irregular and no tendency could be observed.

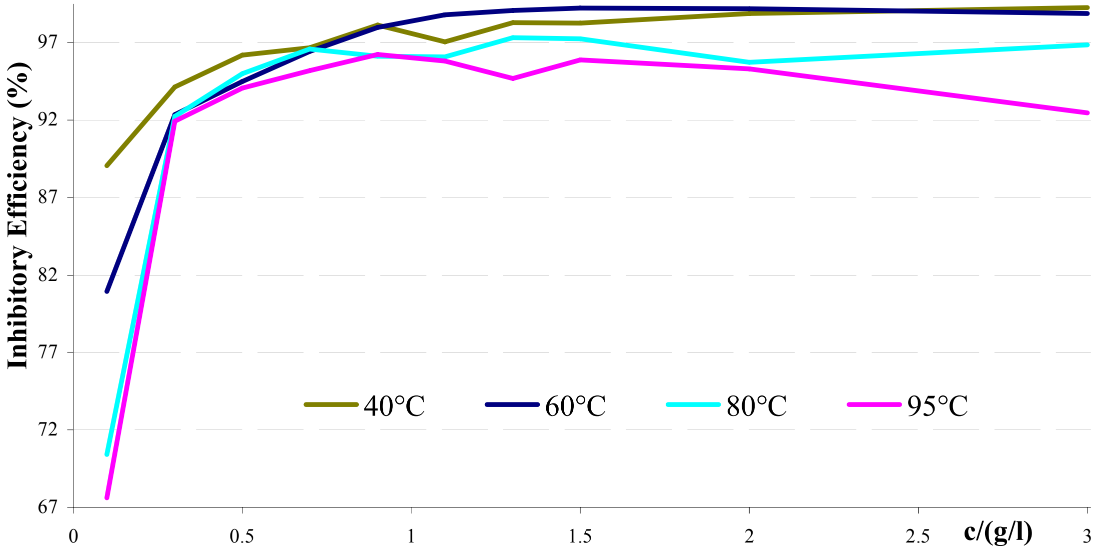

Figure 62. Effectiveness of the inhibitor BD at different temperatures.

For the experiments made at different temperatures an Arrhenius plot can be made so as to show the changes of the activation energy with the temperature. The fact that the effectiveness of the inhibition decreases with the temperature is related to the fact that its desorption increases with the temperatures[118]. In **figure 63** the Arrhenius plots are shown to become confluent at concentrations higher than 0.9 g/l. This is in agreement with the fact that the inhibitory effectiveness reaches a steady state around a concentration of 1.1g/l.

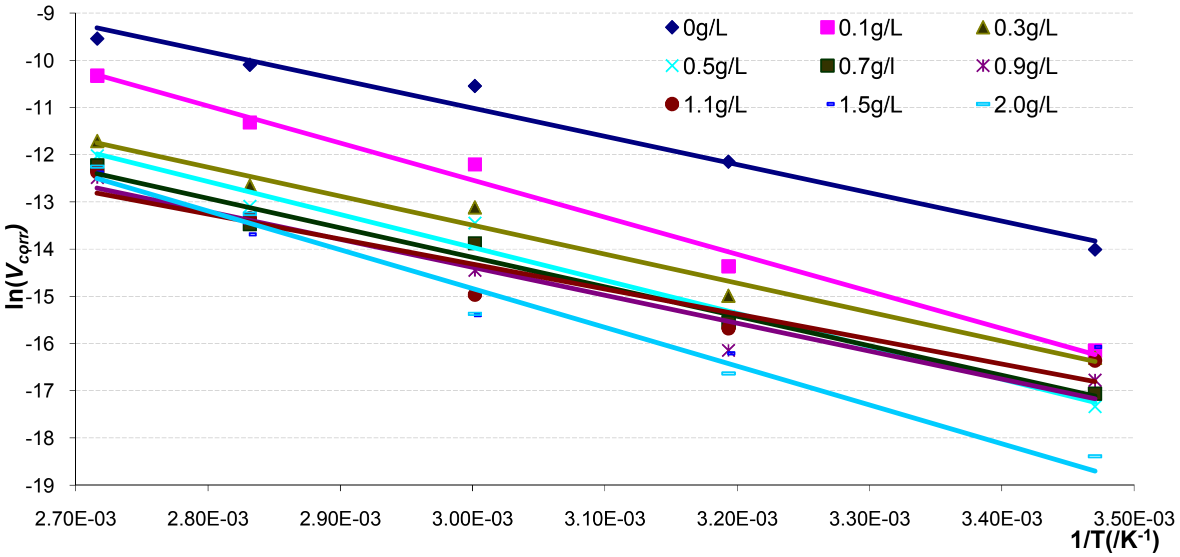

Figure 63. Arrehnius plots for the calculation of the activation energy (E_a) of the inhibition reaction.

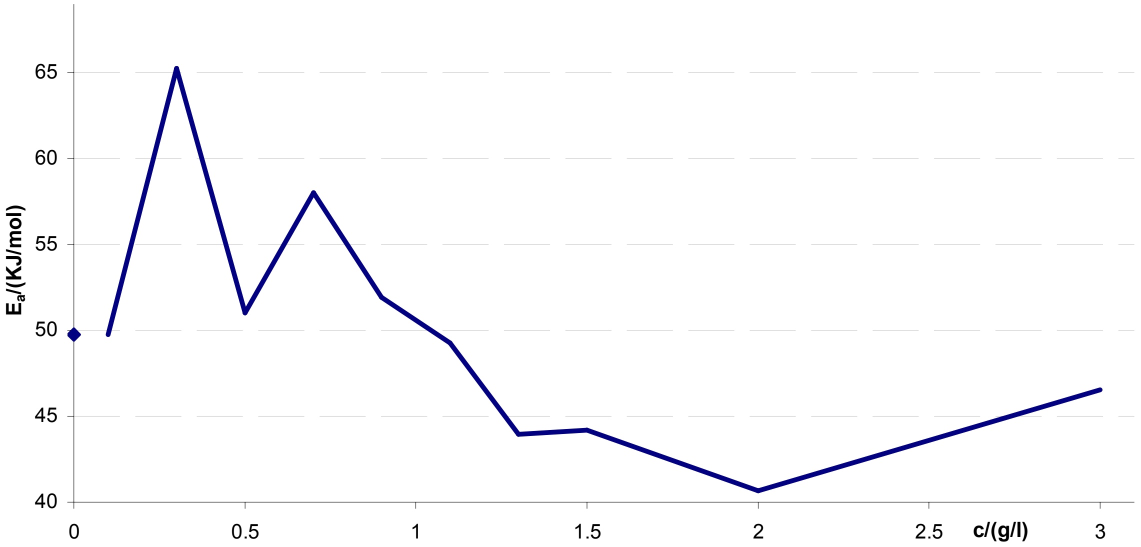

Figure 64. Changes of the activation energy of the activation reaction with the concentration of BD.

It can be seen in **figure 64** that the activation energy behaves very irregularly. The influence of the temperature in the side reactions taking place is an important factor. These side reactions depend as well on the particular structure of the studied acetylene derivate. There are not enough detailed studies so that a relation between the temperature, the acetyl derivate structure and the reactions taking place can be established. Therefore is not possible to compare the inhibition of BD at the different temperatures[68-69].

The activation energy (E_a) at low concentrations goes below that for a solution without inhibitor (49.75 KJ/mol) which is well in agreement with the value given in the literature (46.7 kJ/mol) [119]. This type of inhibition retards the corrosion process at ambient temperatures whereas the inhibition is lower at high temperatures as it is shown in figure **62**.

From an inhibitor concentration of 0.7 g/l onwards the activation energies are mostly below the value in the absence of an inhibitor. Similar results were described by Sanad *et al.*[117] for the case of KI in HCl at different temperatures for different steels. According to several authors[117] these results are related to the strong interaction and the increasing portion of covered surface with the increasing temperature. However in our case this seems not to apply as since the effectiveness of the inhibition decreases with the temperature (**figure 62**).

4.2.2.2 Modelling of the weight loss data

The data obtained for the corrosion rates can be used to study the nature of the interaction between the molecules and the steel surface. Here several models are tested in order to describe the system best.

Langmuir adsorption model

In **figure 65** the Langmuir isotherms for the case of the commercially available inhibitor (CI) and its components (DITU, BD, KI and HMTA) are represented. They have been obtained by applying the equations in *section 2.2.5.2.1*.

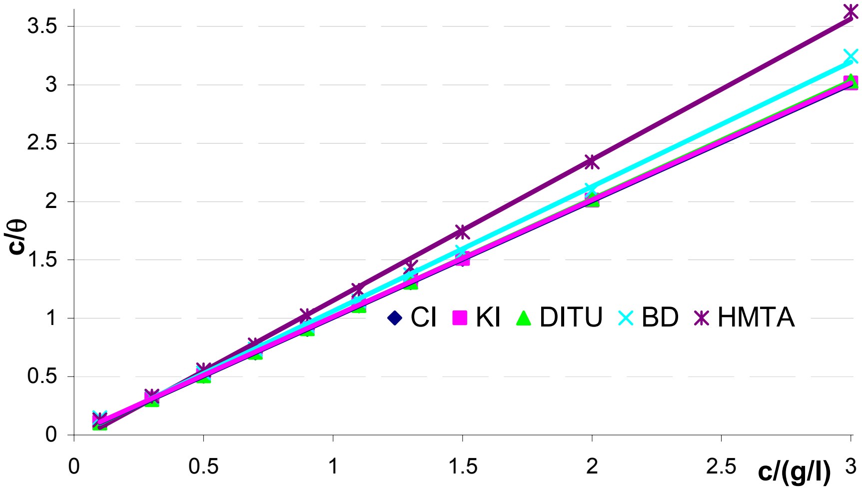

Figure 65. Langmuir isotherms obtained from the weight loss data for the inhibitor CI and for its main components (BD and HMTA for steel B and for CI, KI and DITU for steel C).

The fittings of the data for the different compounds to the Langmuir model are shown to be very good. The R^2 factor and the slopes for the different compounds are very close to one. The free energy of interaction between each single compound or the commercially available inhibitor and the steel surface can be obtained from the coordinate at the origin. The interaction is considered to be a physisorption as the free energy obtained is less negative than -50 kJ/mol [120].

The values obtained from the isotherms represented in **figure 65** for the different inhibitors are shown in **table 10**.

Comp./parameters	Obtained function	R^2	*slope*	*1/k*	*k*	ΔG/(KJ/mol)
CI	y = x + 0.0056	1.000	1	0.0056	178.57	-15.9
KI	y = 1.0019x + 0.0102	1.000	1.0019	0.0102	98.04	-14.3
DITU	y = 1.0098x + 0.001	1.000	1.0098	0.001	1000.00	-21.3
BD	y = 1.067x - 0.0059	0.999	1.067	0.0059	169.49	-15.7
HMTA	y = 1.2075x - 0.0572	0.998	1.2075	0.0572	17.48	-8.8

Table 10. Parameters obtained from Langmuir isotherms for CI and its components.

The isotherms obtained for the pickling in the presence of BD as inhibitor and different temperatures (with steel B) are shown in **figure 66**.

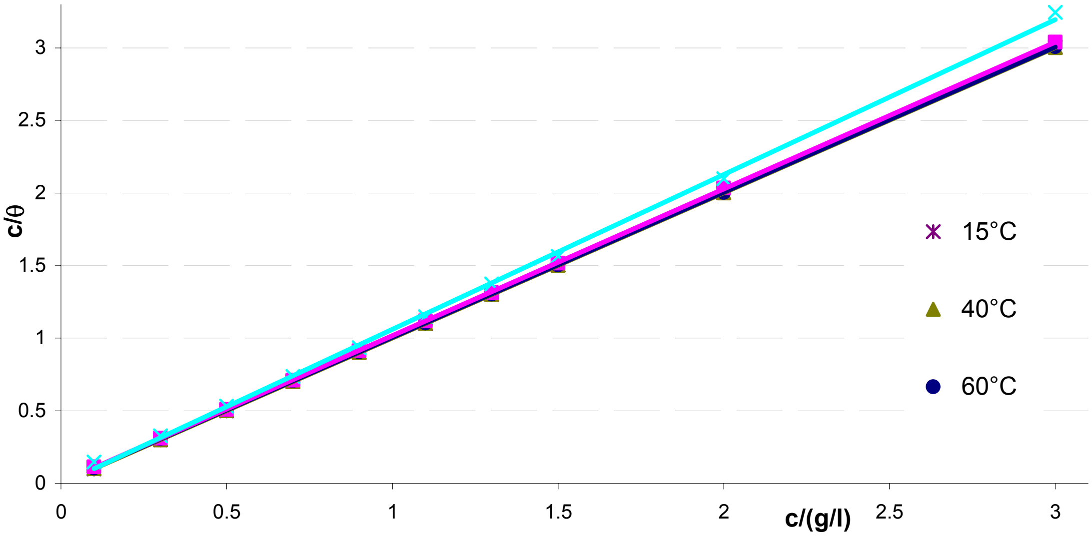

Figure 66. Langmuir isotherms obtained from the data for the pickling in the presence of BD as inhibitor and steel B at different temperatures.

The values obtained from isotherms in **figure 66** can be seen in **table 11**.

T/°C	Function	R^2	Slope	1/*k*	*k*	ΔG/(kJ/mol)
15	y = 1.0012x - 0.0004	1.000	1.0012	0.0004	2500.00	-23.94
40	y = 1.0001x + 0.0009	1.000	1.0001	0.0009	1111.11	-21.46
60	y = 1.0003x + 0.0049	1.000	1.0003	0.0049	204.08	-16.27
80	y = 1.0108x + 0.0058	1.000	1.0108	0.0058	172.41	-15.76
95	y = 1.067x - 0.0059	0.999	1.067	0.0059	169.49	-15.70

Table 11. Parameters from Langmuir isotherms for pickling in the presence of BD as inhibitor.

From the free energies listed in **table 11** it can be seen that at higher temperatures the interaction between BD and the steel surface decreases. This can be explained from the higher kinetic energies of the molecules at higher temperatures, which decrease these attractions. These results agree with the weight loss experiments an increase of the weight loss with the temperature was found.

4.2.2.3 Summary

All components of the commercially available inhibitor were shown to behave as pickling inhibitors under real conditions (20 % H_2SO_4, 95ºC). Some of these substances presented higher inhibitive action. DITU, BD, KI and CI hindrance at most the aggression on the steel.
DMTU and DETU, DITU analogues which contain the thiourea functionality, behaved as good inhibitors under pickling conditions. The molecules were shown to provide higher protection the longer the lateral chain.
Experiments of BD at different temperatures manifested BD’s decreasing efficiency as the temperature raised. The irregular activation energy obtained from the Arrhenius treatment can be explained by the different side reactions taking place at the different temperatures.
When modelling the weight loss data it was observed that only the Langmuir treatment is valid to theoretically explain the behaviour of the tested compounds. This model established physisorption as the kind of interaction taking place between the inhibitors and the surface.

4.2.3 Electrochemical experiments

Different electrochemical experiments were made in the presence of the inhibitors and the results of changes in inhibitor and their concentrations influence the electrochemical behaviour of the material in different pickling solutions as shown in the next sections. Two different pickling solutions were used: a solution of 0.5 % $FeSO_4$ (pH=5.5) and a commercially available solution pH=1 (Titrisol® buffer solution of glycine-HCl at pH=1.00±0.02 (20°C). Merck). This solution was used to work at a low pH as compared to the solution used in the pickling plants. However this solution is less aggressive than H_2SO_4, which prevents the instruments from potential damage.

In order to visualize the resulting corrosion environment, some weight lost experiments at the different conditions were carried out and the results shown in **figure 67**.

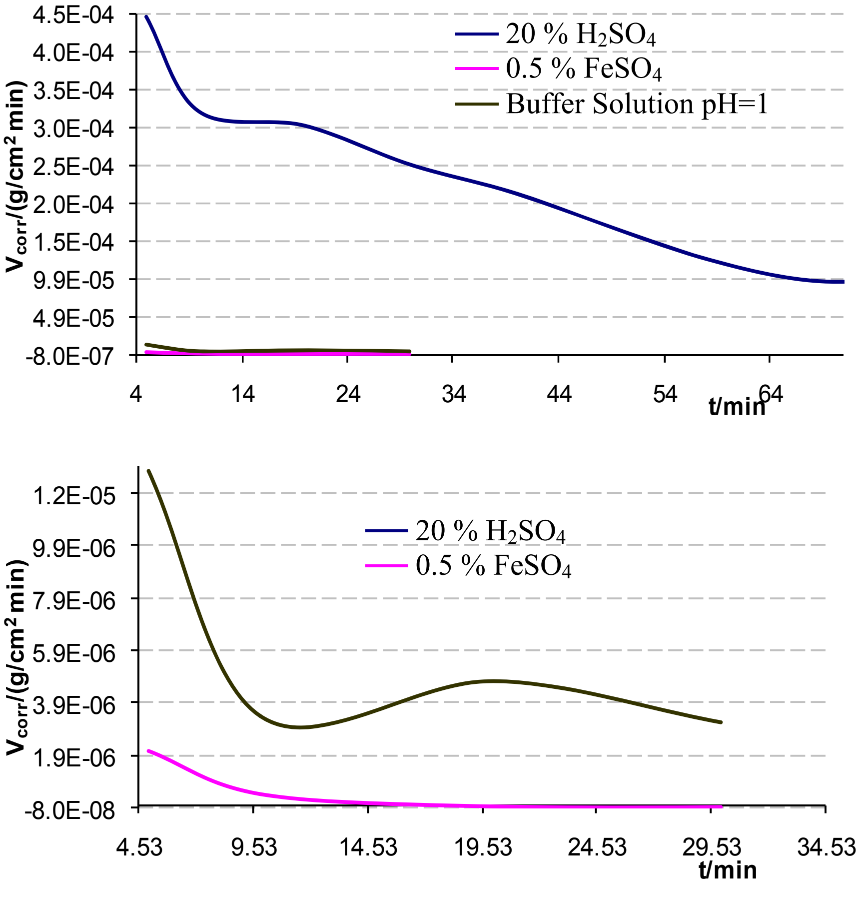

Figure 67. Effect of the different pickling solutions on the corrosion rates.

From the results in **figure 67** it can be concluded that a solution of 20 % of H_2SO_4 is more aggressive and leads to a higher corrosion rate than the other two solutions. For the three pickling solutions there is a decrease in the corrosion rate with time. This is understandable from the formation of a passivation layer and this is consistent with the SNMS analysis results (*section 4.1.2*) which showed that the increased amounts of insoluble elements were present on the surface. The corrosion rate in the case of 0.5 % of $FeSO_4$ becomes even negative values as the steel gains weight. This could be explained in terms of a corrosion of the material and the formation of iron oxides which are heavier than the iron itself. Another possible explanation could be the formation of a chemisorbed Fe_{bulk}-SO_4 species, which indeed was observed in H_2SO_4 (see *section 4.2.4.2*).

4.2.3.1 Open circuit potential measurements (OCP)

The OCP curves obtained at different concentrations in the two different used pickling solutions for each tested inhibitor are compared.

In **figure 68** the OCPs measured for CI at pH=1 and at pH=5.5 with the steel B are shown. A close look on the results shows that the OCPs rise around 200mV for the case of a solution at pH=1. The main difference between the two series of measurements is that at pH=1 the OCP increases slightly once the sample is introduced in the solution and reaches a steady state. At pH=5.5 this steady state is not reached and the OCP decreases during the measurement time. This phenomenon can be found back also in the curve corresponding to the solution without inhibitor. This means that the activity of the surface is increasing the longer it stays in the solution. The relation of these results with the corrosion rate that has been discussed in *section 4.2.3* shows that in a solution with 0.5 % $FeSO_4$ a layer is deposited onto the material. It makes the surface more reactive and corrosion products, which are heavier than the original material, are formed. The presence of CI as inhibitor decreases the reactivity of the surface the higher its concentrations. However the protection is not that good at pH=5.5 as compared to pH=1, which is probably due to the poorer adsorption of the inhibitors to the layer created and to the lower attraction between the inhibitor (with different structure than at pH=1) and the steel in this pickling solution.

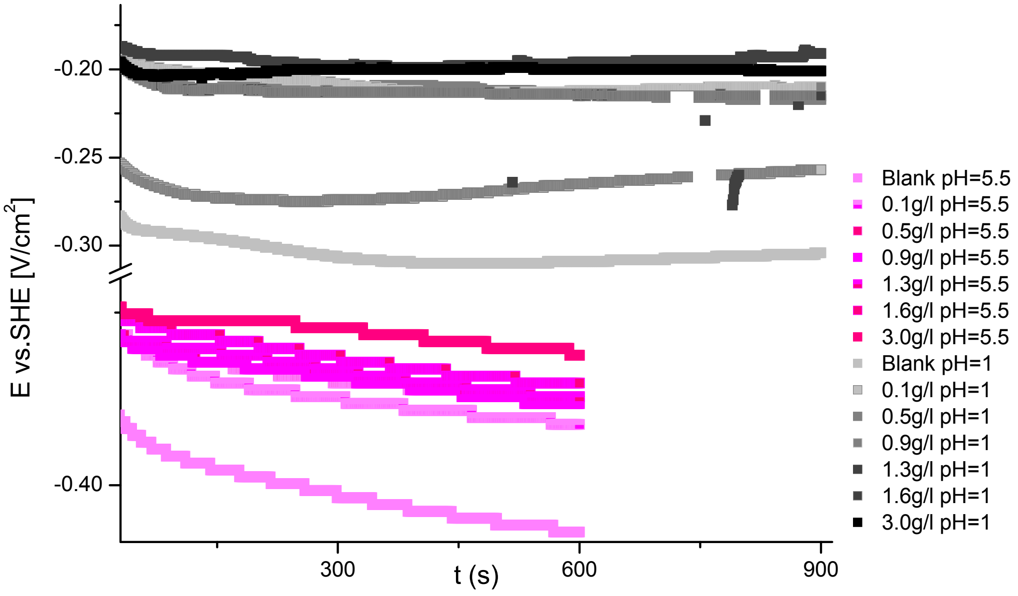

Figure 68. OCP curves measured for steel B in the case of the inhibitor CI at pH=1 and at pH=5.5.

OCP curves obtained for other inhibitors are comparable to those in **figure 68**.

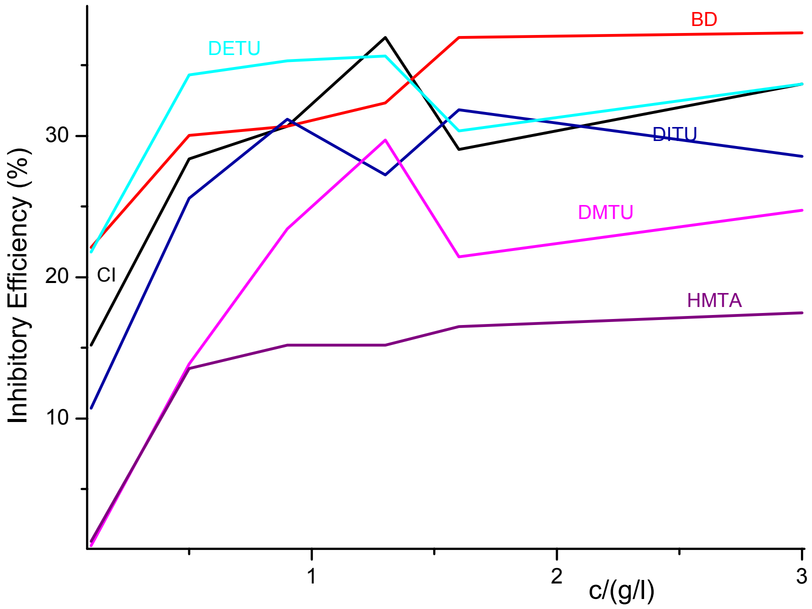

Figure 69. Inhibitory efficiency values obtained for all tested inhibitors with steel B in the pickling solution at pH=1.

In **figure 69** the effectiveness calculated from the OCP values (see *section 2.2.5.1*) obtained for the case of both pickling solutions and the different inhibitors are shown. A negative value of the inhibitory efficiency is obtained when the OCP value for the relevant compound is more negative than the OCP value for the solution without inhibitors.

In general, it can be concluded that the behaviour of the inhibitors improve at pH=1 and this improvement could be both due to the influence of the pickling solution on the steel or to a more effective action in the case of the inhibitor. As mentioned previously, the difference of the obtained results could be due to differences in the activity of the surface at which the inhibitors can adhere more or less [40,72]. The influence of the concentration was found to be always higher at pH=1.

In the group of the most powerful inhibitors DMTU and DITU are shown to be the less effective ones at both pHs and BD, DETU and CI are shown to give the best results for both pickling solutions.

The effectiveness of the inhibitors themselves was found to be greatly different for that obtained from the weight loss experiments (*section 4.2.3*). Besides the fact that there were differences for the solutions used it is also remarkable to see that there is an influence of the temperature (see *section 4.2.2.1*). The fact that the inhibitors have a lower protective behaviour at pH=5.5 can be attributed mainly to two facts:

- the interaction between the structure of the inhibitor and the state of the surface
- the formation of oxides or iron complexes (with the sulphate ion, for example). This would be consistent with the results given in *section 4.2.3*. The inhibitors then stick to the metallic surface but not to the oxides or to other formed compounds.

For the thiourea containing compounds it can be seen how DETU gives a higher OCP than DMTU in both pickling solutions, while in DITU its values drop and at pH=5.5 with DPTU the OCP is even lower. An explanation for this could be the insolubility of the inhibitors as a result of the length and the nature (aromatic groups) of their lateral chains.

The increase of the effectiveness with the length of the lateral chain (for DETU and DMTU) was also found by *Makrides* and *Hackerman*[121] for the case of TU (**figure 70**) and DMTU.

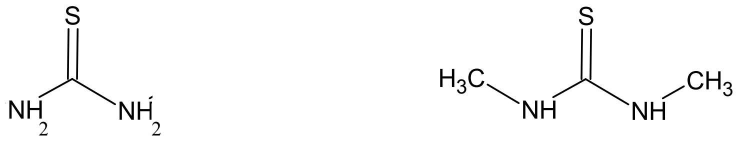

A **B**

Figure 70. Molecular structures for TU (thiourea) (**A**) and DMTU (*N*,*N'*-dimethylthiourea) (**B**).

The potentials that *Makrides* and *Hackerman* obtained in a solution of H_2SO_4 were compared and it was observed that the larger compound (DMTU) was giving more noble potentials than

TU. The form of the curves was nevertheless different from those obtained in our experiments, as the potentials were more negative at increasing concentrations.

The treatment of the data with the Langmuir adsorption model gave no suitable result. Even despite the values of the correlation coefficients were not that bad the deviation of the slope from 1 was not acceptable. This means that under the conditions the experiments were made the behaviour of the inhibitors cannot be described with the Langmuir model.

Nevertheless, a comparison of the Langmuir isotherms for the data of the experiments with BD at room temperature in 20 % of H_2SO_4 with those obtained from OCP measurements in 0.5 % $FeSO_4$ and the commercially available buffer solution of pH=1 can give an idea of how the different solutions affect the adsorption of the inhibitors. In **figure 71** the different Langmuir isotherms are shown and in **table 12** the parameters corresponding to these isotherms are listed.

Solution	**Function**	**R^2**	**Slope**	**1/*k***	***k***	**ΔG/(kJ/mol)**
20% H_2SO_4	y = 1.0012x - 0.0004	1.0000	1.00	0.0004	2500	-23.94
Buffer pH=1	y = 2.5717x + 0.4018	0.9940	2.57	0.4018	2.49	-2.79
0.5% $FeSO_4$	y = 19.511x + 0.092	0.9963	19.51	0.0920	10.87	-7.30

Table 12. Parameters for the Langmuir isotherms given in **figure 71**.

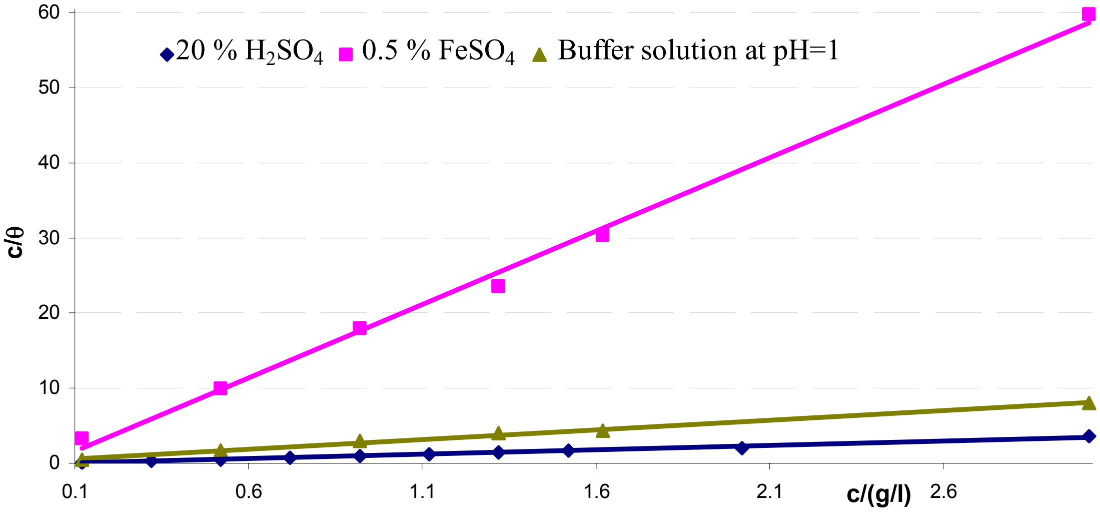

Figure 71. Langmuir isotherms obtained m BD in the case of steel B at room temperature with different pickling solutions..

As expected, the isotherms for the case of 20 % H_2SO_4 and a buffer at pH=1 are similar but the one obtained for 0.5 % $FeSO_4$ is largely different from the remaining two.

It can be said that in H_2SO_4 20% the compound accurately behaves as expected from a Langmuir adsorption model. For the case of the other two solutions, the correlation coefficient is close to one but the slope differs by 79 % in the case of the buffer at pH=1 and by 925 %, in the case of 0.5 % $FeSO_4$ and these deviations are unacceptable.

While in the case BD 20 % H_2SO_4 an adsorption according to Langmuir takes place, the behaviour deviates from this model when a commercially available mixture in a buffer solution of pH=1 is used and the model turns to be completely invalid for a solution of 0.5 % $FeSO_4$.

4.2.3.2 Polarization curves

For the recording of the polarization curves a potential is applied between the steel and the counter electrode and changes of the current density generated are measured. The application of a potential changes the system and has an influence on the sample surface. Studies of the surfaces composition by means of XPS were made in order to study these effects.

4.2.3.2.1 Study of the compositional changes of the surface induced by application of a potential

These experiments were made while keeping the potential during 2 minutes at -0.337 V and immersing a sample of steel B in a solution of 0.5% $FeSO_4$. At this potential an oxidation and a dissolution of the metal are taking place. The experiments were made to see how the surface is affected by the application of a potential and to check if a change of the behaviour of the inhibitor takes place.

For the components, BD and KI, concentrations of 0.1, 0.5 and 0.9 g/l were used. The experiment made with a concentration of 0.1 g/l of BD show that the system is not really stable, as for the two samples at the same conditions significantly different in the results were obtained.

The results for BD are shown in **figure 72**.

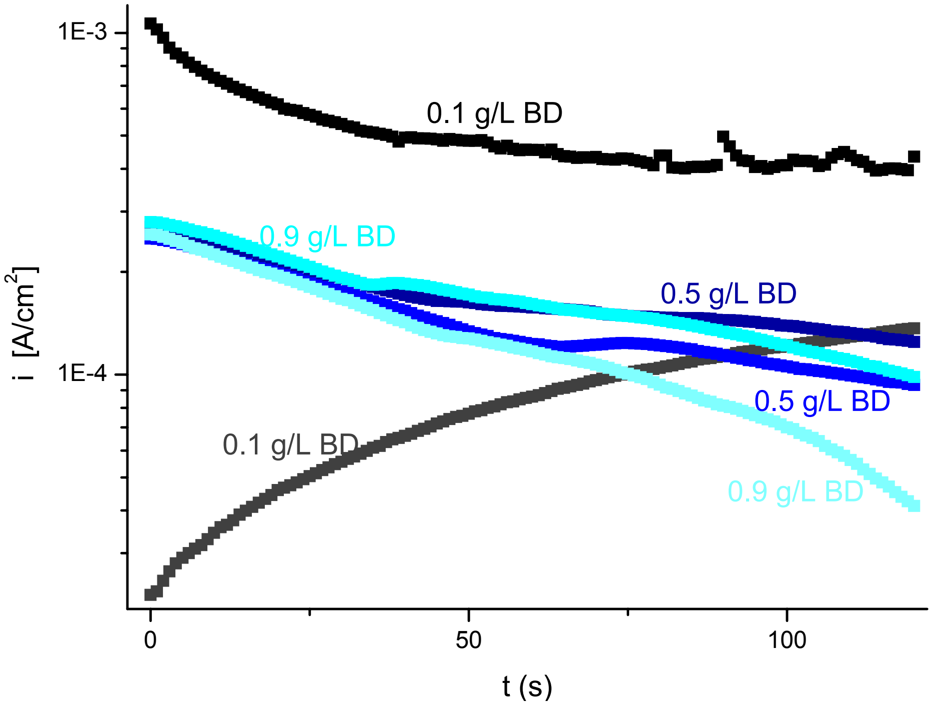

Figure 72. Current density versus time. Curves obtained when -0.337 V are applied during 2 in a BD containing solution.

When the first result, which seems to be out of the range, is not taken into account it can be seen that the current density decreases with time. Also at an increasing concentration of the tested component the current density seems to decrease.

In the case of the KI the results are the represented in **figure 73**:

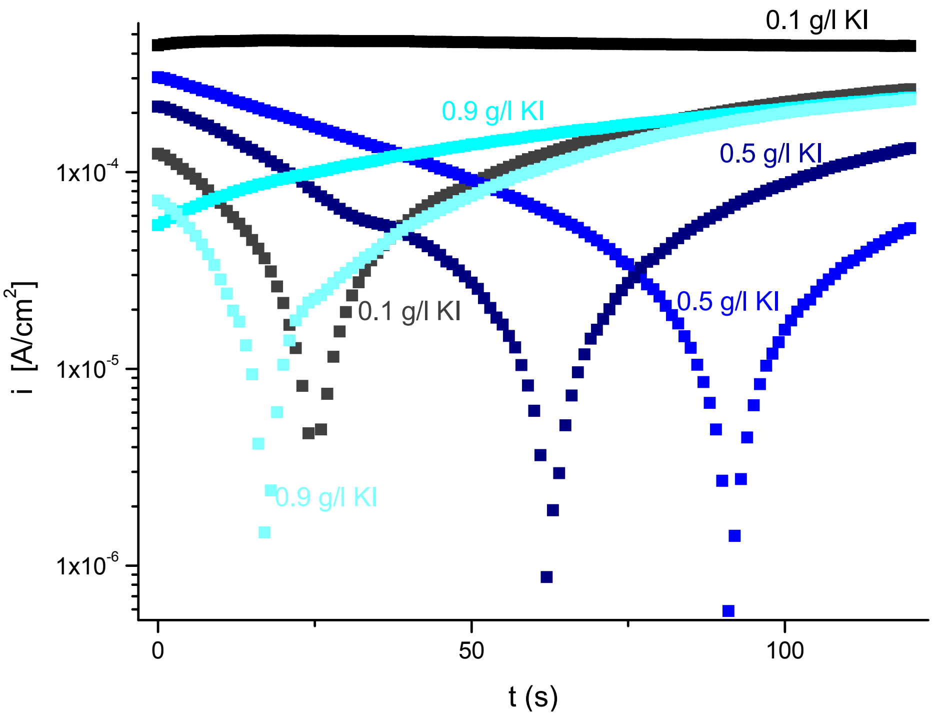

Figure 73. Current density versus time. Curves obtained when -0.337 V are applied during 2 minutes in a KI containing solution.

The graphs have the form of a polarization curve, where the currents are measured in the anodic branch. Generally the current density tends to decrease with the concentration. The current density for the case of a 0.9 g/l concentration of the inhibitor is higher than the one obtained for a concentration of 0.5 g/l.

The influences of the potential of -0.337 V on the surface as studied by XPS measurements can be summarized as follows:

- **S**: With both inhibitors its presence increases when applying a potential (**figure 74 A**).
- **Mn**: In the case of BD, the presence of Mn at surface is higher applying a potential. In the case of the KI it depends on the concentration: at higher concentrations the presence of Mn is higher when the potential is applied and at lower concentrations it is higher without the potential applied (**figure 74 B**).
- **O**: In the case of KI the concentration of O at the surface is higher when the potential is applied. In the case of BD it depends on the concentration: at higher BD concentrations the concentration of oxygen increases when the potential is applied, and at lower BD concentrations the concentration of oxygen at the surface is higher when no potential is applied.

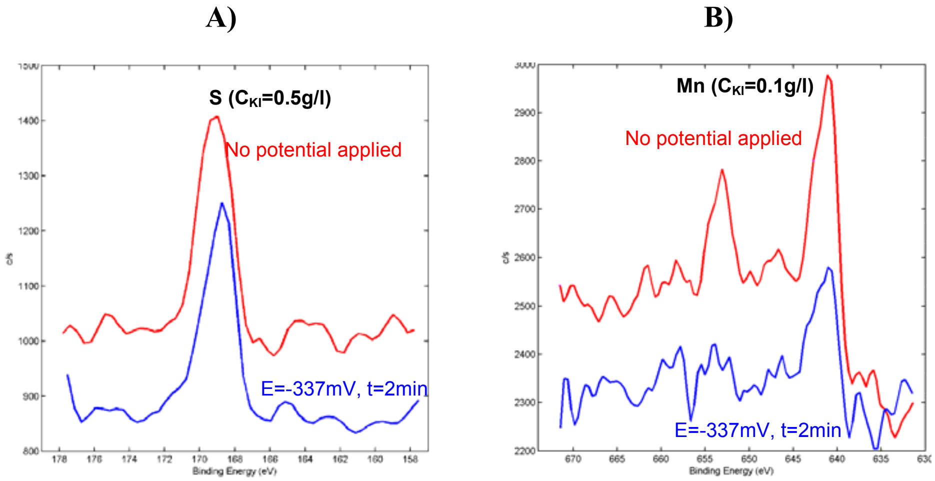

Figure 74. Peaks corresponding to S found at the surface after immersion of steel B in a solution containing 0.5 g/l of KI with and without the application of a potential (**A**) and to Mn found at the surface after immersion of steel B in a solution containing 0.1 g/l of KI with and without the application of a potential (**B**).

- **C**: In the case of KI the concentration of C at the surface is higher when the potential is applied, and in the case of higher concentrations of BD as well. At lower concentrations more C is found in when no potential is applied.
- **Si**: With KI, the concentration of Si is higher when the potential is applied. In the case of BD more Si is found at higher concentrations when no potential is applied and at lower concentrations when the potential is applied.
- **Fe**: With KI the concentration of Fe at the surface increases when no potential is applied. In the case of BD this depends on the concentration: at higher concentrations of KI more Fe is found when no potential is applied and at lower concentrations when the potential is applied.
- **Oxide layer**: Both at high and low inhibitor concentrations the oxide layer becomes thicker when the potential is applied.

A summary on the influence of the application of a potential on the surface composition of the sample is given in **table 13**.

Upon review of the results it can be concluded that the application of a potential affects the system and causes changes in the composition at the surface. These changes also depend on the inhibitor used.

Component/Element		S	Mn	O	C	Si	Fe	Oxide layer
BD	Potential	+	+	>↑C	>↑C	>↓C	>↓C	+
	No potential	-	-	>↓C	>↓C	>↑C	>↑C	-
KI	Potential	+	>↑C	+	+	+	-	+
	No potential	-	>↓C	-	-	-	+	-

Table 13. Influence of the application of a potential of -337 mV on the composition at the surface. (**Key**.- **+**: higher concentration of the element found at the conditions mentioned.; **-**: lower concentration of the element found at the conditions mentioned; **> ↑ C**: higher concentration of the element found at the conditions mentioned when the concentration of the tested inhibitor is high; **>↓C**: higher concentration of the element found at the conditions mentioned when the concentration of the tested inhibitor is low)

4.2.3.2.2 Study of the polarization curves obtained in the presence of the different inhibitors

Polarization curves were recorded in order to study the kinetics of the corrosion process in the presence of different inhibitors.

In **figure 75** and **76** the polarization curves for the different inhibitors at a concentration of 0.9 g/l at pH=1 and pH=5.5, respectively, are shown.

From the results in **figure 75** it can be seen the decreasing current densities of both branches of the curves when the different inhibitors are added to the solution. This means that the tested inhibitors at pH=1 and at a concentration of 0.9 g/l are mixed inhibitors. CI and DETU are shown to be the best inhibitors. Their suppression of the anodic reaction is comparable and CI is the superior inhibitor for the cathodic reaction. HMTA turns out to be the poorest inhibitive compound.

The curves in **figure 76** show that the corrosion reaction itself at pH=5.5 is slower than at pH=1. The shape of the curves is different in both solutions and the curves are wider at pH=5.5 than at pH=1. When comparing the graphs in **figures 75** and **76** it is remarkable how the behaviour of HMTA changes from one case to the other. At pH=1 this inhibitor hinders the corrosion reaction while at pH=5.5 it is promoting it. This enhancement of the current density due to the anodic and cathodic reactions can also be observed with KI and DPGDME. In this solution the better inhibitor for both cathodic and anodic reactions is DPTU. At pH=5.5 the compounds are mostly behaving as anodic inhibitors, whereas at pH=1 both anodic and cathodic reactions are inhibited.

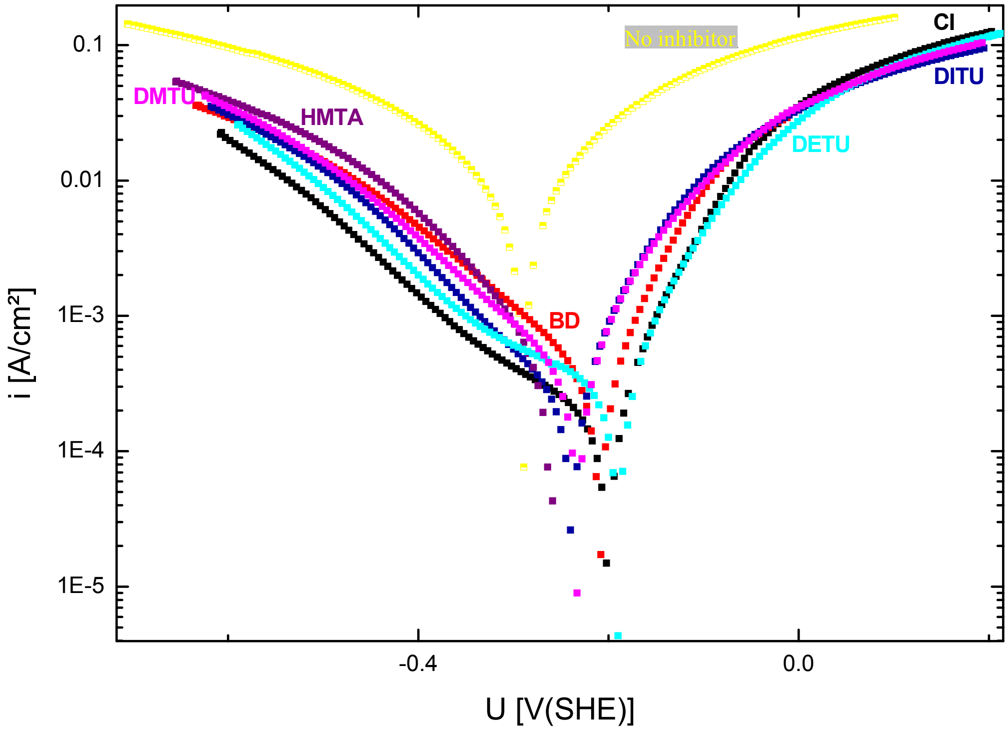

Figure 75. Polarization curves recorded in the presence of different inhibitors (c = 0.9 g/l) at pH=1.

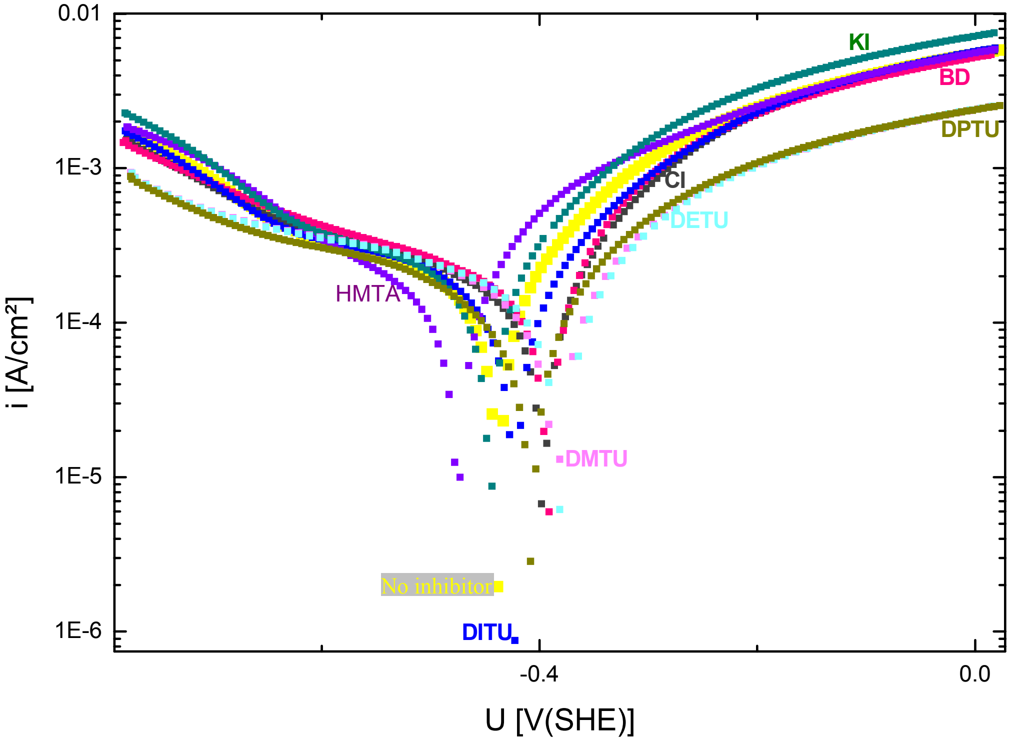

Figure 76. Polarization curves recorded in the presence of the different inhibitors (c = 0.9 g/l) at pH=5.5.

The results of a detailed examination of the polarization curves obtained in the concentration range from 0.1 to 3.0 g/l for different inhibitors are summarized in **table 14**.

Inhibitor	pH=1	pH=5.5
CI	Mixed	Anodic
BD	Mixed (greater anodic effect)	Cathodic with 0.1 g/l Anodic at all other concentrations
DPTU	-	Mainly cathodic
DITU	Mixed	Mainly cathodic
DETU	Mixed	Mainly anodic
DMTU	Mixed	Mainly anodic
HMTA	Mixed	Corrosion promotor (cathodic and anodic)
DPGDME	-	Corrosion promotor (cathodic reaction)
KI	-	Corrosion promotor (mainly of the anodic reaction)

Table 14. Behaviour of the inhibitors at different pH values.

The effectiveness of the inhibitors in the different environments has been calculated (see *section 2.2.5.1*) at their different concentrations from the corrosion potential (E_{corr}) and the corrosion current density (I_{corr}) can be seen in **figures 77** and **78**.

From the results in **figure 77** it can be seen how the highest effectiveness is reached by CI and DETU at higher concentrations at pH=1. DITU, DMTU and BD are shown to be highly effective at pH=1 as well. The effectiveness for the case of HMTA is below the one of DETU and is almost the same as in the case of DMTU at pH=5.5. However, it is much higher than the one of HMTA at pH=5.5. The effectiveness of the inhibitors at pH=1 again seems to be higher than at pH=5.5. Anyhow, when considering the magnitude of E_{corr} the effectiveness of the inhibitors only reaches values up to 38 %, which are comparable to those obtained from the magnitude of the OCP. At pH=5.5 the effectiveness of DETU and DMTU even are higher than the one of CI. The effectiveness of DITU and DPGDME are of the same order and KI, HMTA and DPTU behave rather negatively.

When determining the effectiveness of the different inhibitors from the corrosion current density the effectiveness is higher than when taking the corrosion potential or the OCP value as criterion. Indeed, values of up to 90% may be reached. Accordingly DPTU was not found to be a good inhibitor in the weight loss experiments or when corrosion potentials and OCP values are considered but it is giving the best results for the corrosion current densities, even at pH=5.5.

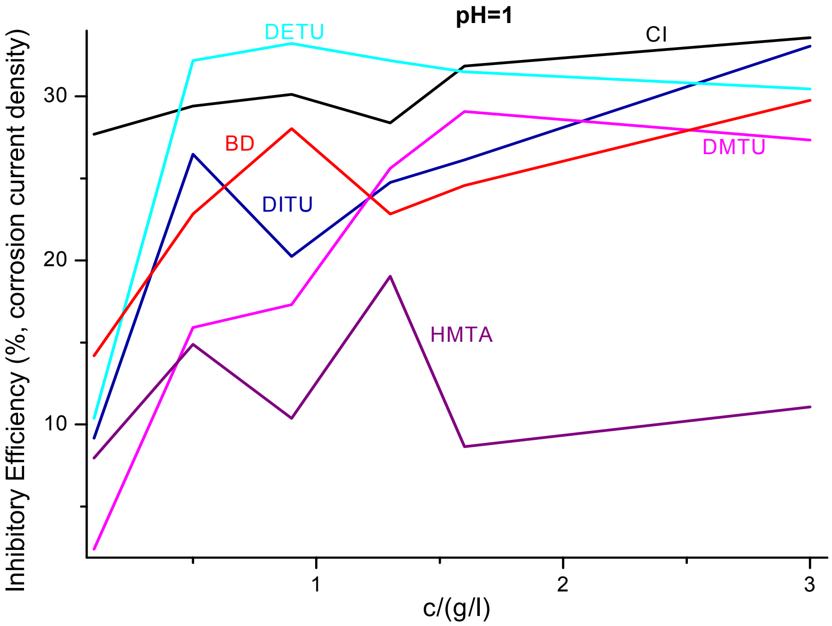

Figure 77. Effectiveness of the different tested inhibitors from the E_{corr} obtained from the polarization curves at pH=1.

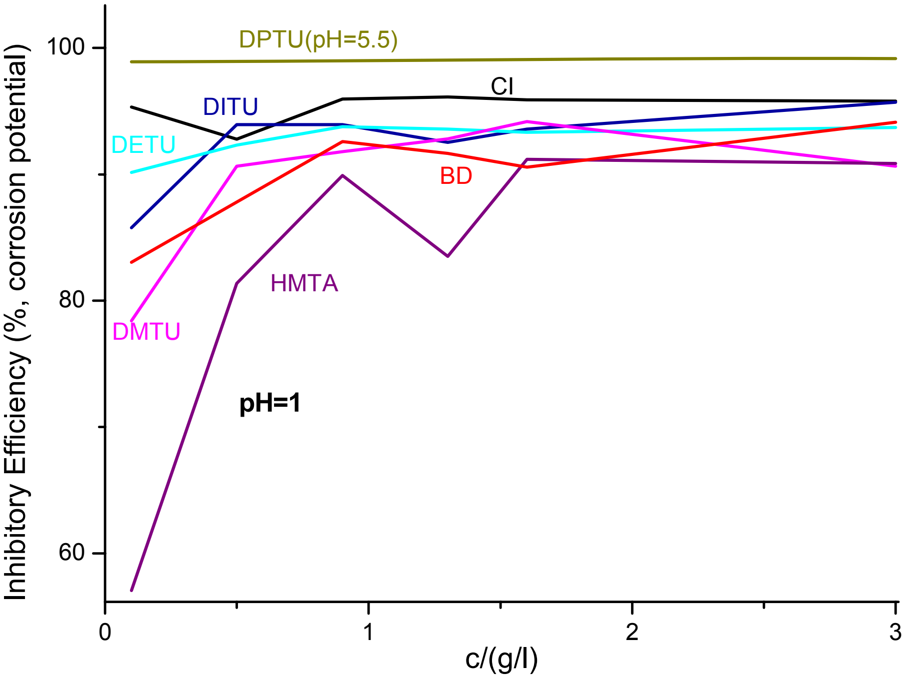

Figure 78. Effectiveness of the different tested compounds from the I_{corr} obtained from polarization curves at pH=1.

For the thiourea containing compounds, the comparison between the different polarization curves is given in **figure 79**.

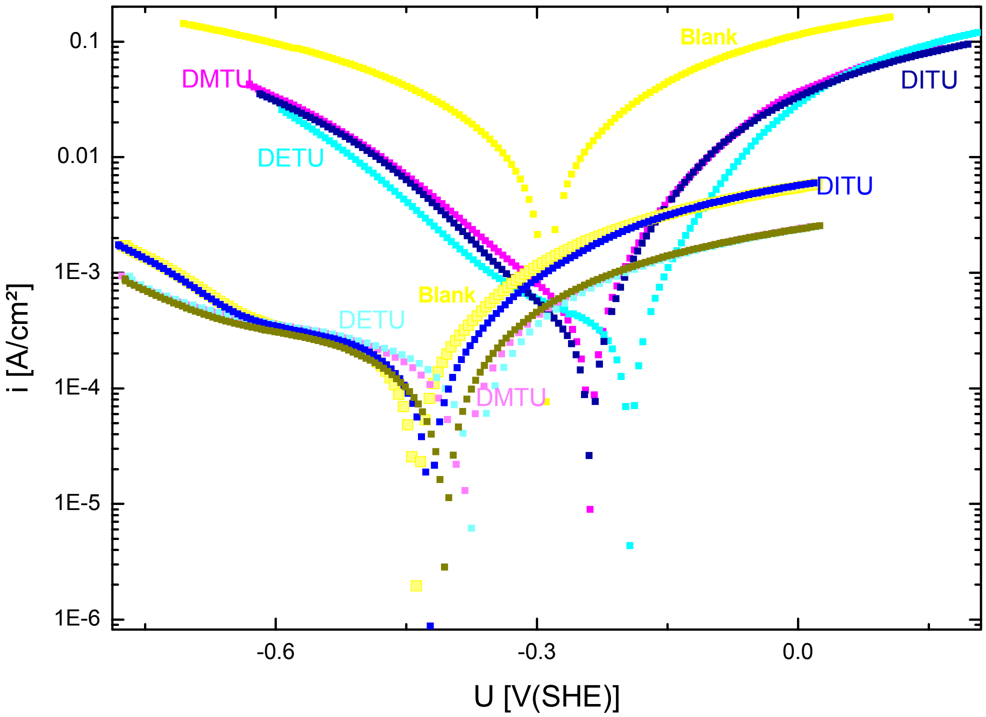

Figure 79. Comparison of the polarization curves obtained for the case of the different thioureas at pH=1 and pH=5.5 for concentrations of 0.9 g/l.

When comparing the polarization curves obtained by the addition of the different compounds of the thiourea family at a concentration of 0.9 g/l it can be seen that:

- The curves obtained at pH=5.5 are shifted towards more negative potentials.
- The current densities along the curve are lower at pH=5.5 than at pH=1.
- At pH=1 the substances behave as mixed inhibitors and diminish both the anodic and the cathodic reaction, while at pH=5.5 they act mainly as anodic inhibitors and do not affect the cathodic process. DITU even gives a passivation in the cathodic branch of the curve at pH=5.5.
- At pH=1 the inhibitors decrease the current densities and displace shift the potential to less negative values from DMTU to DETU. However, the curve given by DITU almost coincides with that of DMTU and here the corrosion current density from the three compounds is the highest.

- At pH=5.5 the curves have lower current densities and are shifted to more positive potentials from DMTU to DETU. DITU gives a higher I_{corr} than the solution without inhibitor and the curve is situated between those corresponding to the solution without inhibitor and the one of DMTU. DPTU gives a corrosion current density higher than the one of DMTU and DETU but lower than in the case of a solution without inhibitor. Its curve almost coincides with that of DMTU.

The corrosion potentials for the case of the different compounds at pH=1 are shown in **figure 77.** The potentials are less negative at pH=1 than at pH=5.5. At both pHs the potentials in the case of DETU are higher than with DMTU. With DITU they again are lower as a result of its insolubility. At pH=5.5 the solubility is lower than at pH=1. At pH=1 the corrosion potential in presence of DITU drop to a value between the one with DMTU and DETU while at pH=5.5 the potential is well below the one with DMTU. Even with DPTU higher corrosion potentials are obtained.

In **figures 75** and **76** it can be seen how at pH=5.5 the corrosion current density is lower than at pH=1. At pH=5.5, the corrosion current density is lower in the case of shorter lateral chain and for DPTU, the lowest corrosion current density is obtained. At pH=1 and with low concentrations the best results are obtained with DETU while at higher concentrations a lower corrosion current density is found in the case of DITU (**figures 78** and **79**).

In **table 15** the data obtained from the respective Langmuir isotherms are shown.

Compound$_{(pH,\ magnitude)}$	**Function**	**R^2**	**Slope**	**1/*k***	***k***	**ΔG/(kJ/mol)**
DPTU$_{(5.5,\ Icorr)}$	$y = 1.0083x + 0.0011$	1.0000	1.0083	0.0011	909.09	-20.8
CI$_{(1,\ Icorr)}$	$y = 1.0413x + 0.0048$	1.0000	1.0413	0.0048	208.33	-16.3
DETU$_{(1,\ Icorr)}$	$y = 1.0657x + 0.0052$	1.0000	1.0657	0.0052	192.31	-16.1
DMTU$_{(1,\ Icorr)}$	$y = 1.0952x – 0.0059$	0.9993	1.0952	0.0059	169.49	-15.7
DITU$_{(1,\ Icorr)}$	$y = 1.0429x + 0.0231$	0.9997	1.0429	0.0231	43.29	-11.5
BD$_{(1,\ Icorr)}$	$y = 1.0592x + 0.0312$	0.9995	1.0592	0.0312	32.05	-10.6
HMTA$_{(1,\ Icorr)}$	$y = 1.0777x + 0.0715$	0.9983	1.0777	0.0715	13.99	-8.1

Table 15. Langmuir isotherms obtained from the polarization curves.

Only for the corrosion current densities (I_{corr}) at pH=1 suitable Langmuir isotherms are obtained, except for the case of DPTU for which a suitable Langmuir isotherm is also obtained at pH=5.5. However no suitable Langmuir isotherm is obtained from the corrosion potentials. The free energies obtained are typical of physisorption and agree with those obtained from the weight loss experiments. In **table 38** the compounds are listed according to the most favourable interaction with the steel surface.

For the case of the thioureas, it was found that the slope value is closer to unit when the length of the lateral chain increases. The value found for the free energy increases from DMTU to DETU. This indicates that the efficiency of the interaction with the steel surface increases with the molecular weight and the length of the lateral chain of the compound. The value for DITU is lower which may be due to its insolubility.

4.2.3.3 Electrochemical impedance spectroscopy

Electrochemical impedance spectroscopy was carried out in order to get information on the different systems as well.

In **figures 80** and **81** impedance and phase diagrams for measurements carried out at pH=1 are presented and results for measurements made at pH=5.5 are shown in **figures 82** and **83**. All measurements were made with steel B.

The impedance diagrams for the solutions used were found to be very different. At pH=1 the behaviour was found to be more capacitive. This could also be observed in the phase diagrams, despite there was only a little increase in the polarization resistance. The resistance of these solutions was found to be much lower than with the 0.5 % $FeSO_4$ solution. This indicates higher aggressiveness of the electrolyte at pH=1 and that a better electron transfer through the solution takes place.

Phase diagrams at pH=1 show that here the inhibitor has more a capacitive behaviour as it is the case for 0.5 % $FeSO_4$. Also a shift of the minimum of the phase curves towards higher frequencies is observed. In both cases the phase curves move towards lower values with the addition of inhibitors, however, not systematically with the concentration.

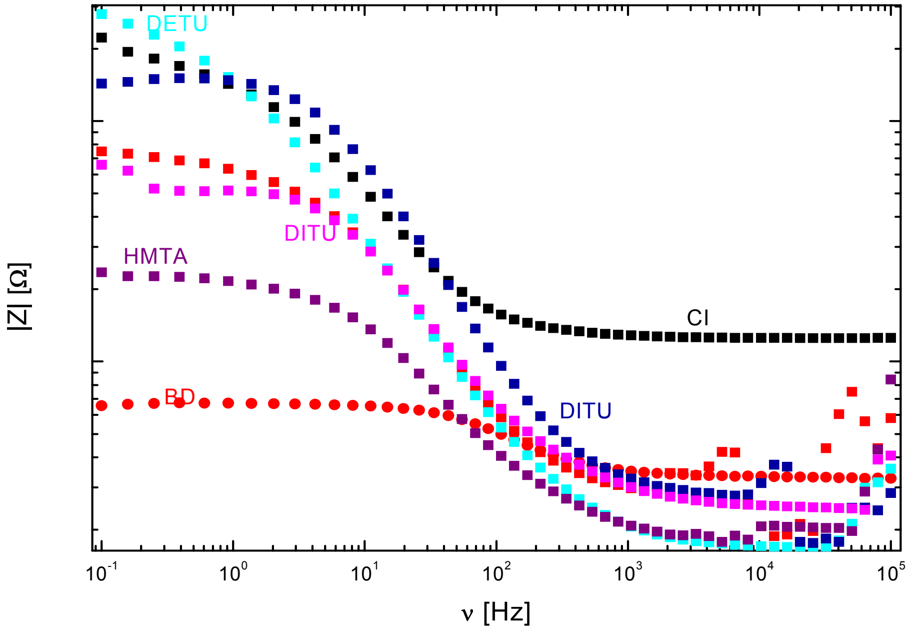

Figure 80. Impedance diagrams obtained for steel B immersed in a commercially available solution buffered at pH=1.

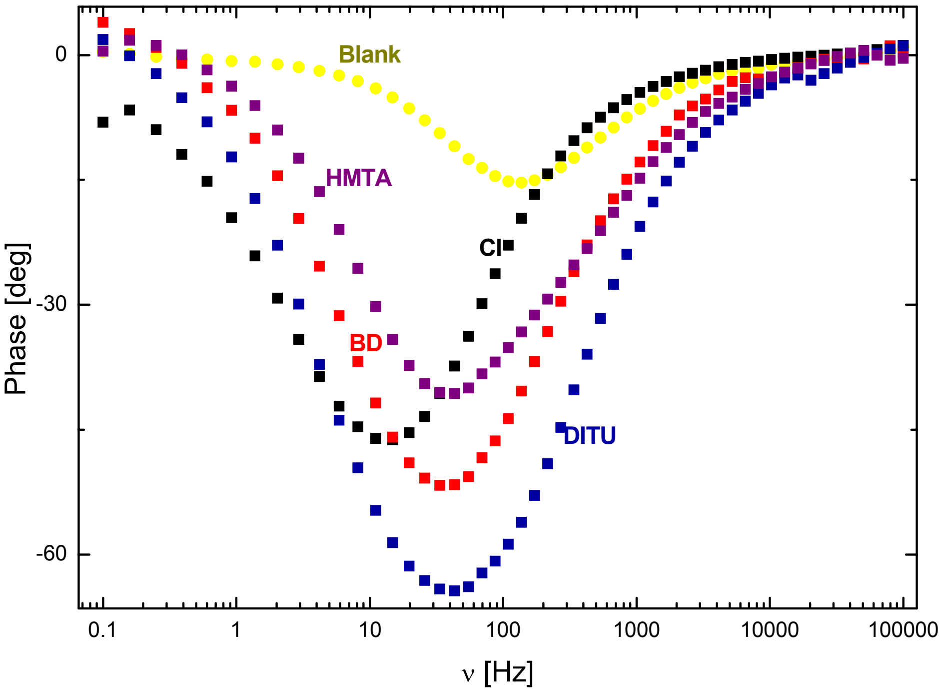

Figure 81. Phase diagrams obtained for steel B immersed in a commercially available solution buffered at pH=1.

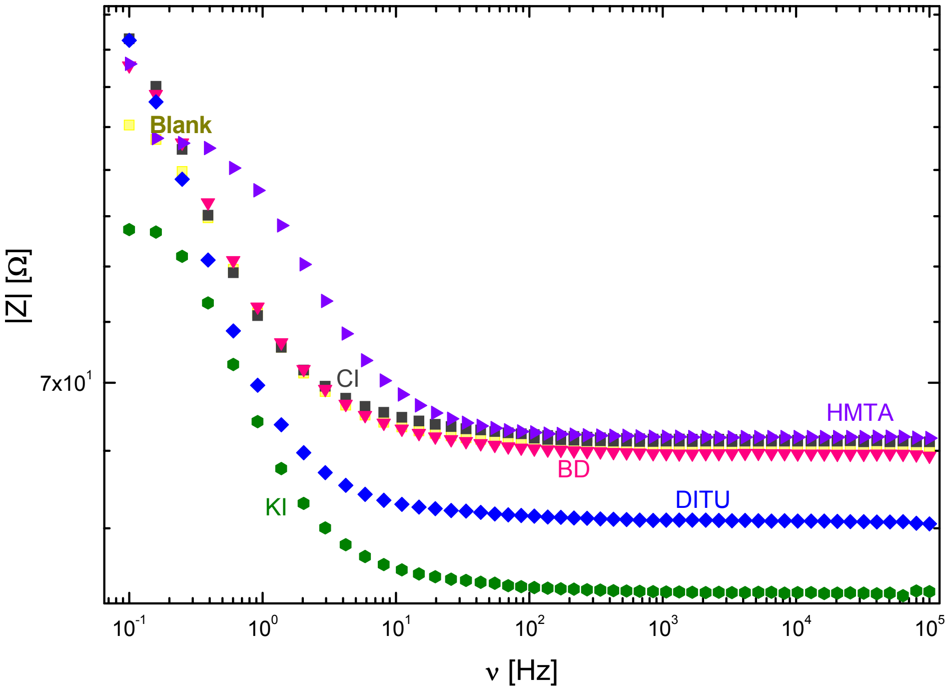

Figure 82. Impedance diagrams obtained for steel B immersed in a solution of 0.5 % $FeSO_4$ at pH=5.5.

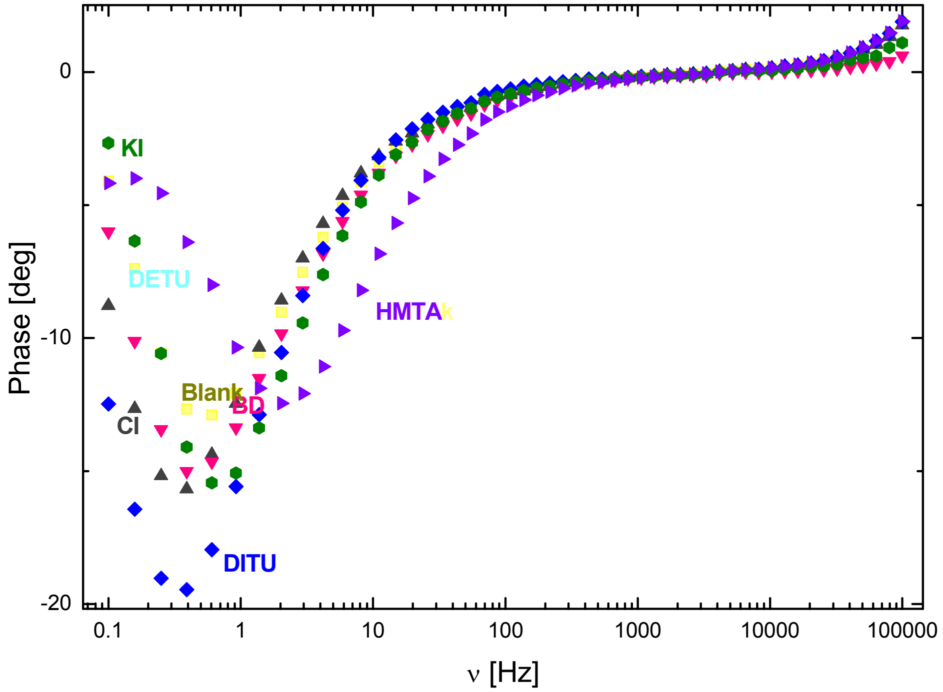

Figure 83. Phase diagrams obtained for steel B immersed in a solution of 0.5 % $FeSO_4$ at pH=5.5.

It was observed that at successive additions of HMTA, DITU, DETU, DMTU at pH=1 of DPGDME at pH=5.5 and of KI at pH=5.5 the resistance of the electrolyte changed. It decreased as compared to a solution without inhibitor. At the addition of DMTU and DETU the electrolyte resistance decreased more than with KI. It further decreased with the concentrations added. On the contrary, when adding DPTU at pH=5.5 the electrolyte resistance increases. This would be the explanation for the high effectiveness calculated from the corrosion current density (see *section 4.2.2.2*). For the impedance and phase curves in the case of DPTU the behaviour at concentrations of 0.5 and 0.9 g/l was irregular. The impedance curves behave very irregular, as they vary parallel at both concentrations and decrease at high frequencies. Subsequently they again smoothly increase up to values of 1000. Phase curves show a capacitive behaviour and the minimum is shifted towards higher frequencies. Regarding the other concentrations they show lower capacitive behaviour than the blank sample and the peaks are displaced towards lower frequencies.

The inhibitory efficiencies as obtained from the polarization resistance are shown as function of the concentrations of the different compounds tested at pH=1 and pH=5.5. The highest effectiveness is reached at pH=1 for the inhibitor CI followed by DITU, DETU, BD, HMTA and DMTU. The effectiveness found at pH=5.5 is much lower. The most effective compounds at this pH are DPTU and HMTA and the less effective is KI. The three thioureas containing inhibitors were found to be more effective than CI in 0.5 % $FeSO_4$ as pickling solution and only is BD more effective than KI.

Among the three thioureas containing inhibitors it was found that at pH=1 the polarization resistance increases with the length of the lateral chain and hence of the molecular weight. The same sequence is found at pH=5.5 at higher concentrations.

4.2.3.4 Summary

The environment used was shown to greatly influence the inhibitory behaviour. In general it could be said that the protection is higher at pH=1, which was shown to be a more aggressive solution.

The application of a potential induces a compositional change on the steel surface and therefore polarization and impedance results are not completely comparable to open circuit potential results.

Higher corrosion current densities at pH=1 were explained by the lower electrolyte resistances found in the impedance diagrams.

KI, DPGDME, HMTA and DPTU at pH=5.5 were shown to behave enhancing the corrosivity of the system by the open circuit potential measurements and polarization curves. The reason of this behaviour is explained by the subsequently decrease of the electrolyte resistance found with EIS when these inhibitors are added to the solution.

CI, BD, DITU, DETU, DMTU and HMTA at pH=1 were found to act as corrosion protectors of the steel surface by all electrochemical techniques.

The influence of lateral chain of the thiourea containing inhibitors is only clear at low molecular weights. The protection increases with the length of the lateral chain. The insolubility of DITU, which is greater a pH=5.5, makes the comparison difficult.

4.2.4 Surface Analysis

By means of surface analysis methods like IRRAS, XPS and TOF-SIMS the steel surface was studied after immersing the sample during certain time in a solution of DPGDME containing DMTU, DETU and DITU in order to investigate if these organic compounds form a stable layer on the steel surface.

4.2.4.1 Studies by means of infrared reflection absorption spectroscopy

In **figure 84** the results of IRRAS obtained after treating the sample with a solution of the different thiourea containing inhibitors during comparable times are shown.

The strong and broad bands at 3340 cm^{-1} are due to the ν (NH) vibration. For this band it can be observed that the adsorption increases with the length of the lateral chains of the molecules.

Between 2976 and 2823 cm^{-1} the bands are due to the alkyl groups. The number of bands at these frequencies consequently decreases when shorter alkyl groups are present in the molecules (for DITU more bands are found than for DMTU). The absorption of the alkyl bands takes place: is also lower than the one of the N-H band. This suggests that a change in the orientation of the groups, the bond N-H would be parallel to the surface and the alkyl groups form an angle with the surface.

Between 1616 and 1475 cm^{-1} bands due to ν (CN), δ (NCN) and ν (CS) vibrations are present. These bands are also very intense, both for DETU and DITU.

The vibrations of the CH_3 groups give bands between 1364 and 1344 cm^{-1}. These bands decrease in intensity with on the size of the molecule.

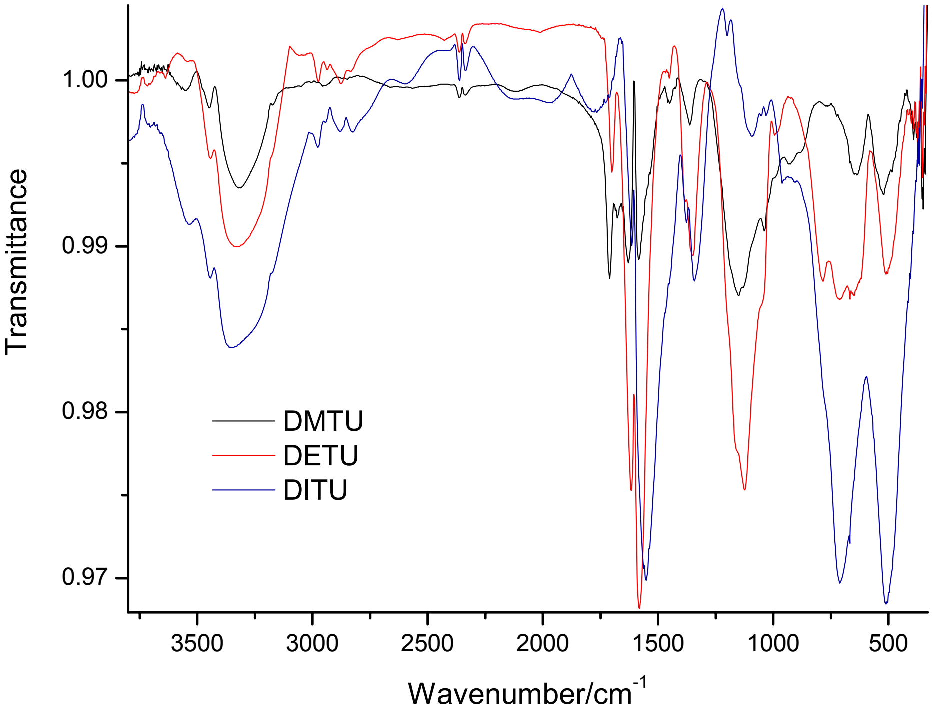

Figure 84. Spectra of the thing layers formed by DMTU, DETU and DITU obtained by means of IRRAS.

4.2.4.2 Studies with X-ray photoelectron spectroscopy (XPS)

Measurements with XPS were made at the surface of a polished steel sample after its immersion in a solution containing 1.5 g/l of DITU during different times (for sample preparation see *section 3.11*). The XPS signals obtained for the different elements at different immersion times are given in **figure 85**.

At a first glance it can be seen that the signal for the elements present in the DITU molecule (C, S and N) tend to increase with the immersion time while the signals of those elements which are not present in the DITU molecule, like Fe and O tend to decrease with the immersion time.

For the spectral lines involving transitions from the 1s orbital two peaks were recognized. The larger one at a binding energy of 285 eV could involve the C of a hydrocarbon or C bound to a N atom. The intensity of this peak is increasing with the immersion time. A small peak was found at 289 eV and this could involve the C-S bond. This peak behaves irregularly with the immersion time, which may be related with its low intensity.

The spectral lines involving transitions from the $2p^{3/2}$ orbital level of S comprise an intensive peak around 169.1 eV which can be related to the formation of the Fe-SO_4.

For Fe the spectral lines involving the $2p^{3/2}$ orbital level of the Fe are found. The peak around 710 eV could be due to Fe_2O_3 or Fe_3O_4 while the one at 724 eV might be due to Fe_2O_3. The minor peaks at 720 and 707 eV could be due to metallic Fe. For all these peaks the intensities tend to diminish when the steel samples stay longer in the solution. This may be due to the fact that then the surface is covered in a better way and that then less Fe species can be detected.

The fact that no peaks are found between 711.5 and 713eV might allow it to conclude that no chemical bonds between Fe and SO_4 are formed, which agrees with the physisorption suggested earlier.

Some assays were made closer to more real conditions. Here H_2SO_4 is used as solvent at room temperature and at 95°C with 0.3 g/l and 3.o g/l of DITU. The surface after these experiments turned out to be inhomogeneous.

At room temperature the amount of S at the surface was found to be higher in the absence of an inhibitor. In this case FeS is detected at the surface while no FeS is detected when DITU is added. This may be due to displacement of the SO_4^{2-} ions by the DITU molecules. The higher the concentration of DITU, the higher was the amount of S found. When the experiments are made at 95°C the amount of S found in the sample without the use of DITU is less than the one found with the solution without DITU at room temperature and also lower than in the case when DITU is added to the solution at 95°C. Also for this sample an FeS peak is detected. This peak can also be observed when DITU is added. This may indicate that no the displacement of SO_4^{2-} ions at the surface takes place but that the DITU is covering the free surface. Nevertheless, the thickness of the oxide layer in both samples in the absence of DITU if found to be more than 200 nm. It decreases to 4 nm in the non-oxidized areas of the samples treated at room temperature and to 5 nm in the non-oxidized areas of the samples treated at 95°C.

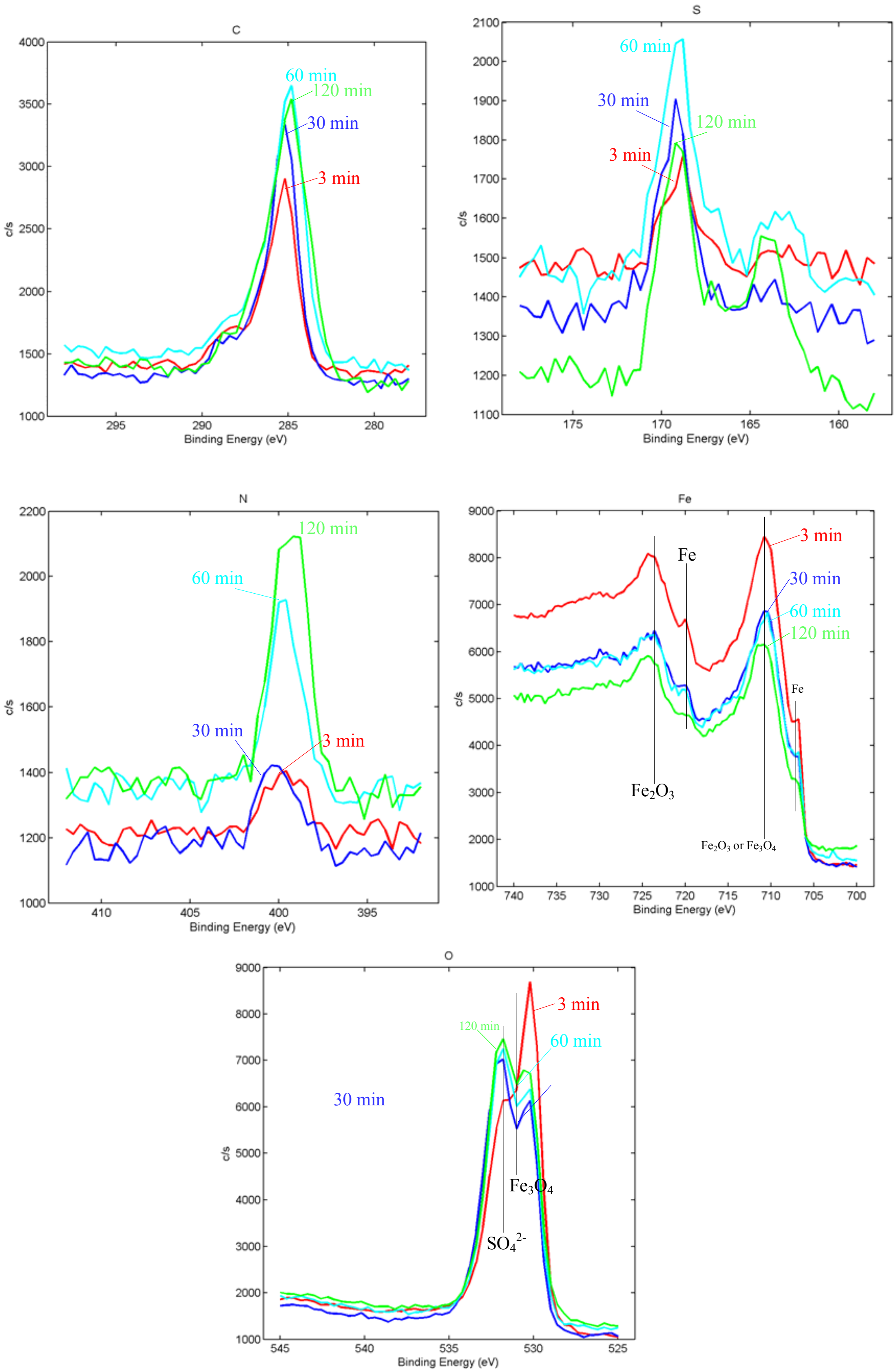

Figure 85. XPS signals for C, S, N, Fe and O peaks from the XPS spectra obtained after different immersion times in a DPGDME solution containing 1.5g/l of DITU.

4.2.4.3 Studies with time-of-flight secondary ion mass spectrometry

TOF-SIMS studies were made of the surface after the steel was treated with a solution containing 1.5 g/l of the different thioureas. The preparation of the samples has been described in *section 3.12*.

The ToF-SIMS peaks in the spectra found for both a positive and a negative polarity of the samples during the treatment with DMTU, DETU, DITU are shown in **figure 86**.

For a negative polarity of the sample during the treatment with DMTU there is a peak for the $[NH]^-$ fragment next to the peak stemming from the $[CH_3]^-$ fragment.

The signal intensity of the $[C_3H_5NS]^-$fragment found from the DETU solution (negative polarity) is not clearly assigned to an analyte fragment ion.

In the case of the sample treated in the presence of DITU, the signal for the fragment ion $[C_3H_8N]^+$ is strong (m/z = 58.065) ion. The signals for the fragment ion $[C_4H_8NS]^+$ (m/z = 102.04) at low mass are on is the shoulder of the peak for the $[C_8H_6]^+$ (m/z = 102.05) fragment ion, which has a high intensity. The peak assigned to the fragment $[C_7H_{16}N_2S]^+$ (m/z = 160.10) at low mass is on the shoulder of the peak for $[C_{12}H_{16}]^+$ (m/z = 160.14) fragment ion, which again has a higher intensity. The peak for the fragment ion $[C_4H_8NS]^-$, is only on flat spectral background stemming from the analyte fragment ions as in the peak for the fragment ion $[C_7H_{16}N_2S]^-$.

The ion $[^{32}S]^-$ stems from the main sulphur isotope, which has a relative natural abundance of 95.02 %. The sulphur isotope $[^{34}S]^-$ is present with a natural isotopic abundance of 4.32 %.

Specific signals from fragment ion as well as from the entire molecule ions of DMTU and DETU with considerable intensities could be detected by TOF-SIMS on the steel samples treated in positive and negative polarity.

The experiments in the presence of DITU were done twice due to the fact that the results found were different from those with the other two thiourea containing compounds. The results were found to be identical. Specific fragment ion signals for DITU could be obtained with considerable intensities only in the smaller mass range and are due to more or less strong fragmentation.

Specific signals for the DPGDME molecule could not be detected in the case of DMTU and DETU. Only when treating the sample in the presence of DITU, slightly increased intensities for ions with a m/z ratio close to the one of the inhibitor could be obtained and this more for positive than for negative polarity.

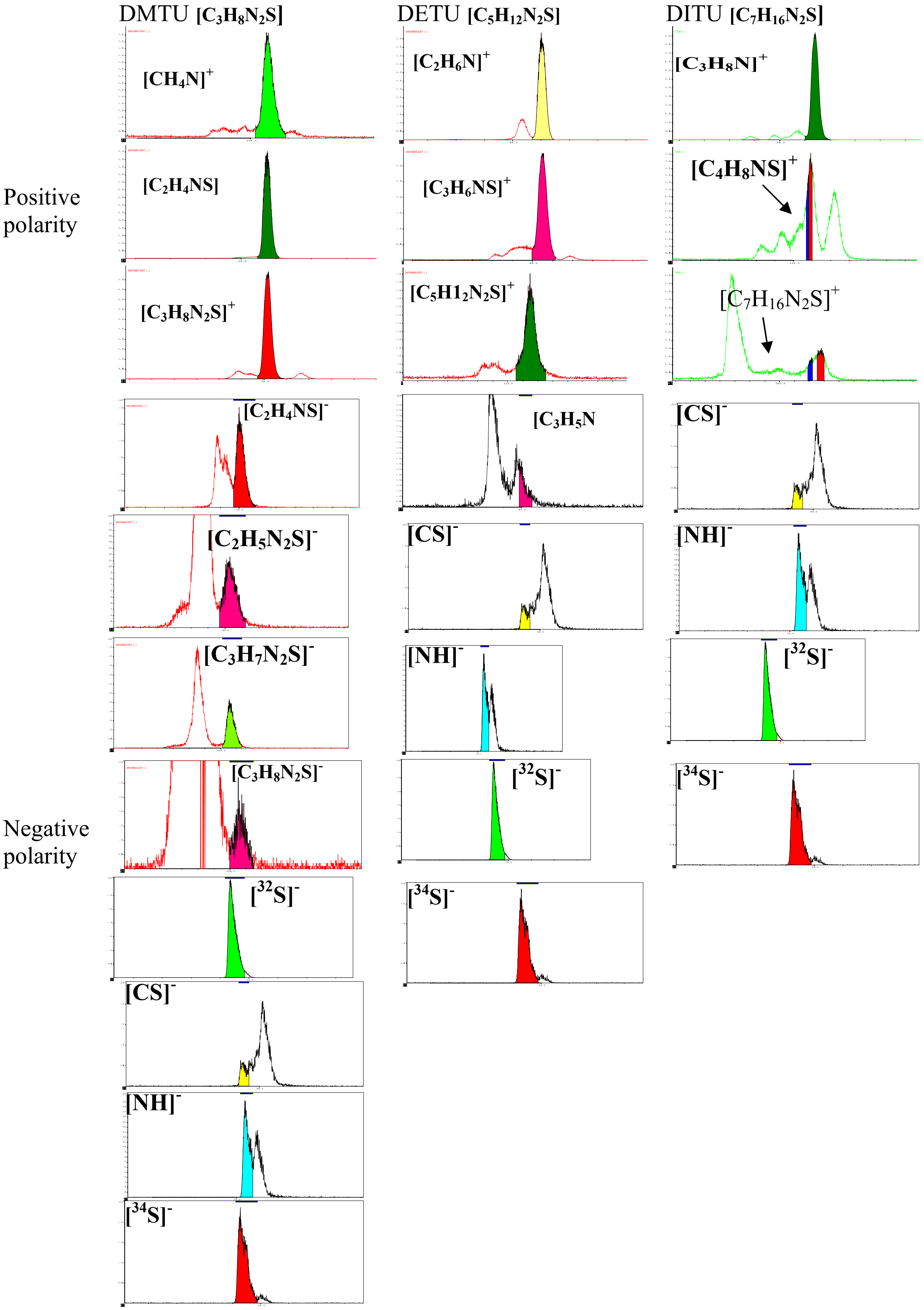

Figure 86. TOf-SIMS spectra obtained or the samples treated in the presence of DITU, DETU and DMTU solutions.

It seems to be obvious that DMTU and DETU are still adsorbed at the steel surface after rinsing in pure solvent. In the case of DITU molecular ions for DITU could not be detected. However, for some specific fragments strong signals in the TOF-SIM spectra are obtained in the case of DITU.

When treating the sample in positive and negative polarity in the presence of DITU the signals for different fragment ions in the TOF-SIM spectra show that significant amounts of DITU adhere to on the steel substrate.

The fact that signals for the positive and negative molecular ions in the case of DITU are absent could be due to diverse factors. It could be due to a quantitative fragmentation of DITU as a result of the SIMS process or to a chemical degradation on the steel substrate before primary ions in the SIMS instrument impact. This might relate with the fact that DITU in solution is less stable than DMTU and DETU. As XPS and IRRAS experiments were made after the same sample treatment and the results obtained for DITU were comparable to those obtained for DMTU and DETU a degradation of DITU in the solution is not probable, the higher molecular fragmentation could then be more likely. Then again two possibilities have to be considered: the higher fragmentation due to a stronger interaction of DITU and the steel surface or the higher stability of the fragments formed.

The interaction between the steel and DITU could be thought to be mainly due to an associate of the steel and a ~NH_2-C(S)-NH_2~ group which is strongly adsorbed to the surface whereas the rest of the molecule would be fragmentising. It could then be more difficult than for DMTU and DETU to desorb the whole molecule. On the other hand, the longer the chain in the ions the more distributed is the charge over the atoms and the more favourable is the situation. Another reason could lay in the fact that the probability to be broken is higher the longer or the more voluminous the molecule.

4.2.4.4 Scanning electron microscopy

In this section the SEM images taken after pickling with and without inhibitor are shown in order to evaluate the protective behaviour of the inhibitors with respect to the surface topography. It can be seen from the results in **figure 87** that differences in surface structure occur as a result of the presence of different inhibitors in the pickling baths.

In **figure 88** the SEM images and the longitudinal sections of two samples of steels A and B which are treated with a solution of 20 % HCl at room temperature in the absence and in the presence of HMTA are shown.

Conditions	SEM	Longitudinal section
50 min in HCl 20 %	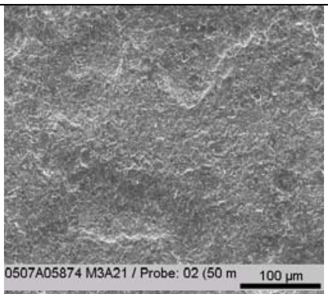	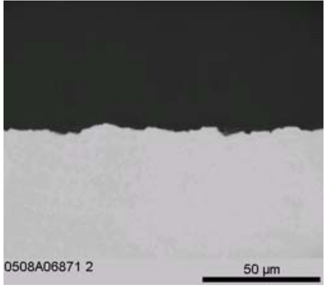
50 min in 20 % HCl + 1.5 g/l BD	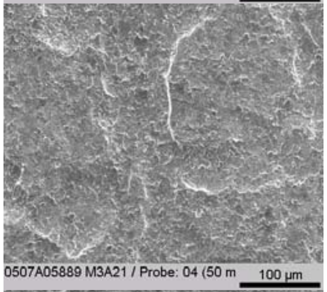	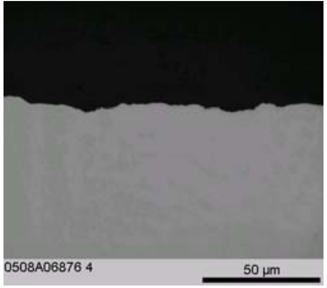
50 min in 20 % HCl + 1.5g/l DMTU	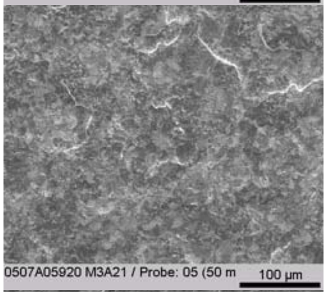	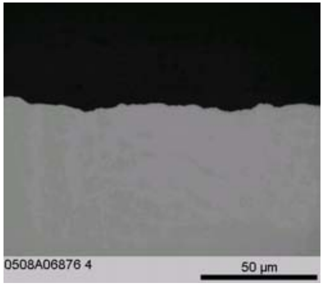
50 min in 20 % HCl + 1.5 g/l DETU	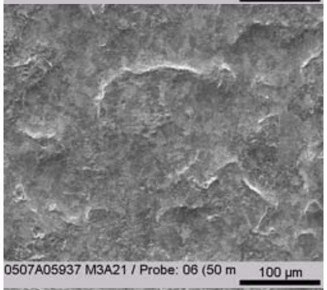	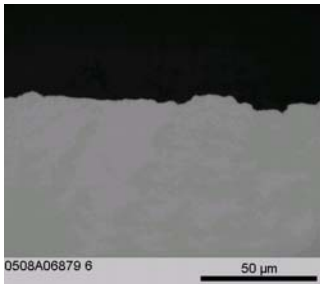
50 min in 20% HCl + 1.5 g/l DITU	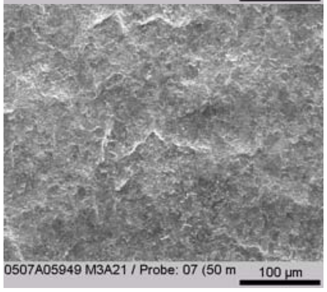	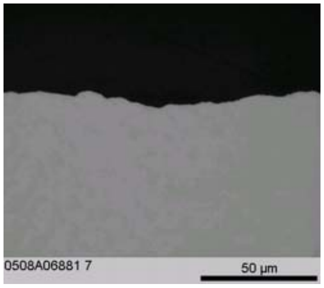

Figure 87. Effect of the presence of different inhibitors addition in the pickling of steel A at room temperature minutes with HCl 20 % during 50.

In the micrograph no appreciable pickling attack is recognizable when HMTA is present while without the inhibitor isolated effects of the acidic attack can be observed.

Conditions	SEM image	Longitudinal section
Steel A 50 min HCl 20%	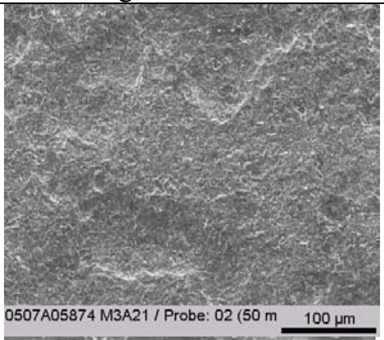	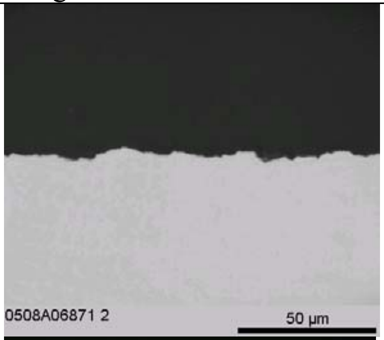
Steel A 50 min HCl 20% + 1.5g/l HMTA	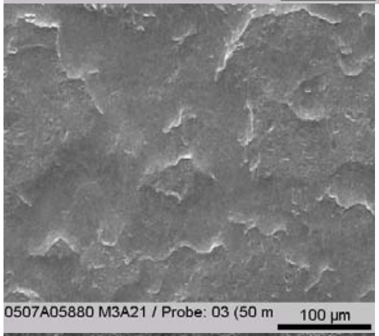	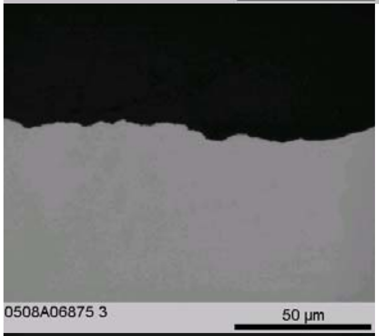
Steel B 3 min in HCl 20%	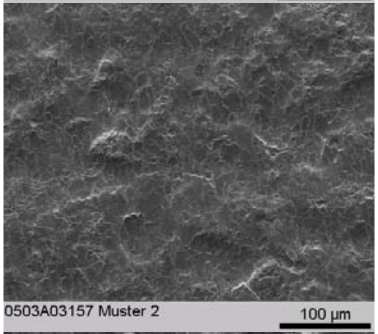	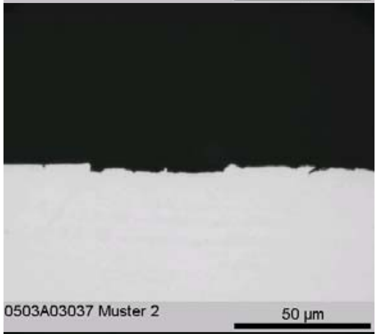
Steel B 3 min in HCl 20% + 3.0g/l HMTA	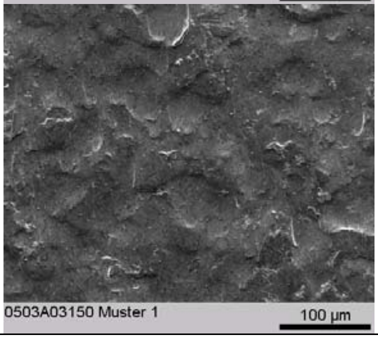	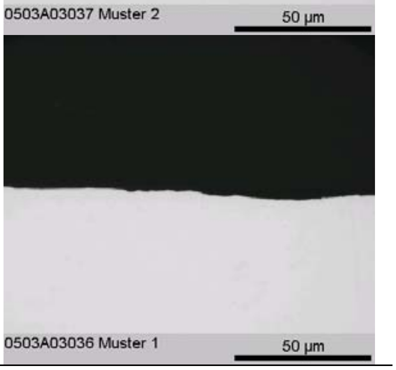

Figure 88. Effect of HMTA addition in the pickling of steels A and B at room temperature with 20 % HCl.

When HMTA is added to the pickling solution the presence of isolated and localized attacks at the grain boundaries can be observed in the SEM image of the sample. This contrasts with the image taken in the absence of an inhibitor. Here the attack at the boundaries and even, but less, at the grain surfaces can be clearly observed. The fundamental topography of the sample is still clearly recognizable. Dried rests can be found on the sample surface. These rests could be due to the pickling solution or to the inhibitor.

In **figure 89** the SEM images and the longitudinal sections of samples treated with 20 % HCl at room temperature in the absence and in the presence of CI are shown.

In both SEM images and longitudinal sections only isolated and weak pickling attacks can be detected. This contrasts with the clear attack at the grain boundaries and at the grain surface when no CI is present. Here only the fundamental topography of the sample is barely still recognizable.

When CI is present some dried residues are found on the surface, which could correspond to dried rests of the pickling environment solution or of the inhibitor.

In the longitudinal section micrograph no pickling attack is observable when CI was present, while when CI was not present the attack is visible and even pores due to pickling can be observed.

In the SEM image only isolated attacks at grain boundaries can be recognized and the topography of sample is maintained while in the absence of CI the surface of the grains shows a strong pickling attack. In this case what are supposed to be the dried rests of the pickling solution are only recognizable when no CI is present.

In **figure 90** the SEM images of the steel surface after 3 minutes of pickling at 95°C with and without inhibitor are shown.

When the pickling is performed in the absence of CI it can be seen how complete grains are removed at the surface. Complete layers are eliminated and the holes where the grains are removed can be observed. From the weight loss it was calculated that the thickness of the lost layer is around 25 μm. After the elimination of the grains a honeycomb relief is left at the surface.

When the process under the same conditions is carried out in presence of 3.0 g/l CI the pickling turns out to be very homogeneous. Some grains are eliminated but without removing a whole layer. Localized effects of pickling can be seen at the grain boundaries but the original topography of the sample is still clearly recognizable. Additionally, what could be rests of the pickling solution on the surface can be observed.

Conditions	SEM image	Longitudinal section
Steel A 50 min in 20 % HCl	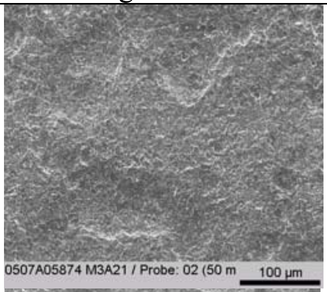	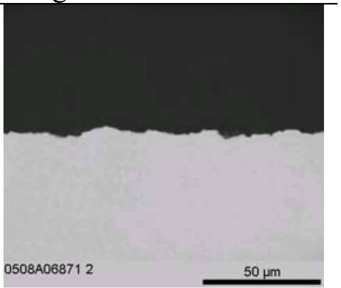
Steel A 50 min in 20 % HCl + 1.5 g/l CI	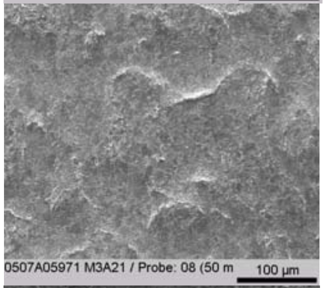	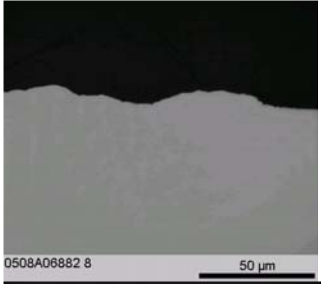
Steel B 30 min in 20 % HCl	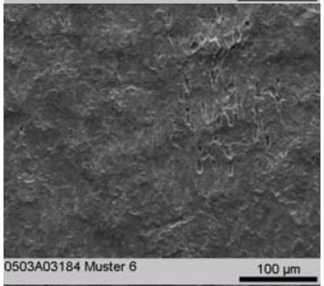	
Steel B 30 min in 20 % HCl + 3.0 g/l CI	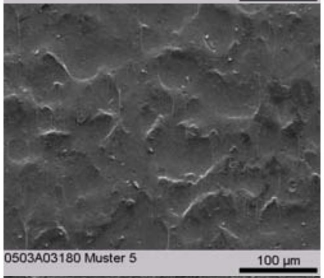	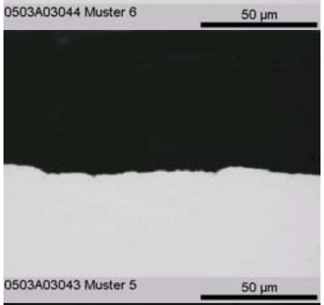
Steel B 50 min in 20 % HCl	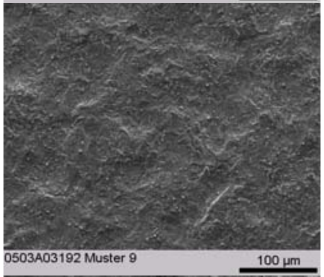	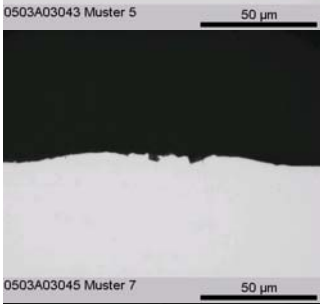
Steel B 50 min in 20 % HCl + 3.0 g/l CI	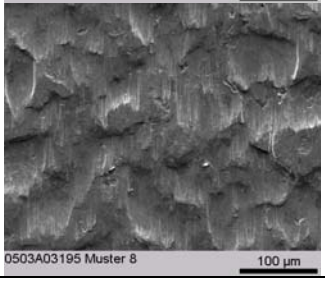	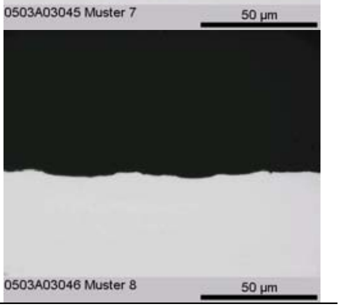

Figure 89. Effect of the addition of CI in the pickling of steels A and B at R.T. with 20 % HCl.

Conditions	SEM image (large scale)	SEM image (small scale)
20 % H_2SO_4 + 0.5 % $FeSO_4$ T=95°C t=3min	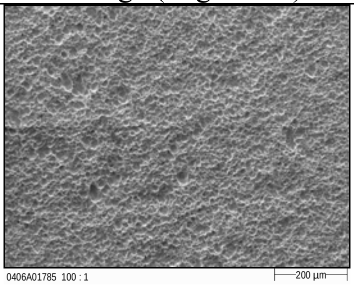	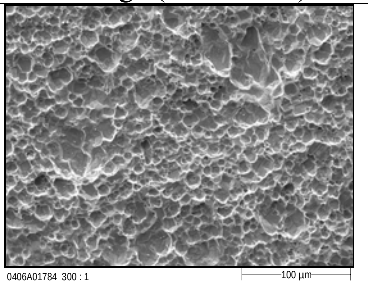
20 % H_2SO_4 + 0.5 % $FeSO_4$ T=95°C t=3min + 3.0 g/l CI	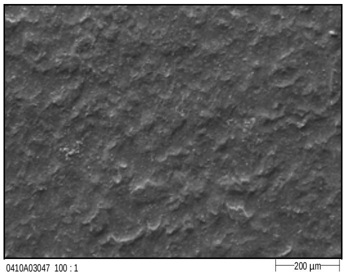	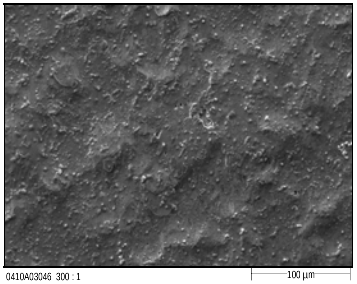
Untreated steel	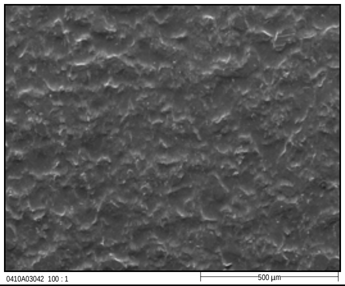	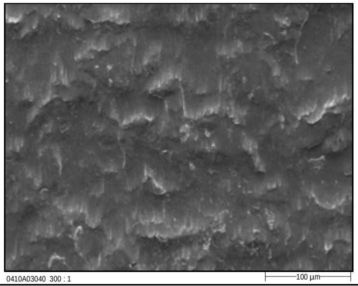

Figure 90. Effect of the addition of CI in the pickling of steel B at 95°C with 20 % H_2SO_4 + 0.5 % $FeSO_4$ during 3 minutes.

4.2.4.5 Atomic force microscopy

The topography of the surface was studied by means of AFM in the liquid phase and in the contact modus so as to investigate the effects of the different inhibitors tested. The buffer was used to minimize the pH changes during the experiment as a result of a dissolution of the material.

Different AFM records of the steel surface after its immersion in different commercially available buffered solutions at pH=1 containing 0.9 g/l of the various inhibitors DMTU, DETU, DITU and BD were made.

The results are shown in **figure 99**. From the records shown in **figure 99**, the surface roughness was measured and the results shown in **figure 100**.

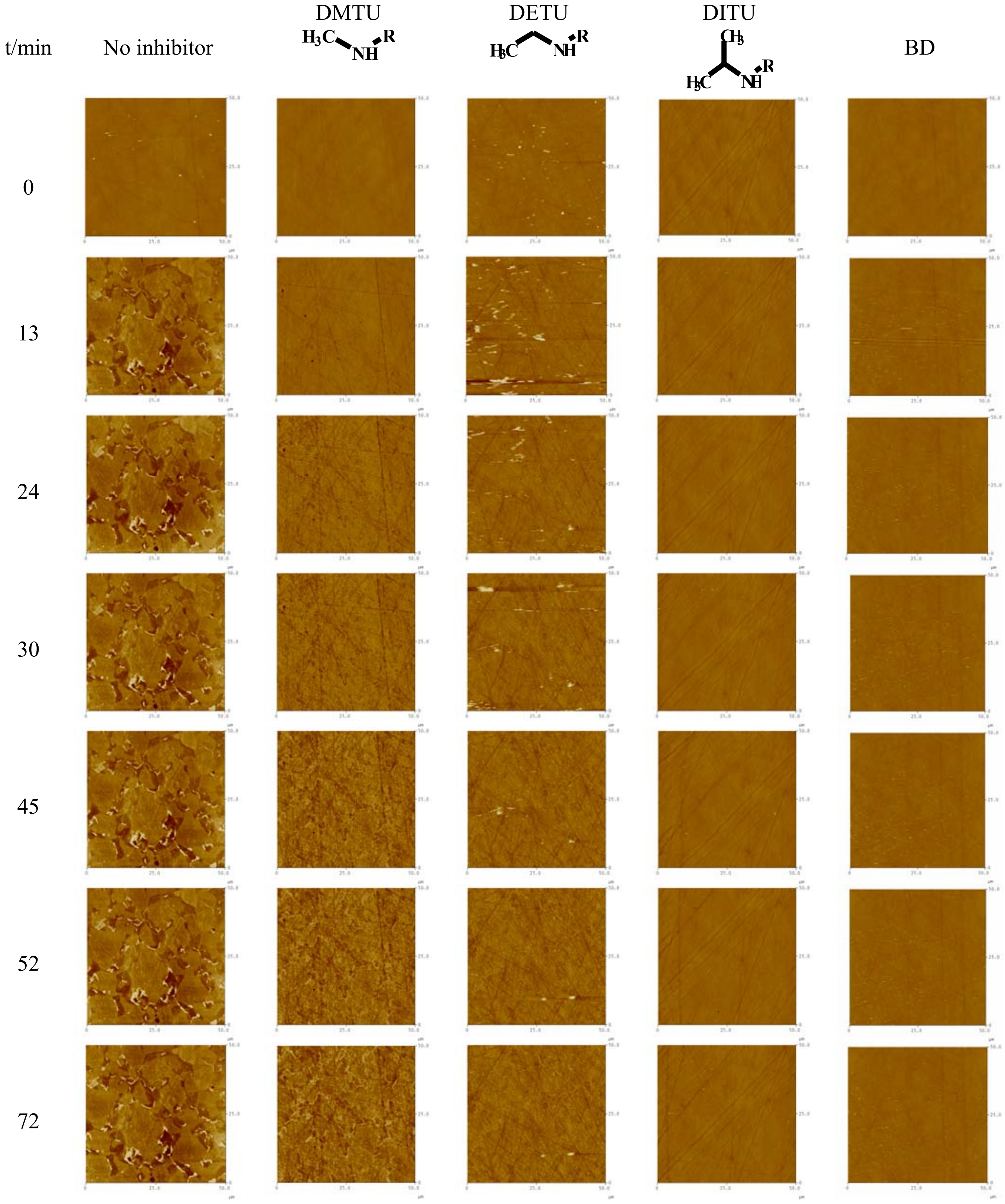

Figure 99. Results of AFM in the liquid phase for the steel surface after immersion in different commercially available buffer solutions containing 0.9 g/l of the different inhibitors (scale: 50 X 50 µm).

From the data shown in **figure 99** it can be concluded that all inhibited solutions tested provide protection against corrosion for the samples when comparing with solution in which no inhibitor is present.

For the inhibitors containing a thiourea, in the records of AFM show that the surface is less affected when the lateral chain is longer. This observation becomes more obvious at higher immersion times. The samples treated with DMTU show to be more affected at the surface than those treated in the presence of DETU und DITU. However, the attack in all cases was less pronounced than in the absence of an inhibitor. This qualitative observation was confirmed by the measurement of the surface roughness of which the results are given in **figure 100**. Here it can be seen that the roughness decreases when inhibitors with a larger lateral chain are used.

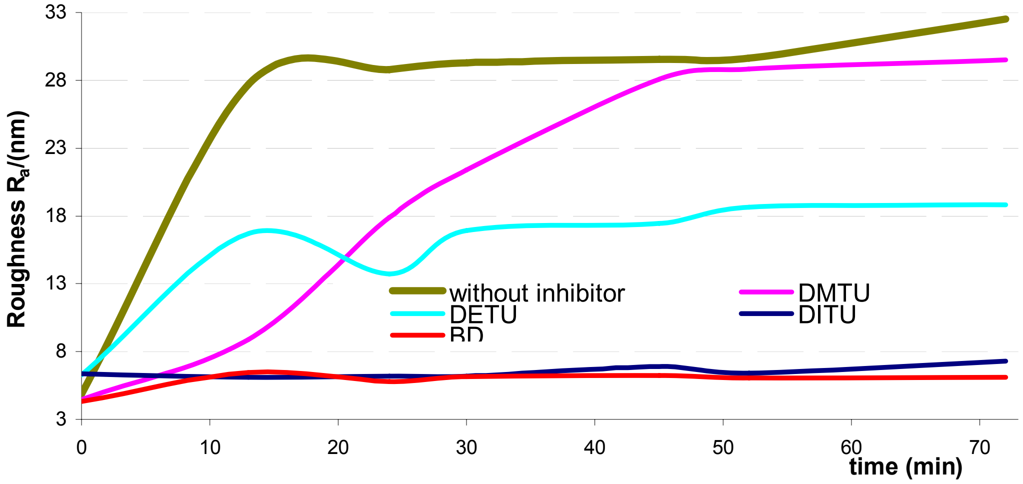

Figure 100. Roughness (R_a) of the steel surface obtained at different immersion times in pickling solutions with 0.9 g/l of DMTU, DETU, DITU and BD.

The effect of BD and DITU in the pickling medium is shown to be optimal with respect to corrosion protection. Their effects are comparable and can be considered to be constant with the concentration. At higher immersion times, however the effect of BD is slightly better than that of DITU, not only because the roughness obtained is lower but also because this parameter becomes more stable.

4.2.4.6 Summary

Results of XPS, IRRAS and TOF-SIMS determined the formation on the steel surface of a layer of thiourea containing compounds (DMTU, DETU, DITU) when the coupon is submerged into solutions of DPGDME containing the molecules.

The adsorption was proved to be most favourable the longer the lateral chain.

In the case of the TOF-SIMS measurements, the results can be summarized as follows:

- Specific fragments of the molecules of the thiourea containing compound were found for the three inhibitors.
- The molecular ion was found for DMTU, DETU and DITU, which testifies that the three compounds were present at the surface after rinsing
- The longer the lateral chain, the fewer molecular ions are found in the TOF-SIMS spectra.
- No fragment Fe-R~ was found, which is in accordance with the physisorptive behaviour of the inhibitors postulated by the former experiments where no chemisorption was confirmed.

The topography of steel pieces is shown to be enormously different when the inhibitors are present in the acidic solutions. The CI in real pickling conditions is shown to protect the steel surface reducing greatly the damage. It reduces the grain elimination in more than a 50%.

The protection of the thiourea containing compounds was proven to be better in a buffer solution pH=1 the longer their lateral chain.

5. Conclusions

The starting point of this work was the study of two topics:

- The effects of pickling in the steel
- The molecules that are part of the commercially available inhibitor used currently at the pickling plants as well as the commercially available solution itself.

The effects of the pickling on the steel surface were studied by means of topographical techniques such as white light interferometry, scanning electron microscopy and atomic force microscopy coupled with secondary mass spectroscopy and weight loss experiments.

The behaviour of the pickling inhibitors was studied by means of weight loss experiments, electrochemical techniques, infrared reflection absorption spectroscopy, x-ray electron spectroscopy and time-of-flight secondary ion mass spectroscopy. Topographical techniques as atomic force microscopy and scanning electron microscopy were also used to study the condition of the steel surface when it had been treated with a pickling solution in the absence and in the presence of the studied inhibitors.

Cold rolled steel was used to make all the studies due to the fact that the results obtained with hot rolled material were shown to be highly dependant on the structure and homogeneity of the scale. With cold rolled the reproducibility of the experiments was better.

5.1 Effects of acid in steels

The investigation of the effects of acids on the surface of low alloyed cold rolled steels yielded the following conclusions:

- A treatment with H_2SO_4 leads to a higher loss of layers than HCl. With topographical studies made with white light interferometry and scanning electron microscopy the pickling with H_2SO_4 could be shown to be more aggressive than the pickling with HCl. Different mechanisms for the pickling with both acids could be proposed: while H_2SO_4 directly attacks the ferrite grain surface and removes the grains completely, HCl attacks mainly at the grain boundaries and it is only a higher pickling times that at the grain boundaries damage occurs. The use of HCl seems to result in a less aggressive pickling, allowing the structure of the surface to be recognizable until higher pickling times.
- When the different concentrations of HCl are compared, the effects of this acid do not vary much between 7 % and 20 %. However, the topography shows how a 7 %HCl solution causes higher roughness. This means that the pickling is less homogeneous. Pickling with 7 % HCl

attacks mainly at the grain boundaries but at higher times a complete removal of grains occurs more clearly than with 20 % HCl.

- By means of white light interferometry it could be visualized how at real pickling conditions a higher roughness at the surface is obtained, due to the higher temperature used. The results of scanning electron microscopy agree with these findings and show how complete layers of ferrite grains were removed.
- The corrosive effect of a commercially available solution buffered at pH=1 could be observed by means of AFM. This solution was shown to cause a very remarkable corrosion of the steel surface. Afterwards the corrosion seems to become constant, which leads to the conclusion of that a passivation layer is formed. The solution seems to cause so-called pitting corrosion.
- The use of H_2SO_4 causes the formation of a passivation layer, of which the composition could be determined by means of secondary neutral mass spectrometry. Approximately until 30 minutes of immersion the concentrations of Cu, Mn, Al, S, Ti, Cr and Si at the surface were found to increase considerably. At long immersion times the concentration of those elements at the surface starts to decrease again. Images of scanning electron microscopy confirm the steady state around 40-50 minutes of pickling.

5.2 Pickling inhibitors

- From weight loss and electrochemical experiments CI, DITU, DETU, DMTU, DPTU and BD were shown to be effective corrosion inhibitors. The interaction between the metal and the compounds was shown to be highly dependant on the pickling solution and the conditions used. Also the nature of the inhibition was found to depend on them. Best results were obtained at lower pHs. It was shown that an adsorption according to Langmuir was followed by the system depending on the conditions used.
- By weight loss experiments it also could be shown that KI, DPGDME and HMTA are pickling inhibitors but at pH=5.5they were shown to be able to act as corrosion promoters as well.
- The protective effect of all inhibitors tested could be visualized by means of scanning electron microscopy. The records showed that the effect on the surface was lower when inhibitors were present. The higher protective effect of HMTA in the case of HCl as compared to the effect in pickling with H_2SO_4 was confirmed. With atomic force microscopy

it could be shown that the thioureas and the BD in a buffer solution at pH=1 has a protective effect as well.

- The interaction between the inhibitors and the steel surface could be shown to be a physisorption by the results of different used methods.
- By weight loss experiments I^- was shown to be more effective than Br^-.
- Comparisson among the different thioureas:
    - The size of the lateral chain was proved to have an influence in the magnitude of the adsorption. An increase in the length results in a best adsorption to the surface.
    - Several techniques lead to the conclusion that the surface is better protected with the lengthening of the lateral chain. The disagreement of some experiments to this statement is attributed to the low solubility of the molecules with higher molecular weight in the tested environment.
    - Weight loss experiments clearly showed a more effective inhibition with the increasing length of the lateral chain. The presence of the aromatic groups of DPTU turns out in the less effective inhibition. Langmuir equation leads to free energy values which increase with the length of the lateral chain.

This work showed the different effects of acids on the steel surface as well as the different mechanism, in the case of acids of different nature and concentration. Different pickling inhibitors were studied with respect to their behaviour by different methods and in different pickling solutions.

It could be shown that the behaviour of an inhibitor depends on its molecular structure. This allows it to predict the inhibitory efficiency on a molecular basis and further to come to a more rational and controlled design of pickling inhibitors.

Further studies could be carried out with respect to the effects of acids at other concentrations, temperatures and the materials.

6. Literature

1. I. L. Rozenfeld, "*Corrosion inhibitors*", McGraw Hill Inc., New York, **1981**.
2. G. R. Brubaker, P. Beverley P. Phippis, (Eds.), "*Corrosion chemistry*", American Chemical Society, Washington, **1979**.
3. A. Benninghoven, F. G. Rüdenauer, H. W. Werner, "*Secondary ion mass spectrometry*", John Wiley & Sons Inc., New York, **1987**.
4. D.M. Drazic in B.E. Conway, J. O'M. Bockris, R.E. White (Eds.) "*Modern aspect of electrochemistry*", vol. 19, Plenum Press, New York, **1989**.
5. F. A. Cotton, G. Wilkinson, C. A. Murillo, M. Bochmann "*Advanced inorganic chemistry*", 6th ed., New York, **1999**.
6. H. E. Jamil, A. Shriri, R. Boulif, C. Bastos, M. F. Montemor, M. G. S. Ferreira, "Electrochemical behaviour of amino alcohol-based inhibitors used to control corrosion of reinforcing steel", *Electrochim. Acta*, **2004**, *49*, 2753-2760.
7. R. Cottis, S. Turgoose "*Corrosion testing made easy: electrochemical impedance and noise*", Barry C. Syrett (Series Eds), NACE International, USA, **1999**.
8. J. Ross Macdonald (Ed), "*Impedance spectroscopy emphasizing solid materials and systems*", John Wiley & Sons, USA, **1987**.
9. D. Schauwinhold, M. Toncourt, R. Steffen, D. Janke, K. Schäfer, H. Jacobi, R. Hentrich, L. Kucharcik, H. Wiegels, H. M. Aichinger, F. Sänger, R. Kümmerling, U. Uhl, W. Decker, R. Pankert, H. Hougardy, W. Dahl, H. J. Grabke, U. Kalla, G. Kalwa, R. Winkelgrund, H.L. Bünnager, V. Brückmann. "Steel", in *Ullmann's Encyclopedia of Industrial Chemistry* Vol. A25, VCH, Weinheim, **1994**.
10. Data from the National Institute of Standards and Technology (NIST) Standard Reference Database 69, June **2005** Release: *NIST Chemistry WebBook*.
11. International Chemical Safety Card 0793, published by the International Programme on Chemical Safety in collaboration with the European Commission, **2004**.
12. Merck ChemDAT database, ®Merck KGaA, Darmstadt, Germany. Last actualization, 28-09-**2007**.
13. Database Chemfinder.com from the CambridgeSoft Corporation, 100 CambridgePark Drive, Cambridge, MA 02140 USA, ©**2004**.
14. J. A. Young, "Chemical laboratory information profile", *JCE*, **2001**, *78*, 1326.
15. From the Material Safety Data Sheet ACC # 09765 from Thermo Fisher Scientific Inc., 2000 Park Lane, Pittsburgh , PA 15275, USA, **2007**.
16. From the Material Safety Data Sheet with product number C1746 from Science Stuff Inc., 1104 Newport Ave, Austin, TX 78753, USA, **2007**.

17. Wang, L.S.; Wu, H.; Desai, S.R., "Sequential oxygen atom chemisorption on surfaces of small iron clusters", *Phys. Rev. Lett.*, **1996**, *76*, 4853-4856.

18. N.N. Greenwood, A. Earnshaw, "*Chemistry of the elements*", Pergamon Press Ltd., Oxford**, 1984**.

19. J. Apraiz Barrero, "Tratamientos térmicos de los aceros" 9. Ed, Limusa Noriega Editores, Madrid, **1997**.

20. M. A. Yescas Gonzalez., "Modelling the microstructure and mechanical properties of austempered ductile irons", Ph.D. thesis, University of Cambridge, Cambridge, **2001**.

21. IUPAC, "*Gold Book. Compendium of chemical terminology*", A. D. McNaught, A. Wilkinson (Eds.), 2nd Edition, Blackwell Scientific Publ., Oxford, **1997**.

22. R. A. Alberty, "*Physical chemistry*" 7. ed., John Wiley & Sons, New York, **1987**.

23. I. N. Levine "*Physical chemistry*" 5. ed., McGraw Hill, New York, **2002**.

24. A. Roig Muntaner, M. Díaz Peña, "*Química física*", Alahambra, Madrid, **1976**.

25. D. A. Jones, "*Principles and prevention of corrosion*", Macmillan Publishing Cy., New York, **1992**.

26. K. E. Heusler, D. Landolt, S. Trasatti, "Electrochemical corrosion nomenclature (Recommendations 1988) Commission on Electrochemistry", *Pure & Appl. Chem.*, **1989**, *61*, 19.

27. F. Mansfeld (ed.), "*Corrosion mechanisms*", Marcek Dekker, Inc., New York, **1987**.

28. W. Bumbulis, G. Köhler, B. Schweinsberg, „Kaltwalzen auf flacher Bahn, *Beizeinrichtungen in Kontaktstudium Umformtechnik*, Teil II", Lüdenscheid, **1982**.

29. I. N. Putilova, S. A. Balezin, V. P. Barnnik, "*Metallic corrosion inhibitors*", Pergamon Press Ltd., London, **1960**.

30. M. N. Salan Ballesteros, "Tecnología de proceso y transformación de materiales", ediciones UPC, Barcelona, **2005**.

31. W.D. Callister Jr., "*Materials science and engineering. An introduction*", John Wiley & Sons, Inc., New York, **1985**.

32. L. L. Shreir, R. A. Jarman, G. T. Burstein, "*Corrosion. Volume 1. Metal/environment reactions*", 3. Ed., Butterwordth-Heinemann Ltd., Bodmin, **1994**.

33. M. G. Fontana, "*Corrosion engineering*", 3. ed., McGraw Hill, Singapore, **1987**.

34. M. Crabtree, D. Eslinger, P. Fletcher, M. Miller, A. Johnson, G. King, "Fighting scale-removal and prevention", *Oilfield Review*, **1999**, *11*, 30-45.

35. R. Y. Chen, W. Y. D. Yuen, “Improvement of pickling characteristics of hot-rolled strip through heat treatment of the oxide scale” presented at *ISS 44th Mechanical Working and Steel Processing Conference*, Orlando (USA), *30*, 17-22,**2002**.
36. G. Hubmer, A. Osterkorn, K. Rendl, R. Puntigam, R. Sestak, W. R. Thiele, “Eine neue Methode zur Endpunktbestimmung beim Beizen von Stahl”, *Stahl & Eisen*, **2002**, *122*, 59-65.
37. L.Prümmer in VDEh (ed.), „*Grundlagen des Beizens in Herstellung von Kaltgewalztem Band*”, Verlag Stahleisen, Düsseldorf, **1970**.
38. J. P. Van’t Hul, G. Sussek, J. Crahay, *“Influence of pickling parameters on zinc coating and cold rolling”*, EUR 20893-Rolling Flat Products, Technical Steel Research Series, European Commission, Luxembourg, **2003**.
39. N. Ipek, B. Holm, R. Pettersson, R. Runnsjö, M. Karlsson, “Electrolytic pickling of duplex stainless steel”, *Materials and Corrosion*, **2005**, *56*, 521-532.
40. G. Schmitt, “Application of inhibitors for acid media”, *Brit. Corr. J.*, **1984**, *19*, 165-176.
41. A. D. Mercer, “Test methods for corrosion inhibitors“, *Brit. Corr. J.*, **1985**, *20*, 61-70.
42. K. J. Laidler, “*Cinética de las reacciones*”, Ed. Alhambra, México D.F., **1979**.
43. J. M. Smith, “*Ingeniería de la cinética química*”, Ed. Continental, México, **1990**.
44. W. Castellan, “*Fisicoquímica*”, Ed. McGraw Hill, México, **1991**.
45. Acros Organics, „*Feinchemikalien Katalog*”, **2004-2005**.
46. Merck KGaA, „*Chemikalien Reagenzien*”, Darmstadt, **2003**.
47. SciFinder Scholar^{TM}, version 2006; Chemical Abstracts Service: Columbus, OH, 2005; RN 2986-17-6 (accessed Oct 17, 2005); RN 105-55-5 (accessed Oct 17, 2005); RN 534-13-4 (accessed Oct 17, 2005); RN 110-65-6 (accessed Oct 17, 2005)
48. Aldrich, „*Katalog Handbuch Feinchemikalien*”, **1996-1997**.
49. „*All in One, Forschungschemikalien, Metalle und Materiallen*”, Alfa Aesar GmbH & Co KG, Kalsruhe, **2006-2007.**
50. European Commission, Directorate-General, Joint Research Centre, “But-2-yne-1,4-diol. Summary risk assessment report” Institute for Health and Consumer Protection, European Chemicals Bureau, Ispra, **2005**.
51. International Chemical Safety Card 1228, published by the International Programme on Chemical Safety in collaboration with the European Commission, **2004**.
52. I. A. Ammar, S.Darwish, “Effect of some ions on inhibition of the acid corrosion of fe by thiourea”, *Corr. Sci.*, **1967**, *7*, 579-596.

53. T. Murakawa, T. Kato, S. Nagaura, N. Hackerman, “A contribution to the understanding of the synergistic effect of anions for the corrosion inhibition of Fe by amines”, *Corr. Sci.*, **1968**, *8*, 483-489.
54. T. Murakawa, T. Kato, S. Nagaura, N. Hackerman, “Differential capacity curves of iron in perchloric acid in the presence of anions”, *Corr. Sci.*, **1967**, *7*, 657-664.
55. N. S. Rawat, G. Udayabhanu, “Synergistic effects of halide ions and benzyl amine on electrochemical behaviour of mild steel in dilute sulphuric acid”, *International Congress on Metallic Corrosion*, 2963-2970, Madras, India, 7-11 Nov., **1987**
56. H. Ashassi-Sorkhabi, N. Ghalebsaz-Jeddi, F. Hashemzadeh, H. Jahani, “Inhibition effect of some polyethylene glycol on the corrosion of carbon steel in hydrochloric acid”, *7th Iran Physical Chemistry Seminar*, 1-8, Isfahan, Iran, 8-10 March, **2005**.
57. H. Ashassi-Sorkhabi, N. Ghalebsaz-Jeddi, “Inhibition effect of polyethylene glycol on the corrosion of carbon steel in sulphuric acid”, *Mat. Chem. & Phys.*, **2005**, *92*, 480-486.
58. E. Slavcheva, G. Petkova, P. Andreev, “Inhibition of corrosion of az91 magnesium ally in ethylene glycol solution in presence of chloride anions”, *Mat. & Corr.*, **2005**, *56*, 83-87.
59. G. Schmitt, “Inhibitors for chemical cleaning treatment” in *Corrosion Inhibitors*, Working Party Report II, The Institute of Materials, UK, **1994**.
60. N. Tabakova, V. Mircheva, "Umweltfreundliche Beizinhibitoren für Stahl" in *Jahrbuch Oberflachentechnik*, Eugene G. Leuze (Ed.), Vol. 61 , Germany, **2005.**
61. P.N. Hurter, T. A. Hatton, “Solubilization of polycyclic aromatic hydrocarbons by poly(ethylene oxide-propylene oxide) block copolymer micelles: effects of polymer structure”, *Langmuir*, **1992**, *8*, 1291-1299.
62. N. Hackerman, E. MacCafferty, “Adsorption and corrosion inhibition with flexible organic diamines”, *Proc. 5th Int. Congress On Metallic Corrosion*, Tokyo, Japan, 21-23 May, **1972**.
63. H. Pirak, W. Wenzel, “Organische Substanzen und die Säurekorrosion des Eisens”, *Korrosion und Metallschutz*, **1934**, *10*, 29-39.
64. K. P. C. Vollhardt, N. E. Schore, “*Química Orgánica*”, 2nd ed., Ed. Omega, Barcelona, **1996**.
65. F.B. Growcock, W. W. Freiner, V. R. Lopp, “corrosion inhibitors of steel in hcl by 1-octiyn-3-ol-i. kinetics”, *Proceedings of the 6th European Symposium on Corrosion Inhibitors (6SEIC)*, Ann. Univ. Ferrara, Italy, N.S., V, Suppl. N.8, 167-181, **1985**.

66. J. O’M. Bockris, N. G. Smart, B. Yang, “On mechanism of inhibitors by acetylenic hydrocarbons”, *Abstracts of the 42nd Meeting Int. Soc. Of Electrochemistry*, Montreux, Switzerland, 25-30 August, IL 4-6, **1991**.

67. M. Utaka, A. Takeda, M. Bender, “Synthesis of endo- and exo-[4(5)-imidazolyl]bicyclo[2.2.1]hept-endo-2-yl trans-cinnamates”, *J. Org. Chem.*, **1974**, *39*, 3772-3777.

68. R. J. Tedeschi, “Acetylenic corrosion inhibitors”, *Corrosion/73*, presented at NACE Annual Conference, Anaheim, USA, March 11-15, paper 24, 24/1-24/13, **1973**.

69. R. J. Tedeschi, P. W. Natali, H. C. MacMahon, “the role of the triple bond in acid corrosion inhibition”, *Corrosion 1969*, presented at 25th NACE Annu. Conf., Houston, USA, March, paper 30, 173-179, **1969**.

70. T. P. Hoar, R. D. Holliday, “The inhibition by quinoline and thioureas of the acid dissolution of mild steel”, *J. Appl. Chem.*, **1953**, *3*, 502-13.

71. H. Kaesche, „Das Elektrodenverhalten von Eisen in perchlorsauren Lösungen von Phenylthioharnstoff“, *Z. Elektrochem.*, **1959**, 63, 492-500.

72. K. Sykut, J. Saba in A. Dabrowski (Ed.), “*Adsorption and its applications in industry and environmental protection*”, Elsevier, Amsterdam, **1999**.

73. A. Frignani, G. Trabanelli, F. Zucchi, M. Zucchini, “Organic substances as inhibitors or stimulators of acid corrosion of iron”, *Proceedings of the 4th European Symposium on Corrosion Inhibitors*, Ferrara, Italy, 15-19 September, 652-673, **1975**.

74. ASTM, “Standard practice for laboratory immersion corrosion testing of metals”, *American Standard Test Method International*, ASTM Designation: G31-72, **1997**, *3*, 95, West Conshohocken (Pennsylvania, USA).

75. N.G. Thompson, J. H. Payer, “*corrosion testing made easy: DC electrochemical test methods*”, vol. 6, NACE International, USA, **1998**.

76. A. J. Bard, L. R. Faulkner, “*Electrochemical method. Fundamentals and applications*”, 2nd Ed., John Wiley & Sons, New York, **2001**.

77. H. H. Girault, “*Analytical and physical electrochemistry*“, EPFL Press, Lausanne, **2004**.

78. P. J. Gellings, “*Introduction to corrosion prevention and control for engineers*“, Delft University Press, Delft, **1976**.

79. K. Hladky, L. M. Callow, J. L. Dawson, “Corrosion rates from impedance measurements: an introduction“, *Brit. Corr. J.*, **1980**, *15*, 20-25.

80. C. H. Hamann, A. Hamett, W. Vielstich, “*Electrochemistry*“, Wiley-VCH, Weinheim, **1998**.

[81] R.C. Alkire, D.M. Kolb, J. Lipkowski, P. Ross (Eds.) "*Diffraction and spectroscopic methods in electrochemistry*", Advances in electrochemical science and engineering, Vol. 9, Wiley-VCH, New York, **1990**.

[82] T. Imae (Ed.), "*Advanced chemistry of monolayers at interfaces*", Interface science and technology, Vol. 14, Elsevier/Academic Press, Amsterdam , **2007**.

[83] J. M. Chalmers, P. R. Griffiths, (Eds.) "*Handbook of vibrational spectroscopy*", Vol. 2, John Wiley & Sons, New York, **2002**.

[84] J. D. Swalen, J. F. Rabolt, "Characterization of orientation and lateral order" in J. R. Ferraro, L. J. Basile (Eds.) *Fourier transform infrared spectroscopy, applications to chemical systems*, Vol. 4, Academic Press, Orlando, **1985**.

[85] W. G. Golden, "Fourier transform infrared reflection-absorption spectroscopy" in J. R. Ferraro, L. J. Basile (Eds.) *Fourier Transform Infrared Spectroscopy, Applications to Chemical Systems*, vol. 4, Academic Press, Orlando, **1985**.

[86] V. P. Tolstoy, I. V. Chernyshova, V. A. Skryshevsky, "*Handbook of infrared spectroscopy of ultrathin films*", John Wiley & Sons, New York, **2003**.

[87] J. F. Moulder; W. F. Stickle, P. E. Sobol, K. D. Bomben, "*Handbook of X-ray photoelectron spectroscopy*", Physical Electronics, Minnesota, **1995**.

[88] M. P. Seah, D. Briggs, in "*Practical surface analysis. Volume 1: Auger and X-ray photoelectron spectroscopy*", D. Briggs, M. P. Seah (Eds), 2nd ed, John Wiley & Sons, New York, **1990**.

[89] R. Payling, D. Jones, A. Bengtson (Ed.), "*Glow discharge optical emission spectrometry*", John Wiley & Sons, Chichester, **1997**.

[90] T. Nelis, R. Payling, "Glow discharge optical emission spectroscopy. A practical guide", Royal Society of Chemistry, Cambrigde, **2003**.

[91] D. Briggs, M. P. Seah (Eds.) "*Practical surface analysis, Volume 2: Ion and neutral spectroscopy*". 2nd Ed, John Wiley & Sons, Chichester, **1992**.

[92] H. Oechsner (Ed.), "*Topics in current physics. Thin film and depth profile analysis*", Springer Verlag, Berlin, **1984**.

[93] J. C. Vickerman (Ed.), "*Surface analysis. The principal techniques*", John Wiley & Sons, Chichester, **1997**.

[94] R. G. Wilson, F. A. Stevie, C. W. Magee, "*Secondary ion mass spectrometry*", John Wiley and Sons, New York, **1989**.

[95] J. C. Vickermann, D. Briggs (Eds), "*TOF-SIMS: surface analysis by mass spectrometry*", IM-Publishers, Surface Spectra, Chichester, **2001**.

[96.] A. Benninghoven, F. G. Rüdenauer, H. W. Werner, “*Secondary ion mass spectrometry*”, John Wiley & Sons, New York, **1987**.

[97.] D. Price, J. E. Williams, “Time-of-flight mass spectrometry”, Pergamon Press, Oxford, **1969**.

[98.] K. Chiba, S. Nakamura, “Characterization of ion species of silicon oxide films using positive and negative secondary ion mass spectra”, *Appl. Surf. Sci.*, **2006**, *253*, 412-416.

[99.] O. Aubel, E. Bugiel, D. Krüger, W. Hasse, M. Hommel, “Investigation of the influence of thermal treatment on interconnect-barrier interfaces in copper metallization systems”, *Microelectronics Reliability*, **2006**, *46*, 768-773.

[100.] N. Yao, Z. L. Wang (Eds.), “*Handbook of Microscopy for Nanotechnology*”, Kluwer Academic-Plenum Publishers, New York, **2005**.

[101.] O. C. Wells, “Scanning electron microscopes”, McGraw Hill, New York, **1974**.

[102.] D. A. Skoog, F. J. Holler, T. A. Nieman, “Principles of instrumental analysis”, 5th Ed., Brooks/Cole Thomson Learning, Belmont, **1998**.

[103.] G. Friedbacher, H. Fuchs, “Classification of scanning probe microscopies (technical report)”, *Pure Appl. Chem.*, **1999**, *71*, 1337-1357.

[104.] C. Daniel, F. Mücklich, “Quantification of periodic surface structures by white-light interferometry”, *Prakt. Metallogr.*, **2004,** *41*, 277-285.

[105.] M. Bossard, “Abstasten mit Licht. Weißlicht-Interferenz-Mikroskopie zur 3D-Oberflächen- und Vibrationsmessung im Submikrometer-Bereich”, *Farbe & Lack*, **2004**, *110*, 27-29.

[106.] M. Roy, I. Cooper, P. Moore, C. J. Sheppard, P. Hariharan, “White light interference microscopy: effects of multiple reflections within a surface film”, *Optics Express*, **2005**, *13*, 164-170.

[107.] J. C. Wyant, “White light interferometry”, presented at AeroSense**,** 1-5 April **2002**, Orlando, Florida.

[108.] P. Atkins, “*Atkins’ Physical Chemistry*” 6. ed, W. H. Freeman & Co. and Sumanas, Inc., New York, **1998**.

[109.] I. Correia Guedes, “*Eficiencia dos inhibidores de corrosao benzotriazol, n-feniltioureia e clorato de hexadeciltrimetil amonia quaternario para ferro puro, aco carbono e aco arbl em meiode acido sulfurico*”, Doctoral Thesis-Ed. Escola Politécnica, Universidad de São Paulo, São Paulo,**1996**.

[110.] B.E. Conway, “*Theory and principles of electrode processes*“, The Ronald Press Company, New York, **1965**.

[111] ASTM, “Standard test methods for determining average grain size”, *American Standard Test Method International*, ASTM Designation: E112-96 sup. e2, **1996**, *3*, 1-26.

[112] E.Weck, E. Leistner, “*Metallographic instructions for colour etching by immersion*”, Deutscher Verlag für Schwißtechnik (DVS) GmbH, Düsseldorf, **1982**.

[113] M. O. Agwar, P. T. Ndifon, M. K. Ndikontar, “Physicochemical studies of some hexamethylenetetramine metal(ii) complexes”, *Bull. Chem. Soc. Ethiop.*, **2004**, *18*, 143-148.

[114] J. O. Jensen, “Vibrational frequencies and structural determinations of hexamethylenetetraamine”, *Spectrochim. Acta Part A*, **2002**, *58*, 1347-1364.

[115] D. Gambino, E. Kremer, E. J. Baran, “Infrared spectra of new re(iii) complexes with thiourea derivatives”, *Spectrochim. Acta Part A*, **2002**, *58*, 3085-3092.

[116] R. M. Silverstein, G. C. Bassler, T. C. Morrill, “Spectrometric identification of organic compounds”, 4th ed, John Wiley & Sons, New York, **1981**.

[117] S. H. Sanad, A. A. Ismail, N. A. Mahmoud, “Inhibition effect of potassium iodide on corrosion of stainless steel in hydrochloric acid solution”, *J. Mat. Sci.*, **1992**, *27*, 5706-5712.

[118] M. Abdallah, “Rhodanine azosulpha drugs as corrosion inhibitors for corrosion of 304 stainless steel in hydrochloric acid solution”, *Corr. Sci.*, **2002**, *44*, 717-728.

[119] B. A. Abd-El-Nabey, A. A. El-Awady, S. G. Aziz, “Structural effects and mechanism of the inhibition of acid corrosion of steel by some dithiocarbamate derivatives”, *Corr. Prevention & Control*, **1991**, *38*, 68-74.

[120] I. V. Aoki, I. C. Guedes, S. L. A. Maranhão, “Copper phthalocyanine as corrosion inhibitor for ASTM A606-4 steel in 16% hydrochloric acid”, *J. Appl. Electrochem.*, **2002**, *32*, 915-919.

[121] A. C. Makrides, N. Hackerman, “Effect of thiourea compounds on dissolution rate of iron and mild steel - adsorption and inhibition, steady state and potential”, *Industrial and Engineering Chemistr*y, **1955**, *47*, 1773-1781.

[122] M. G. Hosseini, M. Sabouri, T. Shahrabi, “Comparison between polyaniline-phosphate and polypyrrole-phosphate composite coatings for mild steel corrosion protection”, *Mat. and Corr.*, **2006**, *57*, 407-410.

Risks and safety

BD: Toxic, corrosive, harmful

- R21, R23/25, R34, R43, R48/22
- S25, S26, S36/37/39, S45, S46

DETU: Harmful

- R22

DITU: Toxic

- R23/24/25
- S27, S28, S36/37/39, S45

DMTU: Toxic

- R25, R43
- S36/37, S45

DPTU: Toxic

- R25
- S36/37/39, S45

$FeSO_4$: Harmful

- R22

HCl: Corrosive

- R34, R37
- S26, S36/37/39, S45

HMTA: Highly flammable, harmful

- R11, R42/43
- S16, S22, S24, S37

H_2SO_4: Corrosive

- R35
- S25, S30, S45

KI: Irritant

- R36/37/38
- S26, S36

The residues generated were placed into the collection waste system available at the facilities of the Dortmunder Oberflächencentrum.

- **Key:**

R11: Highly flammable.
R21: Harmful in contact with skin.
R22: Harmful if swallowed.
R23/24/25: Toxic by inhalation, in contact with skin and if swallowed.
R23/25: Toxic by inhalation and if swallowed.
R34: Causes burns.
R35: Causes severe burns.
R36/37/38: Irritating to eyes, respiratory system and skin.
R37: Irritating to the respiratory system.
R42/43: May cause sensitization by inhalation and skin contact.
R43: May cause sensibilization by skin contact.

R48/22: Harmful: danger of serious damage to health by prolonged exposure in contact with skin and if swallowed.

S16: Keep away from sources of ignition - No smoking.

S22: Do not breathe dust.

S23: Do not breathe gas/fumes/vapor/spray (appropriate wording to be specified by the manufacturer).

S24: Avoid contact with skin.

S24/25: Avoid contact with skin and eyes.

S25: Avoid contact with eyes.

S26: In case of contact with eyes, rinse immediately with plenty of water and seek medical advice.

S27: Take off immediately all contaminated clothing.

S28: After contact with skin, wash immediately with plenty of ... (to be specified by the manufacturer).

S30: Never add water to this product.

S36: Irritating to the eyes.

S36/37: Wear suitable protective clothing and gloves.

S36/37/39: Wear suitable protective clothing, gloves and eye/face protection.

S37: Wear suitable gloves.

S45: In case of accident or if you feel unwell, seek medical advice immediately (show label when possible).

S46: If swallowed, seek medical advice immediately and show this container or label.

Abstract/Übersicht

The current project develops in the framework of the steel industry, where the requirements in terms of quality of flat products are continuously increasing. The manufacturing process must be controlled and optimized to obtain the desired final quality. Therefore the use of organic additives in the pickling baths, which lead to a more uniform scale removal and avoids the formation of holes. The work presented is a study of a commercial inhibitor used at the moment in the pickling plant as well as each one of it single components: butindiol, diisopropylthiourea, dipropylengylkoldimethylether, methenamine and KI. To obtaind a better understanding of these inhibitors and their action, several investigative methods in different solutions have been used:

- The conditions of real pickling process in H_2SO_4 were reproduces in laboratory and the weight loss assays method was used to determine which of those single components exert a greater effect as a corrosion inhibitor.
- Electrochemical methods (open circuit potential measurement, polarization curves recording and electrochemical impedance spectroscopy) were applied to those components in two different solutions at pH=5.5 and at pH=1.
- X-ray photoelectron spectroscopy (XPS) was used to exemplarily determine the affinity of the diisopropylthiourea and two analogue molecules for the steel surface.
- Infrared spectra of the layers of the thiourea derivatives formed on the steel surface were obtained by using infrared reflection absorption spectroscopy (IRRAS).
- The final state of the steel surface after pickling treatment was checked by atomic force microscopy and scanning electron microscopy.

The above studies on the individual additives allowed the identification of the most effective components within the inhibitor. The adaptation of these results to the Langmuir model provides additional information about a monolayer formation and their inhibition mechanism, namely physisorption. Electrochemical assays agree with the weight loss results and determine they function as mixed inhibitors. All those experiments show a dependence of the measured magnitude on the concentration and show a saturation point at which a maximum effect is reached. XPS and IRRAS experiments show also a dependence of the layer formation with the contact time between the surface and the inhibitor. IRRAS prove the formation of a layer onto the steel surface whose spectra are comparable to the infrared spectrum of the thiourea containing molecules, proving a more favourable adsorption the longer the lateral chain. The images obtained by AFM and SEM show the effect of inhibitors resulting in a less affected and more homogeneous steel surface after the pickling. All those experiments lead to a better comprehension of the used additives action within the pickling process.

The effects of H_2SO_4 and HCl on the steel surface were also studied and two different dissolution mechanisms, depending on the nature of the acid, were established.

Das Projekt entwickelte sich aus den steigenden Qualitätsanforderungen der Stahlindustrie. Der Herstellungsprozess von Stahlbanderzeugnissen muss ständig überwacht und optimiert werden, um die gewünschte Endqualität zu gewährleisten. Aus diesem Grund ist die Zugabe von organischen Additiven in die Beizbäder nötig. Die vorliegende Arbeit ist eine Studie über momentan in den Beizbädern eingesetzte kommerzielle Inhibitoren. Es wurde zudem jeder einzelne Inhaltsstoff untersucht: Butindiol, Diisopropylthioharnstoff, Dipropylengylkol-dimethylether, Methenamine und KI. Die Inhibitoren und ihrer Inhaltsstoffe wurden mit verschiedenen Methoden untersucht,um ein besseres Verständnis ihrer Wirkung zu erreichen:

- Der reale Beizprozess in H_2SO_4 wurde mit den einzelnen Komponenten nachgestellt, und die Wirksamkeit der Komponenten wurde über die Ermittlung des Massenverlustes überprüft.
- Die wirksamsten Komponenten wurden mit elektrochemischen Methoden (Ruhepotentialmessungen, Stromdichte-Potentialmessungen und Impedanzmessungen) in zwei verschiedenen Lösungen mit pH=5,5 und pH 1,0 untersucht.
- Mit Röntgen Photoelektronenspektroskopie (x-ray photoelectron spectroscopy, XPS) wurde exemplarisch die Affinität des Diisopropylthioharnstoff und zweier analoger Moleküle zur Stahloberfläche untersucht. Die Schichten, die sich auf der Stahloberfläche ausbildeten, wurden mit Infrarot-Reflexions-Absorptions-Spektroskopie (infrared reflection absorption spectroscopy, IRRAS) untersucht.
- Der Endzustand der Stahloberfläche nach dem Beizen wurde mit Rasterkraft-Mikroskopie (atomic force microscopy, AFM) und Rasterelektronenmikroskopie (scanning electron microscopy, SEM) ermittelt.

  Die Untersuchungen der einzelnen Additive ermöglichte die Bestimmung des wirksamsten Bestandteils des Inhibitors. Aus der Adaption dieser Ergebnisse auf das Langmuir Model wurden zusätzliche Informationen über die Monolayerbildung und die Mechanismen der Inhibition, namentlich die Physisorption, ermittelt. Die elektrochemischen Messungen stimmen mit den Massenverlustmessungen überein und bestätigen die Behinderung der anodischen und kathodischen Reaktionen. All diese Experimente zeigen eine Abhängigkeit der gemessenen Größe (Ruhepotential, Korrosionstromdichte, Korrosionspotential) von der Konzentration und zeigen einen Sättigungspunkt, bei dem der maximale Effekt erreicht wird. XPS und IRRAS zeigen die Abhängigkeit der Schichtformation von der Kontaktzeit zwischen Oberfläche und Inhibitor. IRRAS Messungen weisen eine Schicht auf der Oberfläche nach, dessen Spektrum vergleichbar ist mit dem Infrarotspektrum der Moleküls. Das deutet auf eine bevorzugte Adsorption langer Molekülketten hin. Die mit AFM und SEM erhaltenen Aufnahmen zeigen den Effekt des Inhibitors anhand eines geringeren Angriffs und einer homogeneren Stahloberfläche nach dem Beizen. All diese Versuche führen zu einem besseren Verständnis der Wirkweise der genutzten Additive beim Beizprozess. Die Wirkung von H_2SO_4 und HCl auf die Stahloberfläche wurde ebenfalls untersucht und zwei verschiedene Auflösungsmechanismen, abhängig von der Art der Säure, festgestellt.

Curriculum Vitae

ACADEMIC TRAINING

- Master (2002-2003, USC). (Formation period of the program for Ph.D. thesis in the Organic Chemistry Department (USC), which accredits the *Researcher Aptitude*).

- Master thesis "Conjugated cyanide additions controlled by a remote stereocentre" realised at the Chemical Sciences Department of the University of Studies from Trieste under the supervision of Prof. Fabio Benedetti, at Trieste (Italy) in collaboration with Prof. Ramón José Estévez Cabanas, from the Department of Organic Chemistry (USC).

- Degree in Chemistry (2001), University of Santiago de Compostela (USC), Spain. Orientation: Chemistry of the Bioactive Compounds.

- Final Degree Work: "Peptidomimetic inhibitors of the AIDS virus protease". Realised under the supervision of María del Carmen Villaverde Cameron-Walker, lecturer of the Organic Chemistry Department (USC).

PRACTICAL TRAINING

- Trainee.

Proyects:

- "Determination of ion conductive polymers specific conductivities"
- "Development of ion conductive polymers with specific properties"

Furth im Wald, 01.10.02 - 31.12.02, Flabeg GmbH.

Supervisors: Dr. Dirk Joedicke, Dr. Regine Niepmann.

RESEARCH FELLOSHIP

- Marie Curie Host Fellowship. Host industry: ThyssenKrupp Steel. Supervisor: Dr. Tamara Appel.

- Project: "Characterisation of oxide layers onto steel surfaces and their elimination by means of acids"

Dortmund, 01.08.03-31.12.04; European Commission, ThyssenKrupp Stahl AG.

- Socrates/Erasmus Program. Host University: Universita degli Studi di Trieste. Supervisor: Prof. Fabio Benedetti.

- Project: "Conjugated cyanide additions controlled by a remote stereocenter".

Trieste (Italy), 01.01.03-30.05.03; European Comission.

Ph.D. THESIS

- ThyssenKrupp Steel in Dortmund under the supervision of Dr. Tamara Appel with adscription to the Hamburg University in cooperation with Prof. Dr. José A. Broekaert. 01.08.03 – 07.11.08.

  Theme: “Study of organic additives used as inhibitors in the steel dissolution in steel pickling baths”.

RESEARCH POSITION

- Research associate. Carnegie Mellon University, Department of Material Sciences and Engineering. Pittsburgh, USA. 01.10.07 – 31.09.09.

- Project: “Fundamental studies on controlling scale growth in alloys through additions of reactive elements”. Advisor: Prof. Sridhar Seetharaman,

CONFERENCE PARTICIPATION

- 4th International Conference on Diffusion in Solids and Liquids (DSL-2008): oral presentation “Fundamental Studies on the Transients Stages of Scale Growth in Fe-22%Cr Alloys Containing Reactive Elements”, July 9-11, **2008**, Barcelona, Spain.
- EUROCORR 2006: oral presentation “Influence of organic additives in steel pickling baths”, Sept. 25-28, **2006**, Maastricht (The Netherlands).
- 9th Symposium Electrochemical Methods in Corrosion Research (EMCR 2006): oral presentation “Influence of organic inhibitors in steel pickling baths”, June 18-23, **2006**, Dourdan (France).
- The European Corrosion Congress-EUROCORR2005: oral presentation “Influence of organic additives in steel pickling baths”, Sept. 4-8, **2005**, Lisbon (Portugal).
- 7. Conference JUNIOR EUROMAT: poster “Influence of organic additives in steel pickling baths”, Sept. 6-9, **2004**, Lausanne (Switzerland).

PUBLICATIONS

- L. M. Fernandez Diaz, J. Zhu, G.R. Holcomb, P.D. Jablonski, D.E. Alman, S. Sridhar, “Studies on Transient-Stage-Scale Growth on Fe-22wt.% Cr alloys containing 120 ppm La + 270 ppm Ce”, *Proceedings: General Abstracts: Structural Materials Division 2009 TMS Annual Meeting & Exhibition*, San Francisco, USA, Feb. 15-18, **2009**. (accepted)

- L. M. Fernandez Diaz, J. Zhu, G. R. Holcomb, P.D. Jablonski, D. E. Alman, S. Sridhar, "Fundamental Studies on the Transient Stages of Scale Growth in Fe-22 wt.% Cr alloys", *Defect and Diffusion Forum*, **2008**, (in print).
- L. M. Fernández Díaz, O. Bendick, C. Ostwald, T. Appel, “Influence of Organic Inhibitors in Steel Pickling Baths”, *Manuscripts Eurocorr 2006*, Sept. 25-28, **2006**, Maastricht, The Netherelands.
- L. M. Fernández Díaz, O. Bendick, C. Ostwald, T. Appel, “Study of the Influence of Some Organics as Thiourea Derivatives and Butindiol in Steel Pickling Baths”, *Materials and Corrosion*, **2006**, *57*, 689-95.
- L. M. Fernández Díaz, O. Bendick, C. Ostwald, T. Appel, “Influence of Organic Additives in Steel Pickling Baths”, *Proceedings of The European Corrosion Congress Eurocorr 2005*, Lisbon, Portugal, Sept. 4-8, **2005**. EFC. (ISBN: 972-95921-1-X).